Crystal Growth

طلاب الفرقة الثالثة- علوم

اعداد

الاستاذ الدكتور/ أبوالوفا أبوالمعارف محمد سالم

كلية العلوم

قسم الفيزياء

العام الجامعي

2023/2022

Abstract

The article contains sections titled:

1. Introduction
1.1. Historical Aspects
1.2. Uses of Single Crystals
1.3. Specification of Crystals
1.4. Commercial Aspects
1.5. Sources of Information
2. Thermodynamic Aspects
2.1. Free Energy and Driving Force of Crystallization
2.2. Phase Relations for Major Components
2.3. Phase Relations for Minor Components
2.4. Interfacial Effects
2.5. Shortcomings of the Thermodynamic Approach
3. Growth Kinetics
3.1. Atomic Structure of Growing Interfaces
3.2. Rough Faces
3.3. Perfect Singular Faces
3.4. Imperfect Singular Faces
4. Transport Effects
4.1. Transport Processes
4.2. Boundary Layers
4.3. Mass Flow of Major Components
4.4. Mass Flow of Minor Components
4.5. Heat Flow
4.6. Interface Stability
5. Practical Considerations

This article summarizes the theory and practice of the growth of single crystals. Today, the growth of crystals having dimensions of some hundred millimeters in diameter and weights over 200 kg under extreme pure conditions is well-matured in industrial scale. The major user of the crystals is the electronics industry.

Growth of crystals demands theoretical knowledge of thermodynamics, kinetics, and transport processes. In practice, some general aspects have to be considered, including choice of raw materials, conditions, methods, and characterization. The industrial and laboratory techniques of crystal growth are discussed. Economical aspects dominate the developments in the future, that is, growing of larger crystals at higher quality to raise yields and device performance. Furthermore, the demand for tighter specifications and increasing range of materials and uses will require more sophisticated methods and an extensive use of automation.

1. Introduction

This article summarizes the theory and practice of the growth of single crystals. Consideration is restricted to cases in which the ultimate product exploits *crystallinity; industrial crystallization,* which uses the crystallization process to purify or to obtain a product in an acceptable form (e.g., granulated sugar), is excluded here, but treated in Crystallization and Precipitation.

1.1. Historical Aspects

Crystals have been grown on a commercially significant scale since about 1950. Before this, almost the only significant activity was the growth of rubies for watch and clock bearings and, after 1940, defense-related activities (e.g., piezoelectric crystals for sonar transducers). However, the origins of the technology occurred much earlier.

According to references [1-4] and the sources quoted, the use of crystallization for the purification of salt can be traced back to 2700 B.C., growth from aqueous solution was being studied systematically in 1600 A.D. and high-temperature solution growth in 1800; and by about 1850, melt growth was a process of scientific interest.

Commercial exploitation on a small scale started around 1900 with the ''Geneva'' rubies grown by the Verneuil process (see Section 6.5 Verneuli Process), first used for jewelry and later for bearings in watches and similar instruments. Until quite recently, there was a reluctance to use artificially grown crystals as jewels; now, however, about half the rubies used as jewels are synthetic, and materials which do not exist naturally are common; cubic zirconia, for example, is in many ways a better gemstone than diamond.

VERNEUIL's first paper [5] on the method that carries his name was published in 1902; the second, more informative paper [6] appeared in 1904. During the next 44 years (up to the invention of the transistor in 1948), many of the methods discussed in Chapters Melt Growth Techniques, Solution Growth Techniques, Vapor Growth Techniques, Solid-Phase Growth Techniques were developed. Thus, SPEZIA's work on hydrothermal growth [7-9] was published between 1905 and 1908. The foundations of growth from the solid were laid in 1912 [10] and 1918 [11]. Also, in 1918 CZOCHRALSKI's paper [12] on crystal pulling from the melt was published. Before that the growth of crystals from the top into the melt was introduced in 1916 by NACKEN[13]. A similar technique with seed selection was then developed by KYROPOULOS in 1926 [14]. The decomposition of halides was used to grow crystals from the vapor in 1922 [15]. After TAMMANN[16] in 1914 studied for the first time the unidirectional solidification of metals in small vertical tubes, the crystallization of bulky melts in containers was described in 1925 by BRIDGMAN[17] and STOBER[18], and the technique was improved in 1936 by STOCKBARGER[19] using a two-zone furnace. Zone melting of metals was initiated in 1928 by KAPITZA[20]. Over the same period, much of the theoretical base of crystal growth was also laid. Thus, in 1904, NERNST[21] applied boundary layer ideas to crystal growth, and the basic ideas of the kinetics of the growth of perfect crystals were formulated in 1922–1928 by VOLMER, KLOSSEL, and STRANSKI[22-24]. Other theoretical aspects were treated by GIBBS, CURIE, WULFF, and KAISHEV.

The year 1949 can be regarded as a watershed [25]; reference [26] gives an account of the state of knowledge at that time and the motivation of workers in the field, who were mainly engaged in

scientific pursuits, i.e., studying crystals and their growth or using crystals in scientific instruments. The synthetic crystals of interest in 1949 were mostly semiconductors (especially germanium). After 1949, most workers were employed directly or indirectly because crystals could be used in commercial products. As a consequence, at this time the Czochralski method, being then as now the most productive bulk crystal growth method (Section 8.1 Sublimation and Evaporation Method), was extended to large-scale production. In 1950 TEAL and LITTLE[27] started the pulling of relatively large germanium crystals for the first transistors at Bell Laboratories. Shortly after, in 1952, TEAL and BUEHLER[28] adapted the Czochralski method for production of silicon crystals. The crystals were real (i.e., dirty, strained, and inhomogeneous as compared to ideal crystals), and these imperfections had to be controlled. For many purposes, one impurity atom per million host lattice atoms is of no importance; however, in a semiconductor device, unwanted impurity atoms at this level can have catastrophic consequences.

Semiconductor devices are made from crystals containing specified amounts of desired impurities (dopants) and preferably no other impurities at a detectable level.

The need for purity led to the invention of zone refining [29] and the floating zone process [30,31]. Zone refining is a process in which a molten zone is passed along a bar. Impurities are usually more soluble in the melt than in the solid, so the zone tends to carry the impurities with it. Passing a succession of zones can produce extreme purity: levels of 1 impurity atom in 10^{10} host atoms have been claimed, but measurement of impurity contents below 1 in 10^{8} is difficult. For details of zone refining, see Section 6.4Zone Melting and [32].

Another impurity-related problem involves the desired distribution of dopants. In 1953 it was shown [33,34] that in many situations the amount of impurity incorporated depends on the phase diagram, the growth rate, and the thickness of the boundary layer at the growth face. The general relation between impurity concentration and growth rate is still an unsolved problem (see Chap. 4 Transport Effects).

The causes of strain and crystallographic imperfections are now known and, at a price, certain crystals can be grown without dislocations and with small (say $< 10^{-5}$) built-in strain.

Chapters Thermodynamic Aspects, Growth Kinetics, Transport Effects, of this article summarize the theoretical problems solved in the last few decades. Chapters Practical Considerations, Melt Growth Techniques, Solution Growth Techniques, Vapor Growth Techniques, Solid-Phase Growth Techniques discuss practical techniques, which have changed markedly. For example, in 1949 crystal sizes were typically a few millimeters. Current linear dimensions are 100 times larger. In 1949, a temperature of 1000 8C controlled to 1 8C represented good technology; today, control to 0.1 8C is routine, and good technology can improve this by a factor of at least five. In 1949, raw materials containing less than 10–100 ppm of impurities were rare and expensive; today, levels over 1 ppm are unacceptable for many applications. To maintain high purity, clean ambients (e.g., laminar flow cabinets if not full clean room facilities) are common. Meanwhile, the growth of crystals with dimensions of some hundred millimeters in diameter and weights over 200 kg under extreme pure conditions is well-matured on industrial scale. Worldwide, there are nearly hundred companies dealing with production of metal, semiconductor, and dielectric crystals, mostly, combined with subsequent highly precise crystal cut and pieces polishing before sale. Yearly, the advanced semi-

conductor magazin *III-Vs Review* publishes a special company directory (see, e.g., [35]) with numerous informations on company profiles and product offers.

In order to meet the rapid developments of device dimension reduction and, especially, nanotechnology during the last decade the growth of crystals with nm and mm dimensions have come to the for. Special target is their multiple arrangement in well-ordered patterns, e.g., by the principle of self-assembly [36]. Beyond the traditional transitions between two phases, the three-phase sequence Vapor-Liquid-Solid (VLS) mechanism (see Vapor-Liquid-Solid Growth) to form nanowhiskers of different materials is more and more applied. Although the VLS mechanism is already known for a long time and was experimentally introduced in 1964 by WAGNER and ELLIS[37], it has now a renaissance on a much higher technological level. More details are treated in, e.g., (z Whiskers). History, fundamentals, technological growth aspects, and applicabilities of fiber crystals with diameters in mm dimensions are summarized in the monograph *Fiber Crystal Growth from the Melt*, Springer, 2004, edited by T. FUKUDA, P. RUDOLPH and S. UDA.

Finally, the epitaxy techniques for growth of monocrystalline thin films and stacks of quasi two-dimensional thin layers from alternating materials (i.e. multi-quantum wells), showing new physical properties on the nanometer scale, have been developed into the challenging field of quasi-two-dimensional crystal growth with important technological applications in micro- and optoelectronics. Since the first experiments by liquid-phase epitaxy (LPE) [38], chemical vapor deposition (CVD) [39], metal organic chemical vapor deposition (MOCVD) [40] in the 1960s, and molecular beam epitaxy (MBE) [41] in 1975, the capabilities of the methods and device quality have been markedly improved. Even combined methods like MBE with metal organic precursors (MOMBE) [42] are now under investigation. Nowadays, the growth of epitaxial diamond films from an activated vapor phase under low-pressure conditions is possible [43]. An overview on modern epitaxy techniques and applications is given in [[3], vols. 3 a, 3 b]. Here only some introductory aspects are referred to in Chapter 8 Vapor Growth Techniques (see also Semiconductors - Epitaxy, Silicon - Epitaxy, Thin Films – Thin Film Growth by Molecular Beam Epitaxy (MBE)).

1.2. Uses of Single Crystals

An ideal crystal is an infinite array (lattice) of atoms, arranged in patterns that repeat in all three spatial dimensions with uniform repeat distances; these lattice spacings are usually a small number (about 10) of interatomic distances. Lattice spacings for inorganic materials range from about 2.5×10^{-8} to 3.5×10^{-7} cm. Lattice spacings for organic materials involving macromolecules can be much larger (up to 10^{-5} cm for polymers, proteins, and viruses).

Real crystals are finite, and the effects of the surfaces can be detected in some cases. Real crystals also have some unfilled lattice sites (vacancies) and atoms in some sites that are not part of the ideal lattice (interstitials). The number of these point defects depends on the temperature and on the growth conditions or the postgrowth conditions in which the crystal comes to equilibrium with its ambient. At low temperatures, the time taken to attain equilibrium can be very long (e.g., years at room temperature). In addition to these thermodynamically predictable point defects, most crystals contain impurity atoms and molecules as well as line defects (dislocations). Except for elemental silicon and germanium, multicomponent bulk crystals (compound semiconductors, oxides, fluorides, etc.) contain dislocations that are mostly inimical to various types of devices due to their surrounding stress field

and electrical activity. Additionally, they act as getters for excess and impurity atoms, and this often leads to precipitations (three-dimensional defects). In most cases, characteristic dislocation arrays, such as cellular and grain structures, are formed, which constitute low-angle grain boundaries. Samples containing low-angle boundaries are strictly polycrystalline, but for many purposes, boundaries involving angular changes of about < 18 are acceptable. However, give the increasing demand for nearly perfect highly integrated thin-film devices with high parameter reproducibility, the presence of a network of subgrains, tilted even by lower angles (down to 20 arcsec), is now one of the most serious defects in substrate compound crystals that can significantly impair epitaxial growth and cause scattering of electronic device parameters. Hence, key targets of the crystal grower are the avoidance of subgrain structures and the achievement of homogeneous distribution of the minimum possible number of dislocations. The other two-dimensional sheet defect is a twin plane involving a rotation or reflection of the lattice structure. Samples containing twin planes are not single crystals in the sense used here, and such samples are unacceptable for many applications.

The existence of long-range order (or the absence of short-range disorder) gives crystals their valuable properties, such as the absence of scattering for long-wavelength photons and particles (e.g., the intrinsic or extrinsic carriers in semiconductors). Here, long means large compared to the interatomic spacing. For photons (e.g., X-rays) and particles (e.g., neutrons and electrons) with wavelengths comparable to the interatomic spacings, systematic interference effects (loosely called diffraction) occur if the wavelength **l** and angle u to the atomic planes fulfill the Bragg condition

$$n\mathbf{l} \frac{1}{4} 2d\sin u \tag{1}$$

where *n* is an integer. This property leads to many uses in scientific instruments.

The existence of long-range order which differs with direction leads to anisotropy of crystal properties. Anisotropic properties are useful, for example, in optical polarizers. Even cubic crystals exhibit some anisotropic properties because they are not completely symmetrical (some have no center of symmetry). The absence of a center of symmetry can lead to useful pyroelectric properties (i.e., the appearance of electric charge on some surfaces of crystals that have been subjected to a change in temperature) or piezoelectric effects (the appearance of charge on the surface of crystals subjected to mechanical strain).

Finally, the absence of short-range disorder can give crystals great mechanical strength: no internal sites exist for the nucleation or easy propagation of cracks.

Table 1 contains some examples of the range of applications and typical materials used in these applications. The list is not exhaustive, and interested readers should consult the appropriate

Table 1. Some uses of crystals

Property exploited	Device	Crystals used
Spatial repetition	X-ray prisms	lithium fluoride
	neutron collimators	metals
Absence of	turbine blades	metals
short-range disorder	gramophone styli	sapphire
(giving strength)	bearings	ruby

	tape heads	ferrites
	wire drawing dies	diamond
	abrasives	diamond, sapphire
Uniformity of (eliminating scatter electromagnetic waves)	lenses, prisms, and optical windows	alkali and alkaline earth halides
	lasers	yttrium aluminum garnet
	microwave filters	yttrium iron garnet
Uniformity <?cnv tableNSNL?> (eliminating scatter of charge carriers)	transistors, diodes, thyristors, and integrated circuits	silicon, gallium arsenide, gallium nitride, silcon carbide
Anisotropy (allowing exploitation of vector and tensor properties)	resonant filters, delay lines	quartz, lithium niobate, zinc oxide,
	Nicol prisms	fluorite
	ultrasonic transducers	Rochelle salt
	gramophone pickups	lithium sulfate
	laser frequency converter	potassium dihydrogenphoshate, barium borate

contributions in this encyclopedia and standard texts on optics, X-ray and particle diffraction, crystallography, solid-state physics, and the strength of materials. In many applications, crystals offer more than one advantage; in particular, the absence of scattering effects is often a significant advantage of single crystals that are used for some other primary reason.

1.3. Specification of Crystals

Like any other product, crystals should be produced to a specification, but this is not always easy: factors influencing device performance and yield are not always known, and changes in fabrication techniques may call for a material meeting a radically changed specification. Thus, from the producer's point of view, a user's specification ''suitable for the application'' may be variable and dependent on factors of which he has no knowledge. Similarly, a specification ''best available'' (implying as pure and as perfect as possible) may also be unsatisfactory: the user's processes might rely on some unspecified impurity or depend on the existence of some imperfections which absorb undesired impurities or modify properties (e.g., diffusion, wettability). The factors that must generally be specified are:

Dimensions and tolerances

Orientation and its accuracy

Gross perfection (low-angle boundaries, twins, inclusions–sizes and volume density)

Crystallographic perfection (dislocation density)

Composition (major component homogeneity)

Dopants (concentration, distribution)

Impurities (maximum concentration of undesired impurities, maximum concentration of all other impurities specified as a total)

In particular cases, other factors may have to be included, and the list will obviously be lengthened if the producer does any post-growth processing such as trimming to size, slicing, or etching. The specification should also include the nature and number of tests to be done. The problems of characterizing crystals are briefly discussed in Section 5.5 Characterization.

1.4. Commercial Aspects

Three types of organizations are engaged in growing crystals:

1. Organizations that specialize in crystal growth and supply crystals to other user organizations
2. Organizations that grow crystals in-house for their own use
3. Organizations that investigate crystal growth

From the worldwide data available, about 500 organizations can be identified that are interested in crystal growth; of these, perhaps 300 are commercial organizations of categories 1) and 2). Few organizations interested commercially in crystal growth employ more than 50 people who work on crystal growth. Academic teams tend to be small (rarely more than 10). Thus, about 15 000 people in industrial organizations are involved with crystal growth, as well as perhaps another 2000 in academic institutions.

The worldwide output of the industry is about 20 000 t of crystals per year. The major user of these crystals is the electronics industry, which consumes about 10 000 t of silicon (mostly grown by the Czochralski technique), 2500 t of quartz (grown hydrothermally), and 800 t of pentelides (pnictides), such as GaAs, InP,GaP, CdTe, or ZnTe grown by the Czochralski and vertical Bridgman techniques. The current market for ZrO_2 skull-melted crystals, over 98 % of which are fabricated into gemstones, amounts to about 1000 t. The engineering industry uses about 2000 t of slowly cooled, nearly single crystal alloys for highly stressed components and 100 t of nonmetallic crystals for bearings, dies, and tools. About 2000 t of low-quality metal crystals are used in transformer cores and components for electric motors. The optical industry uses about 400 t of assorted halides and some silicon or germanium for windows, prisms, and lenses; other crystals, such as ruby or yttrium aluminum garnet, for lasers; lithium niobate, and ammonium and potassium dihydrogen phosphates for various electro-optic devices. Crystals in common use in smaller amounts are triglycine sulfate (for pyro-electric devices); various chalcogenides, such as ZnS or CdTe, for optical components or $Cd_x Hg_{1-x} Te$ for infrared detectors; and lithium tantalate for optical and pyroelectric devices. Altogether, about 200 materials are available commercially as single crystals. Most are used at very low rates (< 1 t/a).

When methods are ranked by annual mass produced, the Czochralski technique is first (about 40 %); other melt growth methods (predominantly the Bridgman technique coming to the for even since the last decade as electronically controlled gradient freeze version) produce another 35 % (increasing), solid-state growth accounts for perhaps 12 %, the hydrothermal technique produces about 8 %, and

other solution growth techniques account for almost all the remaining output. Perhaps 1 % is grown from the vapor phase.

Melt growth usually has the highest volume growth rate. Quartz can only be produced hydrothermally. Solution growth techniques are usually inexpensive in terms of capital and labor costs. Vapor growth tends to be both slow and expensive. However, both high-temperature solutuion (flux) and vapor growth are increased applied for production of numerous modern semiconductors with extremely high melting points (over 2000 8C), such as SiC, GaN, AlN, being important materials for high-power microelectronics and blue-violett wave regions. For further discussion, see Section Selection and Optimization of Methods.

When methods are ranked by value, the order of importance is melt growth (about 50 %), solution growth including hydrothermal processes (25 %), vapor growth (15 %), and solid-state growth (10 %). However, this presentation is misleading because a significant fraction (about one-quarter) of the melt-grown crystals are used to provide substrates for the vapor and solution growth of epitaxial layers. The total value of thin layers and their substrates is about 25 % of the value of all the crystals grown.

1.5. Sources of Information

The primary literature (research papers) on crystal growth is extensive: about four papers are published every day on topics relevant to this article, the majority in three international journals (*Journal of Crystal Growth*, *Crystal Growth Design*, and *CrystalResearchTechnology*, formerly *Kristall und Technik*) and a limited number of conference proceedings. Chemical Abstracts offers *CA Selects Crystal Growth*; this service covers a rather wide field (e.g., industrial crystallization, geological and biological crystallization, as well as the growth of single crystals), allows most of the primary papers to be recognized, covers the patent literature, which is an important source of practical information, and serves as an aid in locating the secondary literature.

Nowadays the abstracts of most current publication and patent citations on crystal growth and epitaxy can be obtained from international databases (e.g., INSPEC with about 4000 journals, Chemical Abstract Service, CRYSTMET, GMELIN, for example) via on-line internet suppliers (e.g., FIZ Karlsruhe).

The secondary literature may be divided into two sections: small area reviews and monographs. Small area reviews are also concentrated; they appear as invited papers at conferences (often in special issues of the *Journal of Crystal Growth*) and in the review journals *Progress in Crystal Growth and Characterization* (Pergamon, Oxford) and *Materials Science & Engineering* (Elsevier). In the 1970s and 1980s numerous reviews were published in a limited number of book series, for example, the series *Crystals* (edited by M. C. Freyhardt) published by Springer (Berlin) or the North Holland (Amsterdam) series *Current Topics in Materials Science* (edited by E. Kaldis).

Fundamental and methodical aspects are reviewed in the *Proceedings of the International Summer Schools on Crystal Growth* (ISSCG) triennially organized by the International Organization of Crystal Growth (e.g., *Theoretical and Technological Aspects of Crystal Growth*, edited by R. Fornari and C. Paorici, Trans Tech Publications, 1998) and *Crystal Growth - from Fundamentals to Technology*, edited by G. Müller, J.-J. Metois and P. Rudolph, Elsevier, 2004). A special chapter on crystal growth

of materials treating fundamental and experimental aspects of production of nearly all important substances is included in the *Encyclopedia of Materials: Science and Technology* Elsevier, 2001.

The literature in monograph form is also extensive. There are texts [44,45] for amateurs or students not specializing in crystal growth. More serious students wanting a broad view should turn to [4,46-50]. Specialists have a wider selection: thus, on low-temperature solution growth, [26] still has much to offer; references [51-53] contain much useful material. The last [53] also covers melt growth, as do [54] and [55]; while these three discuss high-temperature solution growth, the standard text is [56]. For vapor growth, consult [57]. Most texts give some account of the theory of the subject, but [58] is the standard text. A number of highly specialized texts contain pertinent information; for example, [59] covers growth in gels (solution growth in the absence of convection), and the growth of polymers (growth controlled largely by the stereochemistry of the molecules) is discussed in [60].

Historical important papers are collected in the book *50 Years Progress in Crystal Growth*, Elsevier, 2004 edited by R.S. Feigelson. In *Bulk Crystal Growth of Electronic, Optical and Optoekectronic Materials*, John Wiley and Sons, 2005, edited by P. Capper, 17 authors summarize the state-of-art of single crystal production and characterization of semiconductors, sapphire, fluorides, scintillator materials, and quartz crystals. Technological aspects of growth and wafer preparation are reviewed in 29 chapters, written by numerous well-known specialists in *Crystal Growth Technology*, Wiley VCH, 2006 edited by H. Scheel and T. Fukuda. An extensive modern compendium comprising three volumes with a total of about 2500 pages was edited during the period of 1993–1994 by D. T. J. hurle (*Handbook of Crystal Growth*, North-Holland, Amsterdam). Seventy four authors contributed fifty-eight chapters to this almost complete compilation on fundamentals, bulk crystal growth, and epitaxy, which is undoubtedly the leading standard work on these fields at present and will be for some time to come.

Because it is now possible to describe crystal growth processes in a nearly quantitative manner, there is a need for numerical data on physical properties and phase diagrams. The texts just quoted suggest some sources and others are given in later sections. There are two relevant on-line data banks such as the *Electronic Materials Information Service* (IEE, Station House, Nightingale Road, Hitchin, Herts SG 5 IRJ, United Kingdom) or *EVITHERM Date Centre*, which give relevant physical property data and *MTDS* (National Physical Laboratory, Teddington, Middlesex TW 11 OLW, United Kingdom), which gives thermodynamic data; [61] lists a series of relevant off-line data centers. In 2005, the special book on compound semiconductor material data *Properties of Group-IV, III-V and II-VI Semiconductors* was published by John Wiley and Sons.

2. Thermodynamic Aspects

2.1. Free Energy and Driving Force of Crystallization

The precondition for crystallization of a stable solid phase from a metastable fluid (starting) phase is deviation from thermodynamic equilibrium. Figure 1 plots schematically the free energy versus temperature $G(T)$ of two contacting phases in the neighborhood of a first-order phase transition. Only at the equilibrium point are the Gibbs potentials G_s and G_f equal, but away from equilibrium the potentials are different. The difference ΔG denotes the driving force of crystallization or growth affinity as $\Delta G = G_f - G_s$.

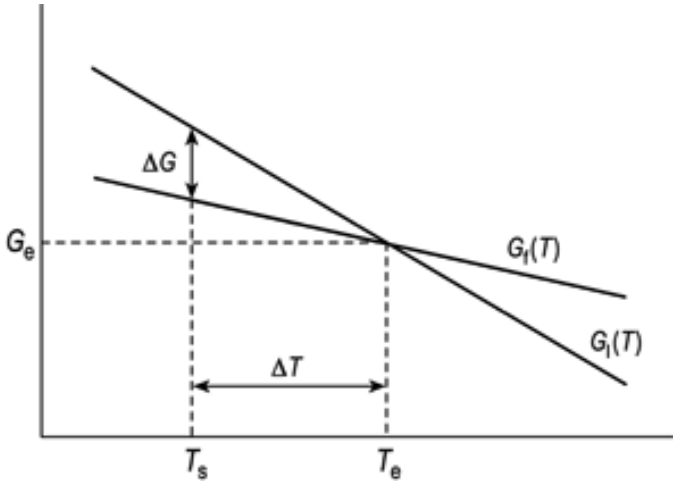

Figure 1. Dependence of free energy *G* of fluid (f) and solid (s) phases on the temperature *T* near the thermodynamical equilibrium (e) D*G* and D*T* denote the driving forces of crystallization and supercooling, respectively

Most crystal growth processes are carried out near equilibrium. Exceptions are vapor growth processes, in particular molecular beam epitaxy, and some techniques involving chemical reactions on the surface of the growing crystal. The driving force for crystallization is usually defined in terms of the free energy released by crystallization. This free energy change D*G* can be related to more easily measured system parameters for supercooled melts, supersaturated solutions, and supersaturated vapors:

1. *Supercooled Melt.* For a melt supercooled by D*T* (at a temperature T_e–D*T*),

$$DG \approx DH\, DT/T_e \tag{2}$$

where D*H* is the enthalpy released by crystallizing 1 mol of solid and T_e is the temperature at which the solid and liquid are in equilibrium, in this case the melting point. If D*T* is large or D*H* is small, D*H* in Equation (2) must be corrected to allow for the difference in specific heats of the solid and the liquid. Doing this introduces an additional term in DT^2 [53, Chap. 3]. Values of D*T* rarely exceed 10 K. Values of DH/T_e usually fall within a range of 10 to 100 J K^{-1} mol^{-1}, and values of D*T* are typically 1 K. Hence, D*G* is about 100 J/mol, and $DG < RT$.

For instance, a propagating (111) face of a dislocation-free silicon crystal requires a supercooling of about D*T* = 4 K [63] (maximal 7 K [62]). By inserting this value in Equation (1) together with the material parameters D*H* = 50 kJ mol^{-1} and melting point T_e = 1693 K, a driving force of crystallization at least of D*G* = 118 J mol^{-1} can be deduced.

2. For a *supersaturated solution*

$$DG \approx n\,RT \ln(1 + Dc/c_e) \approx n\,RT\, Dc/c_e \tag{3}$$

where *n* is the number of ions formed in the solution by one molecule of the solute, *R* is the gas constant (8.31441 J mol^{-1} K^{-1}), *T* is the temperature, and D*c* is the amount by which the solute concentration exceeds the equilibrium concentration c_e. The relative supersaturation

$$s \approx Dc/c_e \tag{4}$$

is often used. Typical values of s are less than 0.1. A driving force of crystallization of about 500 J/mol was found for perfect NaCl crystal growth from aqueous solution [48]. If D*H* is the enthalpy of solution, Equation (2) can also be used to describe growth from a solution cooled by

DT below its saturation temperature. Some degrees of supercooling were ascertained for the growth of quartz single crystals under hydrothermal conditions [48].

3. For a *supersaturated vapor*

$$\mathrm{D}G \approx RT \ln(1 + \mathrm{D}p/p_e) \approx RT\,\mathrm{D}p/p_e \tag{5}$$

where Dp is the amount by which the actual partial pressure of the material exceeds the equilibrium value p_e. If DH is the enthalpy of vaporization, Equation (2) can be used to express DG in terms of cooling the vapor from its equilibrium temperature. Typically $\mathrm{D}p/p_e < 0.1$ and DG is ca. 1 kJ/mol.

The values of T_e, c_e, and p_e are given by the phase diagram which describes equilibria involving pure, unstrained single crystals. To describe the growth of doped or strained crystals, terms involving elastic strain energy must be added [64]. Similarly, any departure from the phase diagram condition (e.g., the application of hydrostatic pressure, electric or magnetic fields) requires minor modifications of the expressions for DG. Such effects at most change growth rates by factors of three.

In the simplest possible free energy–spatial position model of a crystal–fluid interface (Fig. 2), an energy barrier G_I separates the crystal from the fluid. Therefore, the transfer rate from the fluid to the crystal should be proportional to $\exp(-G_I/RT)$, and the rate from crystal to fluid should be proportional to $\exp[-(G_I + \mathrm{D}G)/RT]$. Thus, the net rate of transfer to the crystal should depend on $\exp(G_I/RT) \cdot [1 - \exp(-\mathrm{D}G/RT)]$ which for $\mathrm{D}G \ll RT$ reduces to $\mathrm{D}G\exp(-G_I/RT)/RT$.

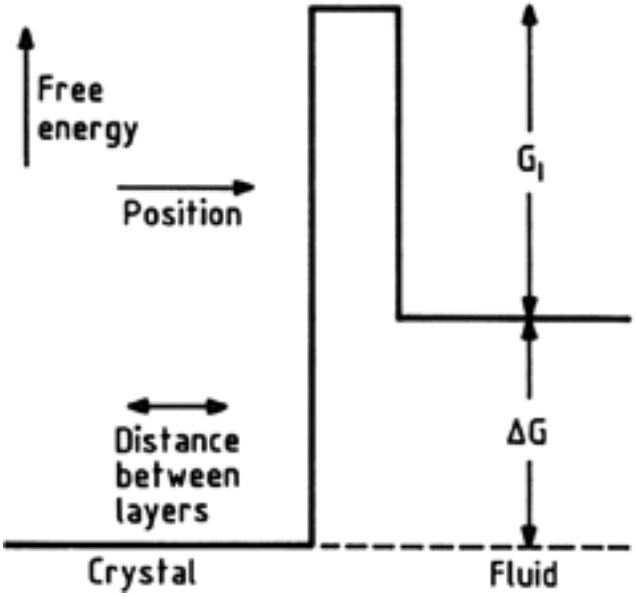

Figure 2. Free energy as a function of position for a simple model of crystal – fluid interface

The determination of the concrete value of G_I is somewhat problematical. Approximately it denotes the activation energy for volume diffusion in the fluid phase, that is, viscous flow in the melt (on the order of 5–50 kJ mol^{-1}[65]). At a crystal–solution interface, solvate shells form or disintegrate, and this requires higher activation energies (desolvation or dehydration energy), yielding G_I in aqueous solutions of 50–100 kJ mol^{-1}[48].

2.2. Phase Relations for Major Components

Because crystals are usually grown in near-equilibrium situations, the actual equlibrium states as described by the phase diagrams should serve as a useful guide to the conditions needed. However, drawings lack accuracy and, for exact work, analytical or tabulated numerical data are preferred. In a well-designed crystal growth system, temperatures can be established with errors of less than 1 K; pressures, between 1 and 5 %; and compositions, 0.1 %.

For introductions to the theory of phase diagrams from the point of view of crystal growth, see [58,66,67]. Reference [68] gives an excellent account of the determination of phase diagrams. Techniques have since been automated, but the basic problems are unchanged and several researcher's years of work are still required to determine a three-component phase diagram. For further information on the principles involved, see the standard texts [69-71]. A literature search is necessary to obtain the latest data on any particular system. A bibliography up to 1956 is given in [72]. Data for many binary systems can be found in [73-76]. Oxide systems are covered by [77-79]. Reference [80] gives data for glass-containing systems. For data on the solubilities of materials, see [81]. Numerical data for calculation can be obtained from [82,83], and [84], and from the data banks discussed in Section 1.5 Sources of Information. A journal (*Calphad*) is devoted to phase diagram calculation, and data on actual systems appear in many journals; in particular, diagrams relevant to crystal growth often appear in *Journal of Crystal Growth, Journal of Materials Science, Journal of Solid State Chemistry,* and *Journal of the Electrochemical Society*. The *Phase Diagram Handbook* with its updating service [85] provides contemporary data on binary diagrams.

Figures 3–6 show some typical diagrams; data for these are taken largely from the sources listed above or from [86], in which the phase diagrams of electronic materials are discussed. When phase data are vital, a literature search followed by a critical review of the data should be undertaken. Typical differences found thereby are 1 to 10 K for temperatures, 0.1 to 1 % for compositions, and 5 to 15 % for pressures. Selecting ''best available'' values is not easy: when many data are available, median values are probably the best choice, and this has been done in Figure 3–6.

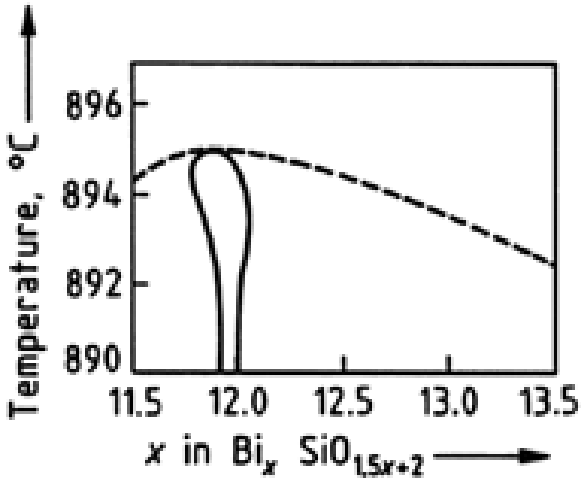

Figure 3. Phase diagram near the maximum melting point of Bi_x $SiO_{1.5x+2}$ grown in air

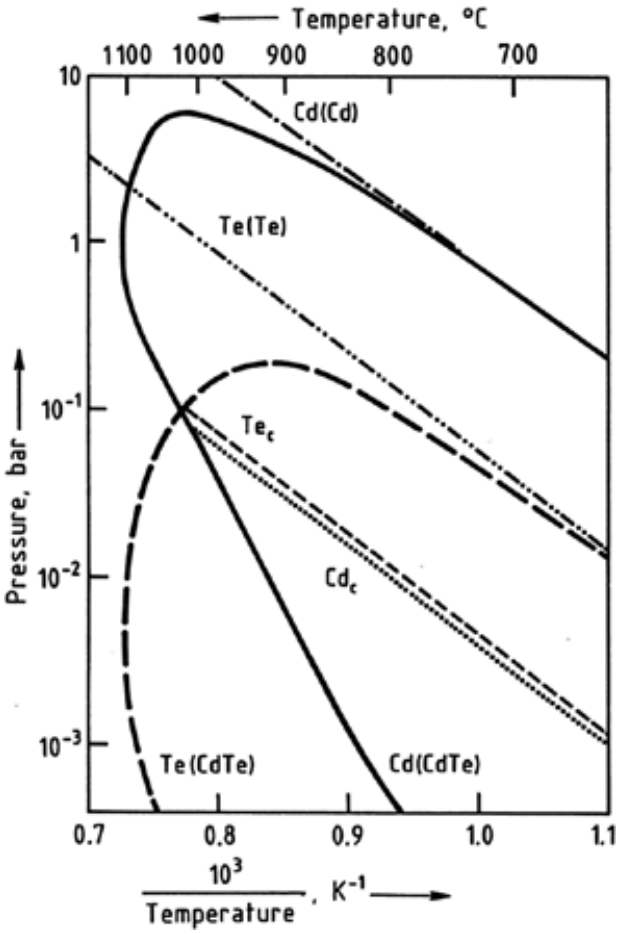

Figure 4. Pressures in the Cd – Te system near the compound CdTe

The convention X (Y), e.g., Te (CdTe), is used to indicate the partial pressure of material X over material Y. The symbols Te_c and Cd_c refer to the partial pressure of Te and Cd for the congruently vaporizing solid

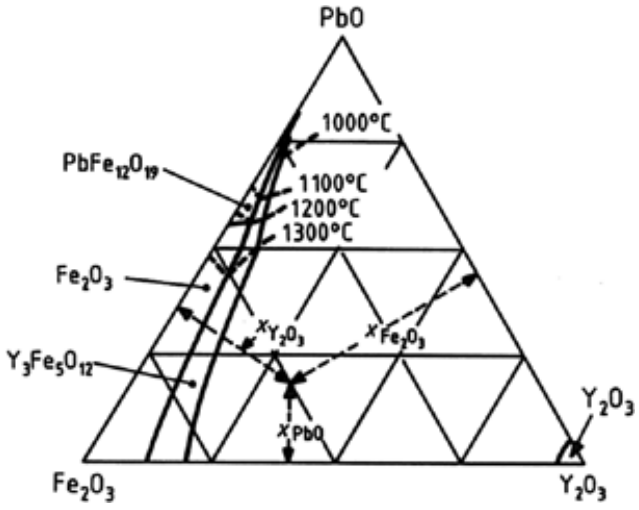

Figure 5. Liquid compositions in the Fe_2O_3–Y_2O_3–PbO system in equilibrium with the indicated solid phase

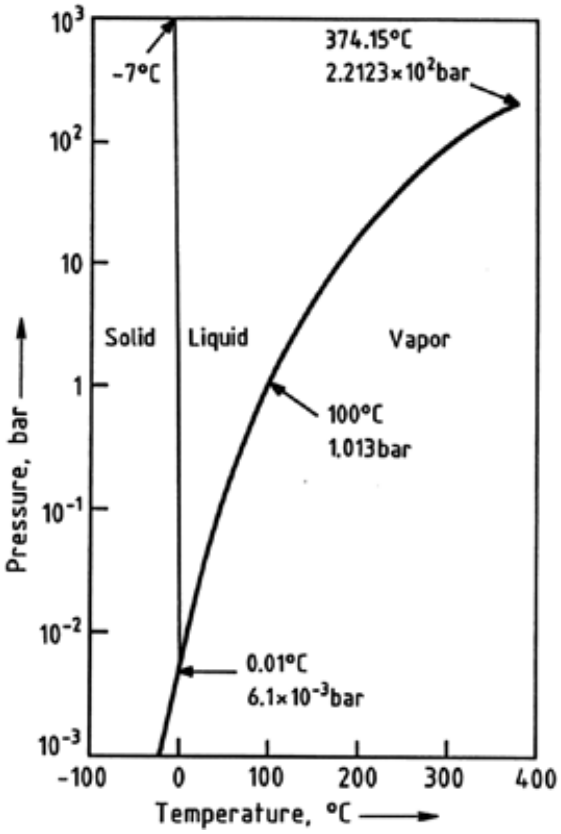

Figure 6. Pressure–temperature diagram for water

Figure 3 shows that part of the phase diagram of the system SiO_2–Bi_2O_3 in air, which is of interest for the growth of the material loosely described as $Bi_{12}SiO_{20}$. The solid line gives the composition of the solid, and the broken line gives the composition of the liquid. At any temperature, the liquid represented by a point on the broken curve is in equilibrium with the solid represented by a point on the part of the solid line nearest to it at the same temperature. The diagram illustrates the wide range of compositions that exist for compounds usually assumed to have a constant composition.

When the growth takes place in pure oxygen, the curves are shifted to the left and the maximum melting point occurs at x = 11.6. In argon + 0.5 % oxygen, the curves are shifted to the right and the maximum melting point is at x = 12.0.

The formula can differ quite significantly from the idealized value, and at any temperature below the maximum melting point, only two solid compositions can be in equilibrium with a melt.

Figure 4 gives data about vapor pressures of interest in the growth of CdTe. When this formula is written in the form $CdTe_y$, the maximum deviation y lies at 850 8C between about $1 - (1 \times 10^{-4})$ and $1 + (3 \times 10^{-4})$, with a value of $1 + (1.5 \times 10^{-5})$ at the maximum melting point (1092 8C) [87,88]. Large changes in partial pressures are seen to result from these small changes in composition. The dotted lines represent roughly the partial pressures in equilibrium with the solid which evaporates to give a vapor with the same composition as the solid (called the congruently subliming solid). The distance between the lines has been exaggerated by a factor of about 10^4 to emphasize that they are not equal.

At any temperature, the product $p_{Cd}\, p_{Te}^{1=2}$ is a constant. When this condition is observed by annealing at appropriate partial pressures, any composition between the extremes at that temperature can be obtained, but again, only the extreme values can be in equilibrium with a melt.

Figure 5 shows liquid compositions in the system Fe_2O_3–Y_2O_3–PbO which are in equilibrium with the solids indicated in the regions separated by bold lines, the so-called primary crystallization field. The arrows indicate how the molar fractions Fe_2O_3, Y_2O_3, and PbO are represented. For the point shown, the values are 0.50, 0.32, and 0.18, respectively. The broken lines are isotherms. The diagram indicates that, for example, if a liquid containing 50 mol % Fe_2O_3 and 7 mol % Y_2O_3 is cooled from about 1300 8C, the garnet phase should be precipitated. The crystalization field of $Y_3Fe_5O_{12}$ (YIG) is enlarged by the addition of B_2O_3 and PbF_2 to the flux discussed above [89].

Figure 6 shows the phase diagram of water, which is important for hydrothermal growth (Section 7.6 Hydrothermal Growth). Many other diagrams are of interest to crystal growers; for example, plots of solubility against temperature, which over small ranges can usually be represented as a straight line when the logarithm of solubility is plotted against reciprocal absolute temperature.

2.3. Phase Relations for Minor Components

Usually, the crystal being grown, even if it is a compound, is regarded as contributing one component in a phase diagram and the solute another. Thus, in growing a doped crystal from the melt, the system can be considered a binary one. Similarly in solution growth, three components — the solvent, the crystallizing material, and the solute — are being considered. Because only dilute solid solutions are under consideration, to a first approximation, effects resulting from the concentration of the solute (dopant, impurity) can be neglected, and in equilibrium, is

$$x_c \text{ ¼ } x_N \exp \frac{-Dm}{kT} \tag{6}$$

where k is the Boltzmann constant, x_c is the atom fraction of the solute in the crystal, and x_N is the concentration in the nutrient phase. The parameter Dm is the chemical potential difference between a solute atom in the crystal and one in the nutrient phase. This difference is almost always positive: it is more difficult to fit a foreign atom into a crystal than into the nutrient (which is usually a fluid). Thus, the segregation coefficient of a solute

$$k_0 \text{ ¼ } x_c = x_N \tag{7}$$

is usually less than unity. In the general case, $k_0 < 0.1$, but there are many exceptions. It is often possible to use m per mole and to replace k in Equation (6 by R (the gas constant).

It is possible to derive Equation (6) rigorously and to show in an ideal case of melt growth that

$$Dm \text{ ¼ } DH_2 \eth 1 - T = T_2 \text{Þ} - DH_1 \eth 1 - T = T_1 \text{Þ} \tag{8}$$

where DH_2 is the latent heat of fusion of the crystal which melts at T_2 and DH_1 is the latent heat of fusion of the solute which melts at T_1. However, few cases are ideal and it is usually necessary to add extra terms to Dm which imply the attractive or repulsive forces between the crystal and the solvent atoms, that is, the activities in the solid and fluid phases. For a discussion of these, see [48,53,58,70,90].

2.4. Interfacial Effects

The surface of a crystal is a gross discontinuity and has a free energy associated with it. The value of this free energy depends on the orientation of the face and the other phase in contact. In surface studies, this phase is usually a vacuum; in the present case, the other phase is often a liquid; for a

discussion of crystal–liquid interfaces, see [86]. As a first approximation, the surface free energy is

$$g_{SP} \approx \delta 1 - w/u \Delta H_{SP} N_A^{-1/3} \quad (9)$$

where u is the number of nearest neighbors for an atom inside the crystal and w is the number of nearest neighbors in the crystal for an atom on the surface ($w < u$). N_A is the Avogadro number and ΔH_{SP} is the energy required to create 1 mol of crystal from the adjacent phase (i.e., the enthalpy of fusion, solution, or vaporization). A plot of g_{SP} against face orientation gives minima as shown in Figure 7. The cusp-shaped minima give rise to atomically flat (singular) faces. Faces corresponding to less sharp minima may appear to be flat but are not flat on an atomic scale. Typical minimum values of g_{SP} at crystal–melt and crystal–vapor interfaces are in the rangs 0.1–1.0 and 1.0–10 J/m^2, respectively. In solutions g_{SP} is somewhat modified by absorption effects of the solvent atoms or molecules at the growing interface and descreases or increases if the solvent is surface active or passive, respectively [91]. Faces that are not singular are atomically rough. The equilibrium shape of a crystal is bounded by the set of singular faces. Real crystals may show nonsingular faces, particularly those corresponding to nonabrupt minima. In the case of small desorientation (some degree) from the singular plane, stepped faces do appear. They consist of lined up singular terraces with equidistant steps of atomic dimensions. Substrates with such surface morphology are of advantages for epitaxial growth in order to guarantee the continuous layer-by-layer growth mode [50].

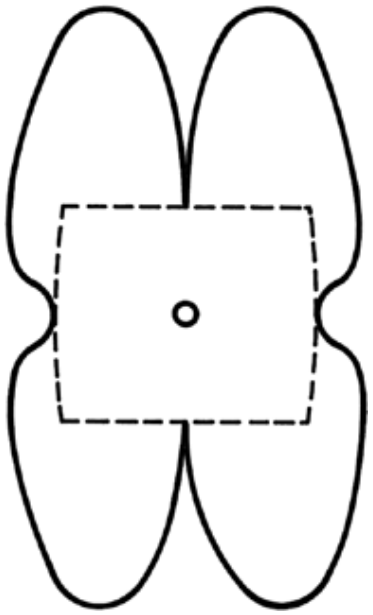

Figure 7. Polar diagram (full line) showing the variation of surface free energy with orientation The broken line gives the shape of the cross section of the crystal

In general, the state of the surface plays an eminent role in advanced epitaxial processes, especially of superthin films and alternating multilayer structures. First the reconstruction of the substrate crystal surface, which causes a reduction in the free surface energy, may influence the nucleation and growth modes of the layer to be grown onto it [90]. Further, very thin films possess de facto the surface features as a whole. Strained structures and atomic ordering effects may appear within few monolayers of multicomponent materials on a misfitting substrate, modifying markedly their physical properties relative to these of the bulk state [92].

2.5. Shortcomings of the Thermodynamic Approach

Equilibrium thermodynamics cannot describe processes involving heat and mass transport. Modeling by use of nonequilibrium thermodynamics (e.g., employing a maximum entropy principle) is possible but difficult. The usual approach is to model the kinetics and transport processes separately and then to combine the results to give a complete description. This approach is adopted here.

3. Growth Kinetics

3.1. Atomic Structure of Growing Interfaces

The central question to be solved by using the kinetic approach is the mechanism by which the fluid atoms enter the crystal interface, i.e., growth mode and velocity on the atomic scale. This first requires the determination of the atomic structure (morphology) of the faces to be grown. At $T = 0$ all faces would to be atomically smooth because all atoms are at the same level. At $T > 0$, however, some atoms can leave the uppermost atomic plane by thermal oscillation, leaving behind vacancies and unsaturated lateral bonds and giving rise to a degree of roughness. Such faces can grow nearly without strain by the so-called normal growth mode because most approaching atoms from the fluid phase can be docked in available vacancies (Section 3.2 Rough Face). With increasing bond strength of a crystalline material, indicated by the enthalpy of crystallization, the less increasing the temperature is able to promote roughening. Perfect faces of such materials (ionic and some covalent crystals), show a marked resistance to growth, which can only be overcame by activating mechanisms such as nucleus generation (Section 3.3 Perfect Singular Faces).

The criterion for transition between a smooth and a rough surface α[93] has the form

$$\alpha = \Delta H \cdot w/RTu \tag{10}$$

where ΔH is the enthalpy of crystallization, w is the number of nearest neighbors of an atom on the face, u is the number of nearest neighbors of an atom in the crystal, R is the gas constant, and T is the absolute temperature. $\Delta H/T$ is the entropy of crystallization: $\Delta H/RT$ for melt growth is often roughly a constant for a given class of materials, e.g., about 1 for most metals. If $\alpha < 2$ the face is rough. If $\alpha > 2$ the face will be smooth like those of oxide crystals with large ΔH, for example. Note that α varies with the orientation of the face. This is especially important for crystals for which $\Delta H/RT \approx 2$, like most semiconductors. In such cases, the w/u ratio in Equation (10) decides whether the given interface tends to be rough or smooth. For instance, silicon crystals have both atomically rough and smooth areas at melt temperature; α becomes 2.6 and 1.7 for the {111} and {100} faces, respectively. Due to the smoothness of the {111} faces they require a higher driving force of crystallization (i.e., supercooling, see Section 2.1 Free Energy and Driving Force of Crystallization) than the rough {100} faces.

On growth from vapor most crystal orientations of silicon (and of most other materials) grow atomically smooth due to the much higher sublimation enthalpy ΔH (ca. 300 kJ/mol at 1000 8C), causing an α of 27. Growth from solution is also characterized by the presence of mostly smooth interfaces because of the markedly lower crystallization temperatures, i.e., low values of $\Delta H/RT$ (α is 15 for NaCl in aqueous solution at room temperature). The kinetic growth modes of such atomically smooth faces (Sections Perfect Singular Faces and Imperfect Singular Faces) differ from the normal mode of rough faces, discussed in Section Rough Faces.

Note that the above analysis is somewhat simplified and valid for thermodynamic equilibrium only because the roughness of the face is restricted to the single-layer solid–fluid model. Especially at higher temperatures, however, one has to allow for a smearing-out of the crystal face at an arbitrary depth [94]. A computer simulation shows that in such cases the transition criterion a_j is 3.2 instead of 2. Further, during the growth (i.e., deviation from thermodynamic equilibrium) the surface is exposed to a driving force (Section 2.1 Free Energy and Driving Force of Crystallization) and a term $-\Delta G/RT$ must be added to the a_j factor that decreases its value as a function of the degree of supercooling (supersaturation). In other words, higher values of ΔG can promote nucleation islands, transforming a former equilibrium smooth face into a roughened one [95].

3.2. Rough Faces

With reference to Figure 2, if a Boltzmann distribution of energies for particles (atoms, molecules) in both the crystal and the nutrient phases is assumed, the particle flows to and from the crystal can be evaluated. The fraction of particles in the nutrient that can cross the barrier into the crystal is given by $\exp[-(\Delta G + G_I)/RT]$ and the fraction in the reverse direction is $\exp[-G_I/RT]$. The actual fluxes are given by multiplying these fractions by a rate constant kT/h, where k is the Boltzmann constant and h the Planck constant $(k/h = 2.084 \times 10^{10}\,\mathrm{S^{-1}K^{-1}})$ and kT/h is an approximation to an atomic vibration frequency. If the spacing between layers is l, then the growth rate on a rough surface is given by

$$f_R = (kT/h)\exp(-G_1/RT)\cdot [1 - \exp(-\Delta G/RT)] \tag{11}$$

ΔG has been evaluated in Equations (2) to (5), and in general $\Delta G/RT$ is small. Thus, Equation (11) can be reduced to

$$f_R \approx \frac{l\,k\Delta G}{hR}\exp(-G_1/RT) \tag{12}$$

According to [96], the diffusion constant in the nutrient can be written as

$$D_S = l^2(k/h)\exp(-G_N/RT) \tag{13}$$

and the final form can be obtained as:

$$f_R \approx \frac{D_S\,\Delta G}{l\,RT}\exp[-(G_I - G_N)/RT] \tag{14}$$

Here, in general, D_S, G_I, or G_N are hardly known, but f_R is proportional to the supercooling $\Delta T/T$ or the supersaturation, either $\Delta c/c$ or $\Delta p/p$. Equation (14) applies only to systems near equilibrium. In systems remote from equilibrium (e.g., molecular beam growth systems), Equation (11) does not apply, and the incoming and outgoing fluxes must be evaluated in some other way (see, for example, Section 8.2 Molecular Beam Epitaxy). Many examples of growth following Equation (11) or (14) are known, but care must be exercised in claiming the validity of these demonstrations because an equation of similar form can be obtained by consideration of transport processes (see Section 4.4 Mass Flow of Major Components).

3.3. Perfect Singular Faces

In equilibrium, a perfect singular face is essentially atomically flat. Depositing an atom or molecule on such a face produces a large increase in free energy. However, a cluster of atoms or molecules can be stable on the face, but the probability of depositing a cluster is much lower than the probability of depositing one particle. Thus, the growth rate f_{PS} on a perfect singular face is expected to be smaller than f_R, the growth rate on a rough surface.

The size of a stable cluster may be modeled by a cluster in which every atom makes half the bonds it would if it were inside the crystal. For a crystal with a diamond lattice (e.g., germanium or silicon), the critical nucleus is 3 atoms on {111}, 2 atoms on {110}, and 1 atom on {100}. Thus {111} and {110} are singularfaces, whereas {100} and all other faces are rough. Hence, at any supercooling, growth rates on {100} greatly exceed those on {110} which, in turn, exceed those on {111}.

Neither consideration of bonding nor the use of a¸ allows calculation of growth rates. To do this, the critical free energy of a nucleus DG^*, must be calculated. As a nucleus grows, the free energy rises to DG^* and then decreases so that further growth is rapid. In macroscopic terms, the free energy associated with a cylindrical nucleus is

$$\mathrm{D}G_N = g_{CN}^2\, \mathrm{p}rh - \mathrm{D}G\, \mathrm{p}r^2h \tag{15}$$

where g_{CN} is the surface free energy per unit area, r is the radius of the nucleus, and h is its height. The first term is the increase in free energy due to the extra surface created by the nucleus. The second term is the decrease in free energy obtained by solidifying some of the nutrient phase. By differentiating Equation (15), the following is obtained:

$$\mathrm{D}G^{\omega} = \mathrm{p}h_{g_{CN}} \tag{16}$$

and the critical nucleus has a radius g_{CN}/DG. The rate of formation of critical nuclei [48,97], is proportional to $\exp(-\mathrm{D}G^{\omega}/RT)$ and to f_R.

Two limiting cases can be distinguished. The first occurs when the nuclei expand rapidly (see Eqs. 21 and 22), in which case

$$f_{PS} = h\,\mathrm{d}N/\mathrm{d}t \tag{17}$$

$$= A_2 \exp(-B_2/\mathrm{D}G) \tag{18}$$

where N is the number of nuclei per unit area, and A_2 and B_2 are constants. The second occurs when the nuclei expand slowly, in which case

$$f_{PS} = h\,\mathrm{p}\, f_R^{\,2} \left(\frac{\mathrm{d}N}{\mathrm{d}t}\right)^{1/3} \tag{19}$$

$$= A_3 (T\,\mathrm{D}G)^{2/3} \exp(-B_3/T\,\mathrm{D}G) \tag{20}$$

where A_3 and B_3 are constants. The conditions for rapid and slow lateral expansion of the nuclei depend on the size L of the face. Rapid expansion corresponds to

$$h\, f_R \quad L\, f_{PS} \tag{21}$$

and slow expansion corresponds to

$$h f_R \quad L f_{PS} \tag{22}$$

Intermediate cases ($h f_R \approx L f_{PS}$) are difficult to express in analytical form.

The use of macroscopic quantities is reasonable for large nuclei. However, for small nuclei (a few molecules), macroscopic quantities have no meaning. If there are n^* molecules in the critical nucleus, another approach can be used [98-101], to show that with rapid spread,

$$f \text{ ¼ } A_4 \, D G^{1 \text{ þ } n^{*}} \tag{23}$$

and with slow spread,

$$f \text{ ¼ } A_5 \, D G^{1 \text{ þ } n^{*}=3} \tag{24}$$

where A_4 and A_5 are constants.

As can be seen from Equations (18)–(24), the nucleation-related growth rate at atomically smooth faces depends exponentially on the driving force of crystallization DG. Thus, so-called exponential growth modes occur.

Examples of all four relations have been discussed; e.g., see [53, Chap. 3].

3.4. Imperfect Singular Faces

Imperfect singular faces have permanent steps. However, creation of a permanent step is difficult. Consider an artificial vicinal face, i.e., one composed of shallow steps with wide singular treads and short rough risers. Figure 8 shows a sequence of interface positions for a system in which $f_R = 2 f_{PS}$. In real cases, f_R is expected to exceed f_{PS} by much larger factors. The argument about bonding suggests that atoms depositing in the corners (ledge sites) between the treads and the risers will more easily satisfy the condition to make half the possible bonds, but it is possible to consider lattices in which this condition is not obeyed. For example, if in a simple cubic lattice, the treads are (100) and the risers (010), an isolated atom in the ledge site (Fig. 9 A) will only make 2 of its possible 6 bonds so that, even at ledge sites, nuclei of 2 atoms will be needed. [This, of course, is less than the 4 atoms arranged in a square needed to form the stable nucleus on a perfect (100) plane.] However, if the treads are (100) and the risers are (011), an atom in the ledge site forms 3 bonds (Fig. 9 B) so that multiatom nuclei are not needed.

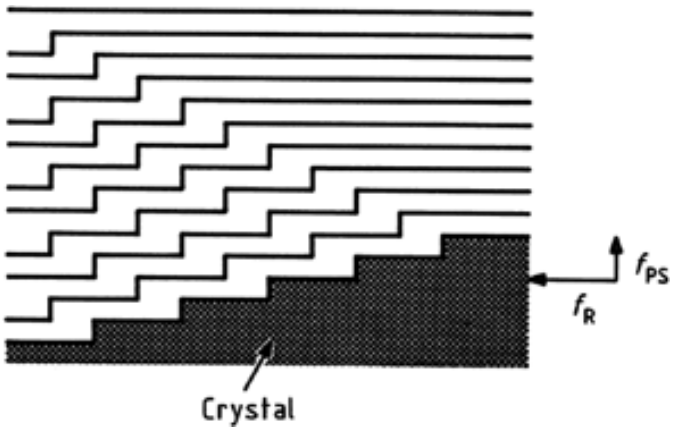

Figure 8. Sequence of interface shapes on a vicinal face
The crystal is at the bottom of the figure and the sequence starts from the bottom

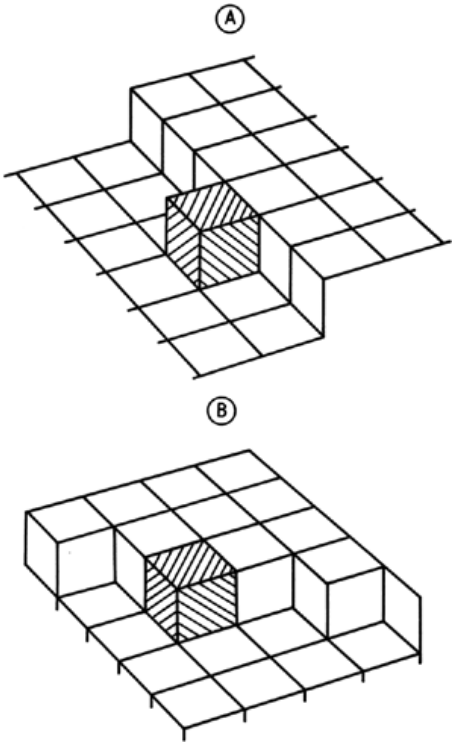

Figure 9. Straight ledge (A) and kinked ledge (B)

Two mechanisms can produce permanent steps. The first is the existence of *multiple twin planes* (Fig. 10). This is usually undesirable but gives a growth rate

$$f_T = a_{TW} f_R \quad (25)$$

where a_{TW} is the ratio of the twin spacing to the interatomic plane spacing normal to the twin planes.

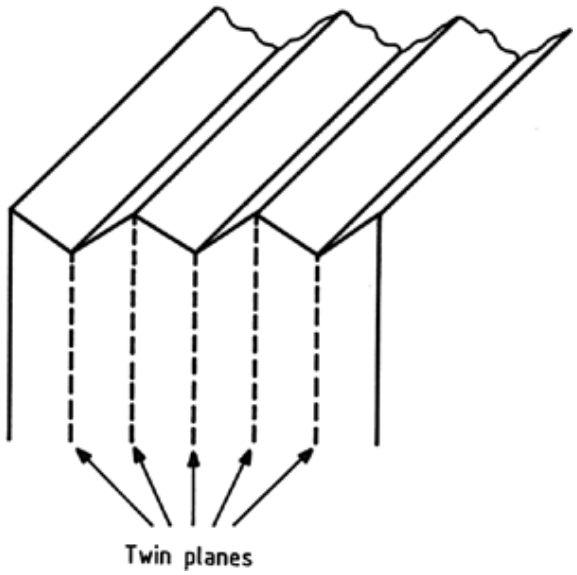

Figure 10. Twinned growth face

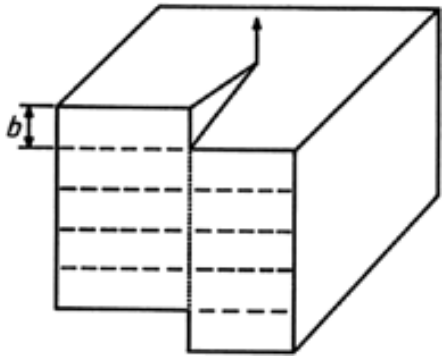

Figure 11. Face intersected by a screw dislocation

The other mechanism is the existence of *screw dislocations*. A screw dislocation (Fig. 11) is a defect produced by making a cut part way through a block of crystal and displacing the outside edge of the cut by a distance *b,* the Burgers vector of the dislocation. Addition of another layer of atoms does not destroy the step produced. In a growth situation, a spiral forms, which is centered on the dislocation axis shown by an arrow in Figure 11; viewed from above, the dislocated face exhibits a continuous ledge as shown in Figure 12. The form of this spiral depends on the symmetry of the crystal lattice. The easiest form to treat is a circular spiral with a radial spacing *S.* It can be shown [53] that

$$S \approx 2_{g_{CN}} V_M = D G \tag{26}$$

although there is dispute about the numerical factor. The fraction of sites which are ledge sites is

$$a_L \; ¼ \; I = 2p \, S \tag{27}$$

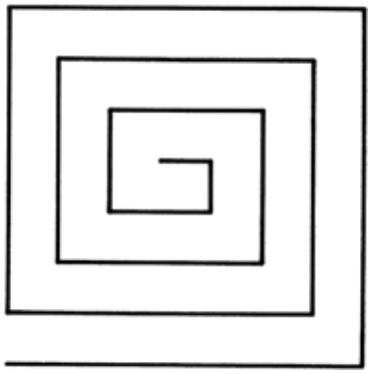

Figure 12. Projection of a face cut by a growth spiral

Hence, assuming that the growth rate is

$$f_D \; ¼ \; a_L \; f_R \tag{28}$$

yields

$$f_D \; ¼ \; I \; f_R \; D G = 4p \, g_{CN} \tag{29}$$

or

$$f_D \; ¼ \; A_6 D G^2 \tag{30}$$

where A_6 is a constant.

A more refined treatment [101] of the growth via surface diffusion yields

$$f_D = A_7 \Delta G^2 \tanh(B_7/\Delta G) \tag{31}$$

which reduces to the normal growth mode

$$f_D \sim \Delta G \text{ when } \Delta G \gg 1 \tag{32}$$

and to the square growth mode

$$f_D \sim \Delta G^2 \text{ when } \Delta G \ll 0 \tag{33}$$

When diffusion in the bulk of the nutrient is a significant limitation, CHERNOV shows that

$$f_D = \frac{A_7 \Delta G^2 \tanh(B_7/\Delta G)}{c_1 + c_2 \tanh(B_7/\Delta G)} \tag{34}$$

where c_1 and c_2 are constants for a given system [102]. Further refinements [103] give

$$f_D \sim \Delta G^n \text{ when } \Delta G \gg 1 \tag{35}$$

where $n = 3/2$ or 5/3. However, in the usually important range (ΔG small), the square law relation still holds.

4. Transport Effects

4.1. Transport Processes

Before the atoms (molecules) pass over from a position in the fluid medium, just beyond the crystal–fluid interface, to their place in the crystal face they must be transported in the fluid over macroscopic distances towards the interface. Such mass transport may proceed by diffusion, forced diffusion (electromigration), buoyancy-free convection, surface-tension-driven free convection, and forced convection (rotation, acceleration, vibration). Further, the heat carried by the species on their way to the crystal by conductive and convective transport must be dissipated in the solid phase by thermal conduction and radiation to maintain a stable propagating interface.

The transport can be fast or slow compared to the kinetics of attachment. Then the rate at which a crystal grows is limited by interfacial kinetics (Chap. 3 Growth Kinetics) or by macroscopic transport, respectively.

In many cases, the growth rate of a crystal can be written in the form

$$f = A_8 \Delta G^M \tag{36}$$

where A_8 is a temperature-dependent parameter and M can take many values: for example, $M = 2/3$, 1, 4/3, 3/2, 5/3, 2, 7/3, 8/3, 3 would be expected and are found [47,53]. Larger values of M might be expected, but more rigorous theory suggests that much larger values of M are improbable and a value of 4 seems to be the largest reported.

In Equation (36) the relevant value of ΔG is that at the growth face. Generally, the value of ΔG can be measured or estimated more easily at some point remote from the growth face. Thus, relating the interface value ΔG_I to some other value ΔG_B in the nutrient phase, presents a problem. The easiest way

to do this is by using boundary layer theory as discussed in Section . To illustrate the approach, it is better to consider a specific variable (i.e., temperature or concentration) rather than the free energy difference which the variable creates.

Figure 13 shows the type of concentration distribution to be expected in a solution growth system. Equation (36) can be rewritten in the form

$$f = A_9(c_I - c_E)^M \tag{37}$$

where A_9 is a constant and c_I and c_E are the solute concentrations at the growth face and in equilibrium with the crystal. Also

$$\sigma = c_B - \int_0^{\infty} \frac{dc}{dx}\,dx \tag{38}$$

which, from Figure 13, can be expressed in the form

$$c_I = c_B - D_S \left(\frac{dc}{dx}\right)_{x=0} \tag{39}$$

This relation defines d_S. For either a solid or a fluid nutrient phase, the flux of solute at $x=0$ is

$$J = D_S \left(\frac{dc}{dx}\right)_{x=0} \tag{40}$$

where D_S is the diffusion constant of the solute.

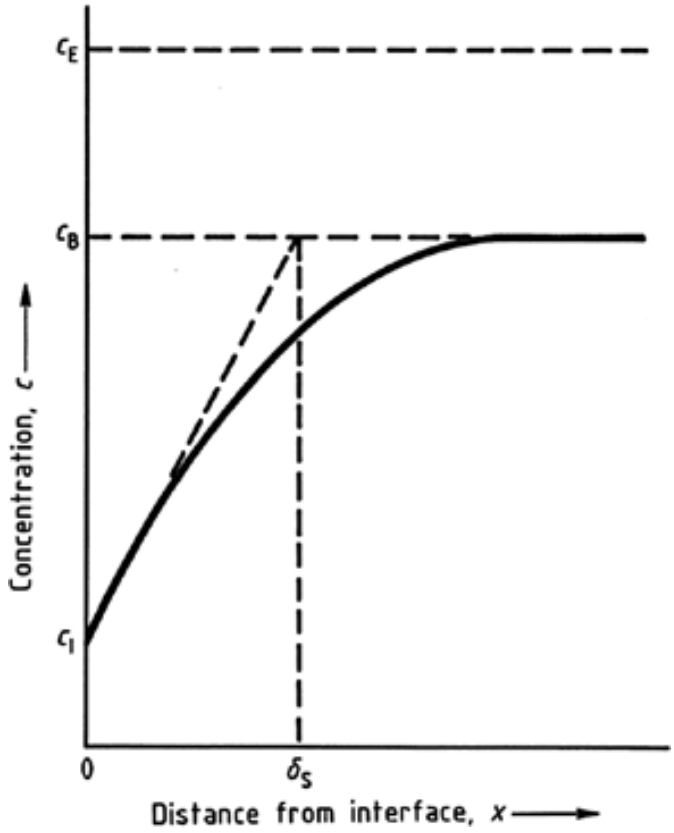

Figure 13. Concentration distribution near a growth face
The crystal is in the region $x<0$

If the nutrient is a solid or an unstirred fluid, it can be shown that d_S is an increasing function of time and so is not useful, but for a stirred, fluid nutrient, d_S is often a constant. The rate of growth of the crystal must be

$$f = V_m J \tag{41}$$

where V_m is the molar volume of the crystal. The rates of growth given by Equations (37) and (41) must be the same; hence,

$$\frac{f D_S}{V_m D} \left(\frac{f}{A_9} \right)^{1=M} = c_B - c_E \tag{42}$$

This general relation for growth from solution in a fluid depends only on the assumption that at the growth face, the flow of solute in the fluid is purely diffusive, which is reasonable because the fluid at this location does not move relative to the growth face.

4.2. Boundary Layers

In a stirred fluid, the distributions of velocity v, concentration c, and temperature T near a growth interface often take the form shown in Figure 14, and boundary layers with thicknesses of d_v, d_S, and d_T respectively, can be defined. In general, these layer thicknesses are different. Furthermore, not all authors use the thicknesses defined by Figure 14.

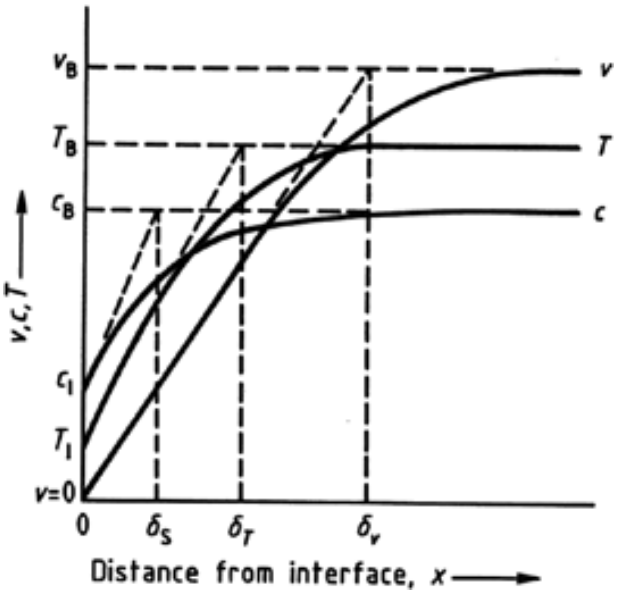

Figure 14. Distribution of temperature (T), concentration (c), and velocity (v) near a growth face, and definitions of d_S, d_T, d_v and interface values c_I, T_I, and v_I

The velocity boundary layer d_v is the most fundamental, and the other two thicknesses are related to this by

$$D_S = D_v (Sc)^{-n_1} \tag{43}$$

and

$$D_T = D_v (Pr)^{-n_2} \tag{44}$$

where n_1 and n_2 vary from 1/3 to 1 (see Fig. 15) and the dimensionless numbers *Sc* and *Pr* are defined in Table 2, which also defines some other parameters.

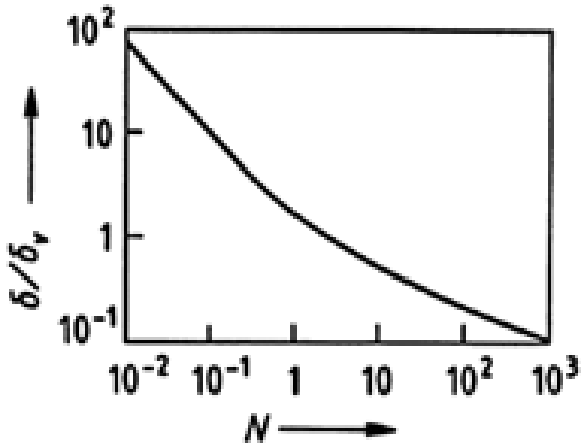

Figure 15. Variation of d/d_v with *N*, where $d = d_T$, when $N = Pr$, and $d = d_s$ when $N = Sc$
The data are for a rotating disk but should be approximately valid in most situations. For $N \leq 0.05$, $d/d_v = 0.701\,N^{-1}$. For $N \geq 200$, $d/d_v = 14;1.00\,N^{-1/3}$. For $N = 0.1$, 0.2, 0.5, 1, 2, 5, 10, 20, 50, and 100, values of d/d_v are 8.06, 4.77, 2.42, 1.56, 1.08, 0.725, 0.546, 0.415, 0.291, and 0.229, respectively. Adapted from .

Table 2. Some dimensionless numbers

Parameter	Symbol	Definition
Prandtl number	*Pr*	$C\eta/K$
Schmidt number	*Sc*	$\eta/\rho D_s$
Reynolds number	*Re*	$L\rho v/\eta$
Grashof number (for heat transfer)	*Gr*	$g L^3 \beta \Delta T \rho^2/\eta^2$
Grashof number (for mass transfer)	Gr^0	$g L^3 \alpha \Delta c \rho^2/\eta^2$
Rayleigh number (for heat transfer)	*Ra*	$C g \beta \Delta T L^3/K\eta$
Rayleigh number (for mass transfer)	Ra^0	$g \alpha \Delta c L^3/D\eta$

[a] *C* = specific heat; η = dynamic viscosity = νρ; *K* = thermal conductivity; D_s = diffusion constant; ρ = density; *g* = acceleration due to gravity; *L* = typical system dimension; β = (1/ρ) d*ρ*/d*T* = thermal expansivity; α = (1/ρ) dρ/d*c* = solute expansivity; *T* = temperature; *c* = concentration; *v* = velocity. Δ*T* and Δ*c* are changes of *T* and *c* along *L*.

Figure 14 has some practical consequences for the crystal grower. In liquid metals, with typically low Prandtl numbers ($N = Pr$ 1), the thermal boundary layer d_T extends farther into the fluid than the velocity transition region d_v because heat transport by conduction dominates over that by convection. However, in molten oxides and aqueous solutions with typically low thermal conductivity ($Pr > 1$), d_v is somewhat broader than d_T. Whereas in the last case the temperature distribution in the melt (i.e., temperature gradient near the interface) is markedly influenced by the mass flow mode, in metallic fluids the temperature field introduced by the heating furnace remains largely unaffected by convection. Compared to multicomponent melts (fluxes) with Schmidt numbers $N = Sc$ of 10 and

higher, this value for gases ranges between 0.1 and 1. Thus, in gases d_c and d_v extend about the same distance. In liquids, however, d_v exceeds d_c considerably, and therefore in front of the interface, the region of major concentration change, the flow velocity is reduced to relatively small values that barely influence the concentration profile.

Boundary layer theory cannot be applied indiscriminately. A boundary layer model can only be valid if

1. the Reynolds number

$$Re \text{ ¼ } Lv{=}n > 1 \tag{45}$$

   where L is a dimension of the growth face and v is the velocity of the face relative to the bulk of the fluid which has a kinematic viscosity n;
2. the dimension of the system normal to the growth face greatly exceeds d_v; here ''greatly'' implies a factor of about 5; and
3. the Reynolds number in Equation (45) is such that the flow does not become turbulent. The upper limiting Reynolds number for a rotating disk is about 2000 and for flow along a flat plate about 5000.

A variety of methods are used for stirring in crystal growth systems (Fig. 16) and under further developments (see, e.g., [104-106]). These and many other techniques can be described in terms of the following models.

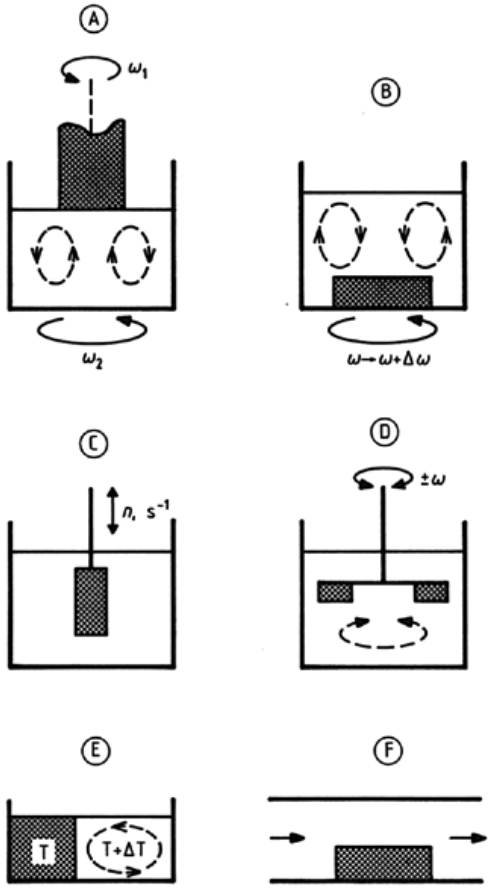

Figure 16. Methods of stirring used in crystal growth
A) Rotation of a pulled crystal; B) Accelerated crucible rotation technique (ACRT); C) Vibration of a plate; D) Reversed rotation; E) Natural convection; F) Forced convection (v = rotational frequency; n = linear frequency)

Rotating Disk or Cone. For an infinite disk rotating at a rate v relative to a semi-infinite fluid with the disk on the fluid surface

$$D_v \approx 1.613 \left(\frac{\nu}{\omega}\right)^{1/2} \nu^{1/2} \tag{46}$$

where n = h/r is the kinematic viscosity. The model fits reasonably well, but an error will generally be introduced by using Equation (46) for a finite disk. Figure 17 gives experimental data for pulled germanium crystals rotated at 90 rpm, which suggest 10 % radial variations in d_T for a finite crystal with an essentially flat face. For a cone with an included angle 2 u, d_v is given by Equation (46) if v is replaced by v sin u.

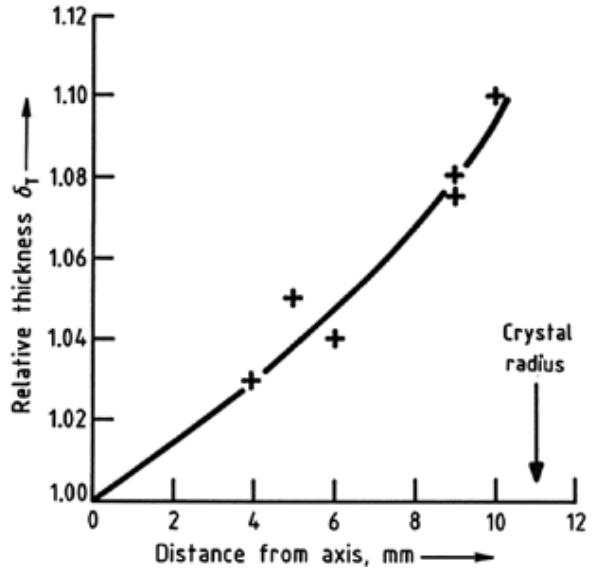

Figure 17. Thickness of a thermal boundary layer relative to the value on the rotation axis as a function of radial position

Wedge or Plate. Figure 18 gives d_v for a wedge with included angle 2 u in a flow with a relative velocity *v*. The value for a plate (*v* is the denominator)

$$D_v \approx 2.93 \left(\frac{\nu x}{v}\right)^{1/2} \tag{47}$$

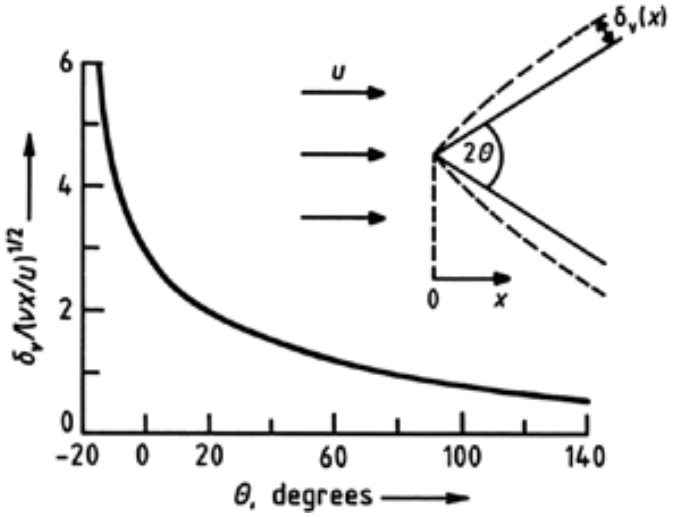

Figure 18. Value of d_v on a wedge
Note that the origin of *x* is the point on the wedge furthest to the left. For u ≤ 908, the origin is the apex. For u ≤ 0, the boundary layer is on the trailing face. For u ≥ 908, the boundary layer is that within a concave wedge; as u ! 1808, d_v tends to the depth of the re-entrant face. Note that *x* is measured parallel to the flow

is obtained by making u = 0. The layer thickness varies with position (x) except for the case u = 908; u > 908 corresponds to a concave apex, and u < 0 corresponds to a wedge facing downstream. For u < — 17.98, the flow breaks away from the surface (i.e., d_v ! 1).

Plate Vibrating in Its Plane. A plate vibrating in its plane at n Hz gives a boundary layer with

$$D_v \frac{1}{4} \delta 2n=n\text{Þ}^{1=2} \tag{48}$$

but produces appreciable stirring only in a layer with thickness about 2.2 $(n/n)^{1/2}$.

Convectively Driven Flow. Convection may occur when there is an adverse density gradient in the fluid phase. Here, adverse is taken to mean that the density increases upwards vertically or in any direction horizontally. This gradient might be caused by a temperature gradient giving the commonly occurring thermal convection. However, growth can also cause density gradients which may give rise to convection. Any horizontal gradient appears to cause convection, but a vertical gradient seems to cause convection only when the Rayleigh number (either *Ra* or *Ra*◊, Table 2) exceeds some critical value which is typically in the range 1000–2000 for systems with low aspect ration h/D with h the height and D the diameter of the melt column. In the case of increasing melt height, like in full-charged Czochralski crucibles or vertical Bridgman containers, the critical Rayleigh value may increase drastically of some orders of magnitude [58]. In fluids with horizontal temperature or solution gradients (e.g., horizontal-boat crystallization techniques), where the Grashof numbers are more representative, even a threshold-free natural convection can take place [58]. If the velocity v of the convective flow is known, d_v can be deduced from the data given for wedges or plates. Computer programs and experimental models are available for calculation and observation of v in most crystal growth arrangements (e.g., [108-112]). In principle v varies as L^n, where L is the system dimension in the direction of the gradient and $n = 0.5$.

Accelerated Crucible Rotation. Consider the system shown in Figure 16 B rotating at v radians per second. If a change Dv is imposed, radial and vertical flows are initiated and these give a boundary layer with a thickness

$$D_v \frac{1}{4} \delta n=Dv\text{Þ}^{1=2} \tag{49}$$

which is established in a time of order Dv^{-1} and which decays with a time constant of about

$$t \frac{1}{4} \text{⁞}n\delta 0{:}618=H^2 \text{ Þ } 14{:}7=A^2\text{Þ}]^{-1} \tag{50}$$

where H is the depth of the fluid and A is its radius. This method of stirring (the accelerated crucible rotation technique, ACRT [113]) is useful because stirring is induced without a mechanical connection to the inside of the crucible, but changes in the rotation rate at intervals of less than t are required. In a time t, the velocity distribution change only extends to a distance of approximately

$$h \frac{1}{4} t\,\delta Dv\ n\text{Þ}^{1=2} \tag{51}$$

from the growth face.

Nonsteady Magnetic Field. There are various possibilities of arrangement of time-dependent magnetic fields in melt growth systems–rotating, travelling (down- or upward), and alternating (pulsed).

Rotating field, causing a torque in the liquid $t_M(B^2, v_M)$, with magnetic induction B and rotating field frequency v_M, can be used for effective promotion of convective flows in electrically conducting melts [114,115]. Traveling and alternating fields can be applied for damping of the convection streams and control of the morphology of the propagating phase boundary [116-120]. Nonsteady fields are generated by using certain electromagnetic coil configurations surrounding the melt zone. Then the velocity boundary layer thickness d_v decreases according to

$$D_v \sim e^{-t_M ð B^2; v_M þ} \tag{51a}$$

This concept, well known from metal casting, has been revived for the melt growth of semiconductors, especially by zone melting, to homogenize the composition and to damp temperature fluctuations by means of well-controlled forced convection. Only very low values of B (a few mT) are necessary for an effective action [121]. For more information, see also [122-124].

4.3. Mass Flow of Major Components

In an idealized melt growth system, the composition of the solid with respect to major components is the same as the composition of the melt, and consideration of the mass flows of major components is rarely necessary: the systems can usually be described completely by considering only heat flow (see Section 4.5 Heat Flow). In the case of growth of compounds, minor differences usually exist between the compositions of the solid and the melt (i.e., growth near, but not exactly at the maximum melting composition); however, the defect or excess quantities of the components are small and can be treated as impurities by the methods discussed in Section 4.4 Mass Flow of Minor Components.

In growth by evaporative methods (e.g., molecular beam epitaxy), the fluxes of the major components can be calculated directly from the parameters of the source and its distance from the growth face (see Sections Sublimation and Evaporation Methods and Molecular Beam Epitaxy).

Strickly speaking, due to the mass balance at the growth interface, i.e., equality of the fluid influxes $j_f = r_f v_f$ and solid outfluxes $j_s = r_s v_s$ (r = mass density), the mass transport rate in the fluid perpenticular to the interface v_f is related to the incorporation rate in the solid v_s by the density ratio r_s/r_f as

$$v_f ¼ ð \%_s = \%_f v_s þ \tag{51b}$$

and may, therefore, differ if $r_s \neq r_f$ leading to a decelerating or accelerating mass flow of the major component in the fluid if r_s is less or greater than r_f, respectively. At the melt–solid transition this difference is small ($r_s \approx r_f$) and the above approximation is valid. In vapor growth systems, however, where $r_s/r_f \approx 10^3$, a pronounced fluid mass flow of the major component, the so-called advection or Stefan flow, can be induced [4,58].

In growth from a solid phase (Chap. 9 Solide Phase Growth Techniques), the two solid phases are usually assumed to have the same composition with respect to major components (and, indeed, often minor components).

4.4. Mass Flow of Minor Components

Figure 19 shows the distribution of a solute near the growth interface for the usual case ($k < 1$) and for $k > 1$, which is unusual but does occur. Two segregation coefficients can be defined:

1. the interface segregation coefficient (for definition of symbols, see Fig. 19)

$$k_I \text{ ¼ } c_S/c_I \tag{52}$$

which can sometimes be made equal to k_0 (the value deduced from the phase diagram) and

2. the effective segregation coefficient

$$k_{eff} \text{ ¼ } c_S/c_{BN} \tag{53}$$

As is shown in Section 2.1 Free Energy and Driving Force of Crystallization, a propagating interface requires a certain deviation from thermodynamic equilibrium. The incorporation of minor components is also controlled by atomic processes. To account for this, a kinetic segregation coefficient k_i is often introduced. Its derivation, however, is somewhat problematical because of the actual concentration c_I immediately at the interface is unknown (see Fig. 13). Different theoretical approaches to the formulation of k_i, especially in the case of atomically smooth faces, are presented in [4,48], for example. In general, for growth from a melt involving atomically rough interfaces and near-equilibrium conditions, k_i equals k_I, and the above equations are justified.

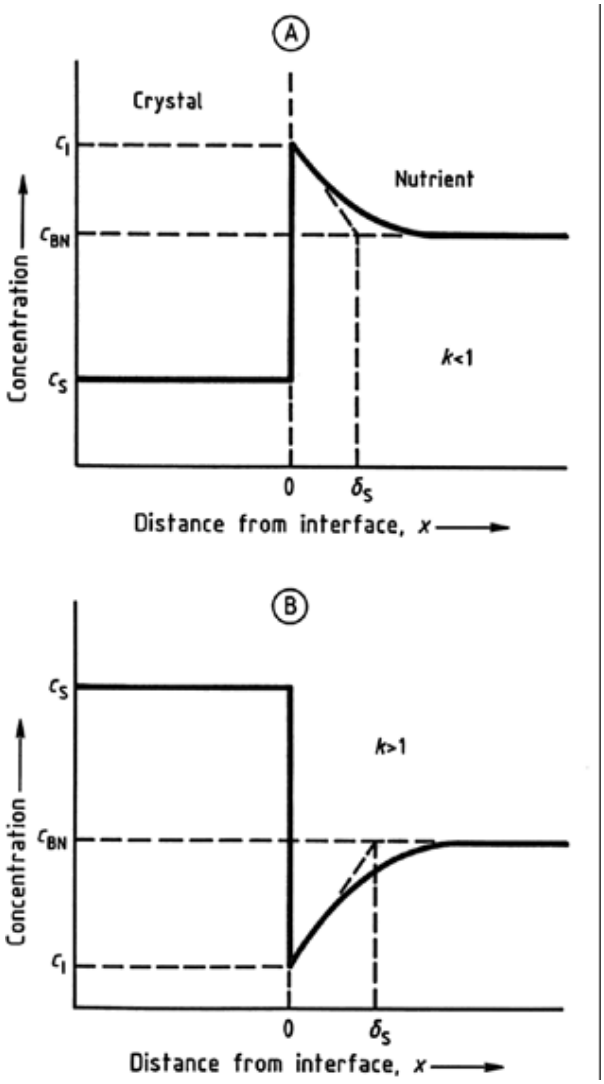

Figure 19. Concentrations of a minor component near a growth face for $k < 1$ (A) and $k > 1$ (B)

For a macroscopically flat growth interface, a one-dimensional equation

$$D_S \frac{\partial^2 c}{\partial x^2} + f \frac{\partial c}{\partial x} = \frac{\partial c}{\partial t} \tag{54}$$

can be solved with the boundary condition

$$D_S \left(\frac{\partial c}{\partial x}\right)_{x=0} = c_I (1 - k_I) f = D_S (c_I - c_{BN})/D_S \tag{55}$$

In a steady state, $\partial c/\partial t = 0$ and the solution is [33,34]

$$k_{eff} = \frac{k_I}{k_I + (1 - k_I)\exp(-f\, d_S/D_S)} \tag{56}$$

which, for small values of $f\, d_S/D_S$, reduces to

$$k_{eff} = \frac{k_I}{1 - f\, d\,(1 - k_I)/D_S} \tag{57}$$

These relations have been repeatedly verified and shown to be excellent approximations, provided that d_S is calculated by using Figure 15 rather than one of the limiting formulas and that there is no growth-induced flow. Thus, for example, Equation (54) applies for melt growth if the densities of the solid and liquid are identical. If this condition is not obeyed, then f must be replaced by a parameter $f^{\omega} = (1 + D)f$, where D is a constant for the particular system and f^* is the growth rate measured relative to fluid particles near the growth face (i.e., roughly at $x = d_S$).

It is permissible to assume that $\partial c/\partial t = 0$ if changes occur at rates that are slow compared to the time (roughly D_S^2/D_S) needed to modify the solute distribution in the boundary layer. This time is usually less than one second so that Equation (54) is generally valid and may be used to describe the effects of changing either the growth rate or the boundary layer thickness d_S. Such changes can obviously occur as a result of apparatus imperfections which can be mechanical (changes in rotation rates, etc.) or thermal (lack of perfection in temperature control). However, the most intractable problems are caused by thermal oscillations. These are time-dependent variations in the convection currents in the system, which occur in particular ranges of the Rayleigh numbers Ra and Ra'[58,110]. Because the Rayleigh numbers depend on L^3 (Table 2), large fluid volumes are more prone to thermal oscillations than small ones and the occurrence of thermal oscillations provides a major limitation on the size of crystal growth systems. The obvious methods of minimizing the problem are (1) to work with minimal density gradients (e.g., keep temperature gradients small), (2) to design the apparatus to have effectively small dimensions (e.g., add baffles, which can be porous), and (3) to maximize viscosity (for conductive fluids, this can be achieved by applying a magnetic field [94]). The critical values of Ra and Ra' are usually several times the value needed to initiate convection (say > 2500). For Ra or Ra' greater than this value, both the oscillation amplitude and its frequency increase with Ra or Ra'.

4.5. Heat Flow

Crystal growth is always accompanied by a latent heat (the enthalpy of crystallization DH_C). In most cases, DH_C is positive (i.e., heat is evolved), but in a few instances, heat is absorbed, for example, the growth of lithium sulfate from solution in water.

If the subscripts S and N are used to denote the crystal and the nutrient phases, then at any plane growth face in a steady state:

$$K_N \left(\frac{dT_N}{dx}\right)_{x=0} - \frac{\Delta H_C}{V_m} f = K_S \left(\frac{dT_S}{dx}\right)_{x=0} \tag{58}$$

where K is the thermal conductivity at the temperature T, V_m is the molar volume, f is the growth rate, and x is a coordinate axis normal to the face with $x = 0$ at the face. The term dT_s/dx denotes the axial temperature gradient in the crystal near to the interface. Numerous efforts have been directed at its exact determination in growth experiments in the past. For instance, it was shown analytically, that in cylindrical crystals with high emissivity e (metals, semiconductors) pulled from melts (Section Crystal Pulling) at high temperatures (> 1000 8C), the dissipation of the heat is dominated by radiation from the crystal surface, and dT_s/dx equals in good approximation $(\varepsilon\sigma_P T_e^5 a^{-1})^{1/2}$, where σ_P is Planck's constant, T_e the melt temperature, and a the crystal radius. Computer calculations, including enthalpy of crystallization, thermal conductivity, convection in the fluid phase, and radiation processes, can provide almost realistic knowledge on the course of steady and nonsteady temperature fields in growing crystals ([109,110], for example). Nowadays, even convective processes such as turbulences in the gas phase within the growth chamber are being included in the models [125].

If the nutrient is a stirred fluid, the first term is $K_N(T_{BN} - T_I)/\Delta T$ (see Fig. 14). In melt growth, if T_{BN} varies by ΔT at a rate which is slow compared with the response times of the boundary layer $(\Delta T^2/\kappa_N)$ and the crystal (a^2/κ_S), then the growth rate changes by

$$\Delta f = (K_N V_m/\Delta H_C)(\Delta T/\Delta T) \tag{59}$$

where κ is the thermal diffusivity $(K/C\rho)$ and a is the radius of the crystal. The change ΔT can be caused by a malfunction of the control system or by thermal oscillations. To evaluate the effect of ΔT on the concentration of a solute, $\partial k_{eff}/\partial f$ is calculated from Equation (54) and multiplied by Δf. In solution growth or other methods, the same ideas are used, but the dependence of growth rate on the interface temperature is a complicating factor. (In melt growth, the interface temperature can be regarded as a constant. This is not the case in any other method of growth.)

Dislocations. Uniform heat flow in a growing crystal has no significant effect. A nonuniform flow promotes the dislocation multiplication due to thermomechanical stress such as edge dislocations (Fig. 20). Consider a rod-shaped crystal growing in the z direction with a plane growth face at $z = 0$ and a radius a. The temperature distribution is given by

$$\frac{\partial T}{\partial t} + f\frac{\partial T}{\partial z} - \kappa\nabla^2 T = 0 \tag{60}$$

where f is the growth rate and κ is the thermal diffusivity. It is assumed that the growth face is the isotherm $T = T_I$ and that heat is lost from the curved surface at a rate $h(T - T_0)$, where h is the heat transfer coefficient. Then, provided the crystal is fairly long (say 6 a, although the solution for shorter crystals is known):

$$T - T_0 \approx \frac{(T_I - T_0)(1 - hr^2/2a)}{(1 - ha/2)} \exp\left[-\left(\frac{2h}{a}\right)^{1/2} z\right] \tag{61}$$

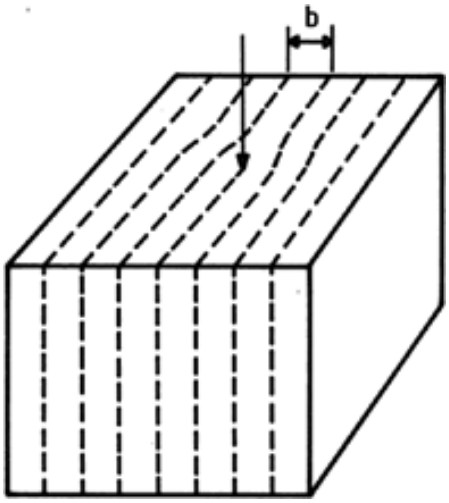

Figure 20. An edge dislocation (arrow)
The broken lines are the intersections of atomic planes with the faces of the crystal. The dislocation axis shown by the arrow is at right angles to the Burger's vector *b,* which, in this example, is one interplanar spacing

and

$$\frac{@T}{@r} \approx -\frac{\delta T_1 - T_0 \flat}{\delta 1 - h\,a{=}2\flat\, a} \exp\left(-\frac{2h}{a}\right)^{1=2} z \tag{62}$$

When circles of constant *r* are considered, it can be seen that this radial gradient will give rise to hoop stresses and if the material is plastic, it will at some magnitude of hoop stress, deform to give dislocations. (If the material is brittle, it will crack at a critical hoop stress.) If t_C is the critical shear stress for plastic deformation and *G* is the shear modulus, then the dislocation density is

$$N_d = \frac{a}{b}\frac{@T}{@r} - \frac{p_C}{G\,b a} \tag{63}$$

where a is the coefficient of thermal expansion. For

$$\frac{@T}{@r} < \frac{t_C}{G\,a\,a} \tag{64}$$

dislocation-free growth is possible. Typically $t_C/G \approx 10^{-3}$ and $a \approx 10^{-5}\ K^{-1}$ so that if *a* is measured in centimeters, the critical value of $@T/@r \approx 100/a$ K/cm.

Also the axial temperature distribution in a crystal may create similar magnitudes of stress to the curvature of the isotherms in the radial direction. It was demonstrated by the thermoelastic theory of dislocation generation [126] that nonlinearities of temperature gradients (second derivations) are the sources of stress. Due to the extremely extensive numerical calculations the following relation is helpful in estimating the stress s in the region behind the growth interface

$$s \approx a\,E\,L^2 @^2 T{=}@z^2 \tag{64a}$$

where *E* is the elastic modulus and *L* the characteristic axial length, which is on the order of 20 % of the crystal diameter. Conclusions can then be made about the dislocation density by comparing s and t_c; no dislocations are generated if $s < t_c$. In semiconductors t_c is in the region of 0.7 (GaAs) to 9 MPa (Si), hence, under similar thermal conditions, dislocation-flawed GaAs and dislocation-free Si crystals are grown. Two-dimensional maps of computer-simulated temperature and stress fields in the growing crystal are now routinely plotted [109].

The local dislocation density can be estimated theoretically from the constitutive law linking the plastic shear rate and dislocation density with the applied stress in the course of the cooling-down procedure of the crystal

$$d\varepsilon/dt = \rho b V_o (\tau_{app} - D\sqrt{\rho})^m \cdot \exp\left(-\frac{Q}{kT}\right)$$

where r is the density of moving dislocations, b the Burgers vector, V_o a pre-exponential factor, m is a material constant, Q the Peierls potential, D a parameter relating r and t, and τ_{app} is the applied stress. Details of this approach can be found in the profound review [127].

Today, the global numeric modeling of the non-stationary elastic stress and related dislocation development in growing crystals is used by implying the history of the thermal field in the furnace and crystal as well as the convection in the melt and vapour phase [128].

Thermal stresses are not the only source of dislocations; in particular, dislocations in the seed crystal usually propagate into the growing crystal and can nucleate at inclusions in the crystal. Further details and an approach to the dynamic dislocation theory, which considers interactions between dislocations already existing in the crystal during the cooling down process, are given in [127].

4.6. Interface Stability

In Chapter 3 Growth Kinetics, the growth rate f was shown to be an increasing function of DG. Thus, if DG increases away from a growth face (as, for example, is always the case in solution growth), a projection on the growth face caused by a fluctuation in the growth process may grow more rapidly than the remainder of the face, and the face is unstable. When this happens, the liquid is said to be constitutionally supersaturated (if the instability results from a concentration gradient), constitutionally supercooled (if the instability results from the combination of a concentration and a temperature gradient), or thermally unstable (when a temperature gradient is the sole cause).

Thermal instability can only arise in melt growth. The condition for thermal instability can be derived from Equation (58) and the condition that $dT_N/dx < 0$ (where x is measured normal to the growth face), which together yield an instability condition

$$K_S \left(\frac{dT_S}{dx}\right)_{x=0} - \frac{\Delta H_C f}{V_m} < 0 \tag{65}$$

Elimination of the instability involves practical steps to increase the first term or decrease the second term on the left-hand side of this relation.

The instability condition for constitutional supercooling can be shown to be approximately [129,130]

$$\left(\frac{dT_S}{dx}\right)_{x=0} < m c_{BN} (1 - k_I) f k_{eff} / k_I D_S \tag{66}$$

where c_{BN} is the concentration of the dopant with distribution coefficients k_I and k_{eff} and a diffusion coefficient D_S. The parameter m is the slope of the liquidus (i.e., $\partial T_E/\partial c_{BN}$), where T_E is the equilibrium temperature on the phase diagram.

The effective segregation coefficient k_{eff} represents the influence of melt convection. In the case of complete mixing ($f d_s/D_s \gg 1$), Equation (54) becomes $k_{eff} = k$, and only a small temperature gradient has to

be established for preservation of interface stability (if $k < 1$). In motionless melts, $k_{\text{eff}} = 1$, and this represents the highest danger of instability. Hence, convection may stabilize growing interfaces against morphological instability.

The instability condition for constitutional supersaturation can be shown to be

$$f > \frac{V_m D_S c_E}{T} \frac{\partial T_N}{\partial x} : \frac{c D H_C}{c_E R T} - \frac{T \partial f / \partial T}{\partial f / \partial (c - c_E)} \tag{67}$$

which points to the role of the temperature gradient in solution growth.

The conditions given above are approximations that ignore some stabilizing forces. In particular, a face growing by nucleation with rapid spread will always be stable and the stabilizing effect of the surface free energy has been ignored. Thus, faces are usually more stable than these relations suggest. For further discussion of stability relations, see [47, 56, 58, 131].

Even if a face is potentially unstable, there is no certainty that the instability will develop. A suitable fluctuation is necessary to initiate unstable growth and it takes time for the instability to develop. For example, in thin-layer growth instabilities are rarely seen, even in systems which must be potentially unstable. However, interface instability does provide a real limit to the maximum obtainable growth rate and, at a given growth rate, to the maximum size of a growth face. (Remember that the maximum value of dT_S/dx falls with face size.)

5. Practical Considerations

5.1. Raw Materials

Many materials with fewer than 10 ppm of impurities are now available. Used with care, such materials yield crystals with about 1 ppm of impurity. Most crystal growers buy their raw materials from specialist suppliers, who supply various grades. Typically, the price paid doubles for each factor of ten reduction in impurity content. Purification is sometimes necessary; thus, most organizations using water as a solvent purify their own water. A process sequence of filtering, reverse osmosis, deionization, and ultrafiltration is typical. In other cases, raw materials may be transferred to the growth system by distillation, which typically removes more than 90 % of the impurities present. When uncommon materials are required, in-house processes become essential, and crystal growth groups often distill or zone refine some of their raw materials.

5.2. Temperature Control

Spatial variations (temperature distribution) involve both uniformity and controlled nonuniformity. To produce regions with low temperature gradients requires the use of structural components with large effective thermal conductivities. At the lowest temperatures employed for crystal growth, stirred fluid baths are widely used. For higher temperatures (over 100 8C), metals (e.g., aluminum up to about 500 8C, copper to somewhat higher temperatures, and various steels up to about 1200 8C) can be useful. Above about 400 8C, liquid-metal filled heat pipes can be helpful, but with a given heat-transfer fluid, the optimum performance of a heat pipe exists only over a small temperature interval. Obtaining

desired gradients over limited distances is more difficult than obtaining a uniform temperature. Essentially, the problem is one of the heat flow that must accompany the gradient. Structural materials with low thermal conductivities (ceramics, mineral fiber wools, and even evacuated spaces) can play a part, but heat transfer in nutrient materials (particularly fluids) and in the crystals being grown can be significant, and considerable ingenuity may be needed to obtain the desired distribution without producing radial gradients that are harmful to the crystal (Section 4.5 Heat Flow).

Fully computer controlled heating systems, consisting of cylindrical multizone side heaters and top and bottom heaters, surrounded by insulating materials, are today of increasing interest due to their ability to realize nearly uniaxial heat flow through the growing crystal [132]. Excellent insulative properties are exhibited by modern carbon materials composed of interpenetrating layers of carbon fibers (calcarb). The very good machinability, low thermal conductivity (ca. 10^{-6} K^{-1}), and high temperature stability up to 2000 8C and above make this material very suitable for numerous high-temperature crystal growth processes that require minimal radial temperature gradients.

The availability of sensitive temperature transducers (thermocouples, resistance thermometers, and radiation sensors) together with solid-state temperature controllers has greatly simplified the designer's problems. However, the targets to be reached have also become more difficult: it is now common to demand temperatures of 1000 8C with variations of less than about 0.1 8C, and in the range 40–100 8C variations of less than 0.01 8C are often requested. The state of the art allows a tenfold improvement on these figures by use of multistage processes.

5.3. Containers and Atmospheres

Both the crystal and the nutrient from which it is growing must be in contact directly or indirectly with some solid part of the growth apparatus, and both may be in contact with an atmosphere. Thus, surface contamination and some contamination of the bulk materials, particularly in the slower growth processes, are expected, because most crystal growth processes occur at elevated temperature.

Solids in contact with the crystal and the nutrient must be selected with care. Graphite is a widely used material which is stable in contact with many solid and liquid halides and semiconductors (however, not with silicon), but reacts with many oxides. Silica (vitreous SiO_2) is used extensively but reacts slowly with molten silicon. Glasses, particularly borosilicates, are used widely, but care must be exercised because some components can be leached preferentially. The platinum metals, particularly platinum and iridium, are useful for work with oxides and halides.

For the growth of semiconductor compounds such as GaAs, InP, and GaP, pyrolytic boron nitride (pBN) has became the most widely accepted crucible and container material because of its high purity, thermal stability (up to 3000 8C in inert gas atmosphere), low out-gasing, and nonwetting characteristics. In particular, using pBN as alternative to quartz in Czochralski and Bridgman growth methods (Sections Crystal Pulling and Bridgman Method) eliminated the problem of silicon contamination, and the semi-insulating behavior of GaAs became apparent in production. pBN is also the most widely utilized container material for MBE sources. For HF induction coupling in the region up to 3000 8C, high-purity glassy carbon ampoules and containers have gained in significance.

In choosing solids for containers, care must be exercised in selecting the grades to be used. Materials which are satisfactory in a pure form may be unsatisfactory in technical grades. For example, pure

platinum is a satisfactory container for alkaline molten oxide materials, but technical-grade platinum contains some rhodium which is easily leached out by these oxides.

Similar care is required in choosing gases for ambients. Water is a common contaminant of gases from cylinders (however, many glasses contain significant amounts of water so that if the absence of water is essential, the correct construction materials must be chosen). Hydrogen is widely used because it can be purified readily by diffusion through heated palladium. Vacuum iscommonly thought to be a clean ''atmosphere.'' However, typical vacuum systems contain appreciable amounts of H_2O, CO, CH_4, and hydrogen (which is difficult to pump away). Water and carbon monoxide usually come from films absorbed on the inside walls of the vacuum system, and methane can be formed by the cracking of pump oils. For further information about vacuum technology, see [133]. Figure 21 shows that relatively low partial pressures give rise to appreciable impingement rates so that one monolayer can form in one second with a partial pressure of about 10^{-9} bar. A partial pressure of about 10^{-8} bar gives an impingement rate equivalent to a growth rate of about 1 mm/min so that thin-layer growth from a vapor at 1 mm/min requires partial pressures of about 10^{-14} bar to avoid contamination at a level of about 1 ppm. Pressures of 10^{-13} bar are currently the state of the art. Thus, if all atoms impinging are incorporated, a contamination of about 10 ppm must be expected. Fortunately, most of the impinging atoms are desorbed before they are incorporated, and crystals are usually purer, by a factor of ten or more, than these estimates suggest.

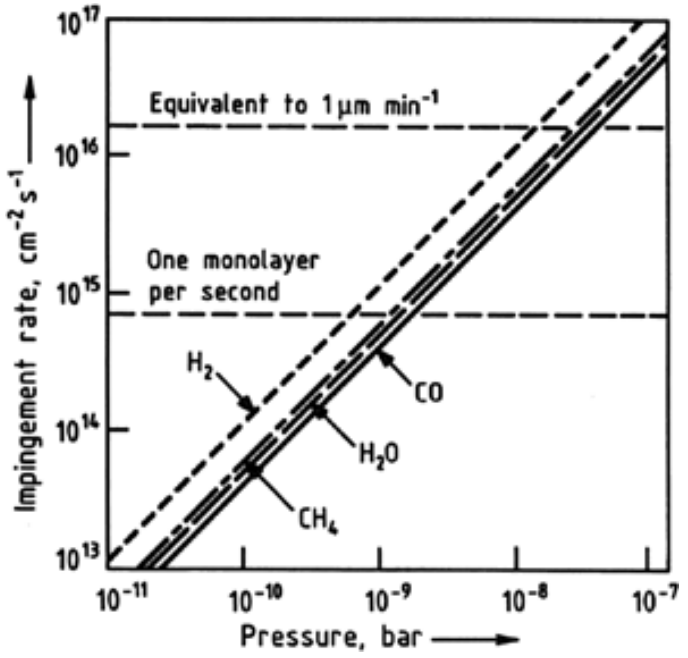

Figure 21. Impingement rates (molecules per unit area per unit time) as a function of partial pressure for typical residual gases in a vacuum system

5.4. Selection and Optimization of Methods

Selecting and optimizing methods of growth requires information about the methods available, the nature of the material, and its use. For example, if thin layers are needed, cutting thin sheets from bulk crystals might be very expensive, but in some cases, this may be the only approach; for example, no

method for producing the a-quartz needed for resonators in thin-sheet form has yet been found. In fact, only a few, rather limited methods exist (Section Crystal Pulling) for making thin, unsupported layers. Most thin-layer growth methods make use of a substrate which cannot be removed easily.

Bulk Crystals. For growing bulk crystals, *melt growth* is likely to be the fastest method (volume per unit equipment time), but it is only applicable to materials that melt congruently and have no destructive phase changes. Also, melt growth involves the highest possible temperatures and, therefore, the maximum possibilities of contamination. Of the available melt growth methods, the Czochralski and floating-zone methods can reliably yield dislocation-free crystals, and the floating zone method can yield large crystals only of materials whose melts have a high ratio of surface tension to density. (Typical ratios are in the range 3 to 300 $cm^2 s^{-2}$ but only materials with ratios exceeding about 100 $cm^2 s^{-2}$ are suitable for floating zone refining.) Due to the marked improvement in container materials (pBN, glassy carbon) and computer-controlled temperature programming, the Bridgman method has achieved a noteworthy renaissance for the relatively cheap production of high-quality crystals with excellent diameter accuracy, and dislocation densities in semiconductor compounds of less than 10^3 cm^{-2} are typical [134]). Skull melting is the cheapest method of melt growth but gives high dislocation densities in irregularly shaped crystals.

Vapor growth techniques probably give the second highest growth rates but are applicable only to materials that are volatile or give rise to reversibly decomposable compounds. Due to the low condensation temperature relative to the melting point, low-temperature single-crystalline phases can be grown directly without passing through harmful solid–solid phase transitions. This phase transition is today more and more used for the growth of materials with high melting point, such as nitrides (GaN, AlN) and silicon carbide, which are of increasing importance for advanced micro- and optoelectronics.

Solution growth techniques are usually the slowest processes and are applicable only to materials that are reversibly soluble.

Solid-phase growth techniques are not used commercially for bulk crystal production because yields are low. All the other methods of growth allow some segregation of impurities so that the crystals can be purer than the starting materials. However, for special materials with high melting points or solid phase transitions, solid-state recrystallization by exploiting the phenomenon of grain growth in thermally stressed polycrystalline samples is under investigation.

Thin Layers. For thin-layer processes, crystals can be grown from solution (liquid-phase epitaxy, LPE), from the vapor (vapor-phase epitaxy, VPE, or molecular beam epitaxy, MBE), or from the solid state (solid-state epitaxy, SSE). In the last case, the solid from which growth takes place is likely to be amorphous. Liquid-phase epitaxy is used quite widely. It is almost the only technique available to make thin layers of garnets for magneto-optic devices (bubble memories, display devices) and for single crystalline phosphors for high-intensity cathode-ray tubes. Liquid-phase epitaxy is also used for semiconductors, where it generally yields layers purer than other methods but usually with rather imperfect surfaces. Molecular beam epitaxy is rather slow but can yield complicated structures with many layers and sharp composition changes; the substrate temperature can be very low, e.g., 100 8C.

Vapor-phase epitaxy using halides (VPE, CVD) or organometallic compounds (OMCVD or OMLPE) is widely employed for semiconductors. Recently, SSE has been used for semiconductors, but proper evaluation of this method requires more experience with a wider range of materials. Choosing the optimum thin-film method is particularly dependent on the use. Almost the only general statement that can be made is that MBE is unlikely to be economic for thick layers. However, it plays a leading role in the production of quantum-size devices such as quantum wells, wires, and dots.

Optimization. Method optimization usually implies an increase in scale, such as larger volumes for bulk crystals, or larger areas for thin layers. In general, large crystals have to be grown at slower rates than small ones if perfection and uniformity are to be maintained, and costs do not decrease as rapidly as they would if the rates could be maintained. Nutrient costs do not decrease with crystal size and are typically one-third of total costs. A larger apparatus uses energy more efficiently, but the energy costs are low (usually < 10 % of total costs). Equipment and labor costs do not rise linearly with crystal dimensions, so some savings are possible. In general, automation is a paying proposition. The extra cost for equipment is usually less than the savings in labor cost, and automated equipment can produce more uniform material with higher yields than manually controlled equipment. Operator errors can easily result in losses that exceed 20 %.

5.5. Characterization

In general, the number of characterization techniques is vast and rapidly growing, so that only the main essentials can be summarized here. With resepect to crystal growth the various characterization techniques can be roughly grouped into three categories:

1. Characterization of composition and purity
2. Structural characterization
3. Characterization with respect to specific physical properties, depending on special material properties and on the application for which the material is intended

Further, analytical methods can be divided into destructive and nondestructive as well as in-situ and post-growth techniques. The development of suitable in-situ techniques is of major importance for advanced crystal growth. Whereas in the case of thin film growth, especially MBE, the in-situ observation and control of the crystallization modes (by RHEED and scanning tunneling microscopy, for example) is already state-of-the-art [135], for bulk growth from the melt this is an as-yet unresolved problem, primarily because of the lack of adequate sensors and analytical techniques. Considerable progress has been achieved in solution and vapor growth by using laser scattering, especially in holographic mode, for the investigation of diffusion boundary layer thicknesses and growth kinetics.

Today it is important that the experimental analytics are combined with modelling of the observed effects. Modelling includes both the simulation of the solid with its various specific structural features and modelling of the effects exerted by a solid with this structure on the analytical probes. Modelling is also necessary for image enhancement.

Skilled personnel can obtain a great deal of data in a nondestructive mode by just looking at a crystal. Visual inspection directly or by microscope (particularly one with an interference, e.g., Nomarski, lens)

reveals surface irregularities on natural faces or other grown surfaces. Networks of grooves suggest low-angle grain boundaries. Isolated straight lines (particularly on lightly abraded faces) suggest twins. Pyramids suggest screw dislocations or stacking faults. Sets of parallel lines suggest concentration striae. On etched surfaces, pits probably indicate dislocations or vacancy clusters. For transparent materials, light-scattering centers in the bulk may be inclusions. Many crystals are transparent in the infrared, and infrared microscopy is a powerful tool. Transparent crystals can also be examined by using polarized light, which readily reveals built-in strains. Such strains, indicating large-scale effects resulting from the simultaneous existence of more than one type of growth face, inclusions or dislocations or internal strain arising from dislocation or impurity distribution, can be revealed by X-ray topography (see, for example, [136]). Similar data can also be obtained by electron microscopy. It is often necessary to know the compositions of crystals, especially the concentrations of deliberately added dopants and accidentally occurring impurities. The spatial variations of composition are also of interest. Thus, it is desirable to find methods which work on small samples. Table 3 gives typical data for the methods commonly used. When the sample size is given as an area times a length, the length is normal to the sample surface. Other methods are less generally used. For further data, see [19,47,137,138].

Table 3. Methods for determining composition

	Method	Sample size	Destructive?	Detection limit (atom fraction)
a	Gravimetry	$20\,mm^3$	yes	10^{-5}
b	Titrimetry	$10\,mm^3$	yes	10^{-5}
c	Electro-chemical methods	$10\,mm^3$	yes	10^{-4}
d	Isotope dilution	$2\,mm^3$	yes	10^{-4}
e	Atomic absorption spectrometry	$20\,mm^3$	yes	10^{-7}
f	AAS (with graphite furnace)	$2\,mm^3$	yes	10^{-8}
g	Solid-source mass spectrometry	$2\,mm^3$	yes	10^{-8}
h	Neutron activation	$0.2\,mm^3$	yes	10^{-9}
i	Charged-particle activation	$2\,mm^2 \times 100\,mm$	yes	10^{-9}
j	X-ray fluorescence	$25\,mm^2 \times 20\,mm$	no	10^{-5}
k	Rutherford backscattering	$1\,mm^2 \times 2\,mm$	no	10^{-3}
l	Electron-probe (X-ray spectrum)	$4\,mm^2 \times 2\,mm$	no	10^{-3}
m	Secondary-ion mass spectrometry	$0.1\,mm^2 \times 10\,nm$	yes	10^{-9}
n	Auger spectrometry	$100\,mm^2 \times 1\,nm$	no	10^{-2}
o	X-ray photo-electron spectrometry	$10\,mm^2 \times 1\,nm$	no	10^{-3}
p	Low-energy ion scattering	$1\,mm^2 \times 1\,nm$	no	10^{-4}

6. Melt Growth Techniques

6.1. Crystal Pulling

The order of the following sections reflects the amount of use that is made of each method; the Czochralski method is used to a greater extent than the other four techniques.

Czochralski Method. The basic sequence of operations in the Czochralski method is shown in Figure 22. A seed crystal is dipped into the melt, and a small amount of the seed is allowed to melt. Pulling is then begun, and the melt temperature is adjusted so that the first portion grown has a diameter just smaller than that of the seed. For dislocation-free growth, the diameter is then reduced to about 2 mm by raising the melt temperature slightly. This diameter is maintained for about 10 mm and then increased to the final target value (dislocations, except those exactly parallel to the seed axis, grow out while this neck is grown). When dislocation-free growth is not required, the diameter can be increased after the first 2 or 3 mm of growth. Decreasing the melt temperature increases the crystal diameter and vice versa. Increasing the rate of pull or the relative rate of rotation of the crystal decreases the diameter. The word relative is used here because many workers may rotate the seed and the crucible in opposite directions. Some workers also raise the crucible to maintain the liquid surface at the same height relative to the apparatus. This is particularly convenient when the system for controlling diameter employs the reflection of a light beam on the curved portion of the melt near the edge of the crystal. The other commonly used method of diameter control involves weighing the crystal or the melt.

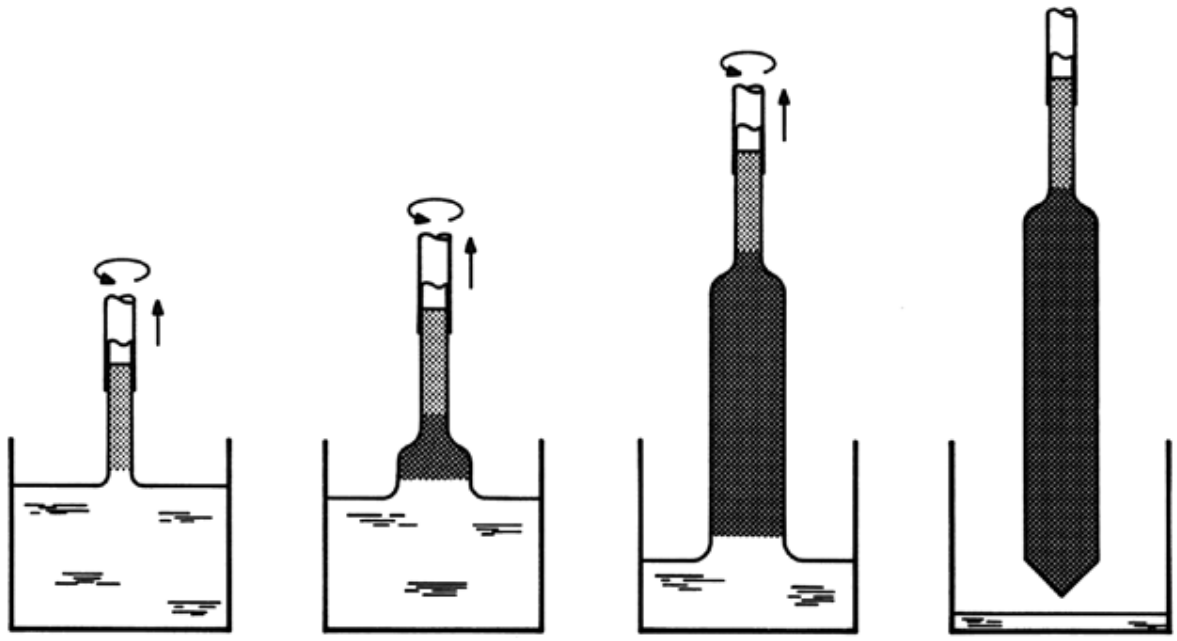

Figure 22. Sequence of operations in the Czochralski method

The rotation and pulling rates used depend on the material being grown and the diameter of the crystal. Larger crystals need slower pulling and rotation. The maximum pulling rate is roughly inversely proportional to the diameter to the power 1.5. Typical rates for 2-cm diameter crystals range from 3 mm/min (silicon and germanium) to 3 mm/h (oxide crystals with low thermal conductivity). Rates as high as 12 mm/min and as low as 1 mm/h have been reported. Crystal rotation rates tend to be proportional to the reciprocal of the crystal diameter. For 2-cm diameter crystals, rates of 5–50 rpm are typical. Crystals of silicon up to 30 cm diameter are pulled (40-cm technology is under development); alkali metal halides can have much larger diameters.

When electrically conducting crucibles are used, power can be supplied by radio-frequency heating as shown in Figure 23, which also illustrates the use of an encapsulant to prevent decomposition of materials with a volatile component. When nonconducting crucibles are used, radio-frequency power may be coupled directly to the melt, but more usually a resistive heater coaxial with the crucible is used. Such heating elements can be made from graphite, silicon carbide, or molybdenum or from resistance wires wound on ceramic formers.

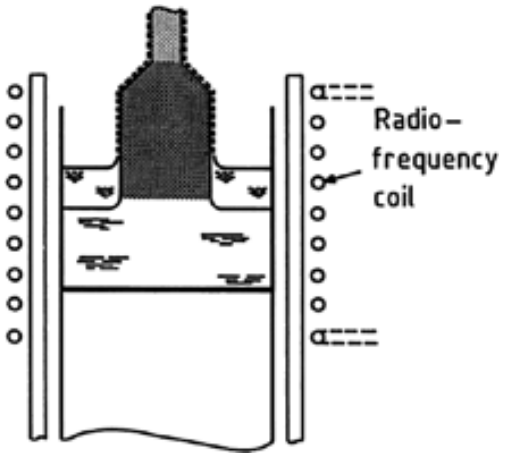

Figure 23. Liquid encapsulated growth by the Czochralski technique (LEC)
This method is used to grow a material with a high partial pressure of one or more component. Use of an encapsulant (usually boric oxide, but occasionally a halide), shown dotted, prevents loss of volatile material from the melt and from the crystal if the pressure in the growth chamber exceeds the sum of partial pressures of the components

Usually, the conventional Czochralski technique is characterized by high temperature gradients and thermal nonlinearities in the growing crystal, which are harmful for materials with low critical resolved shear stress (semiconductor compounds). To decrease the temperature gradients, after-heating systems are used. To prevent dissociative decomposition of the hot crystal surface, in such cases, a closed inner growth chamber with a controlled atmosphere of the volatile component can be used [139].

A comprehensive overview on the Czochralski technique is given in [140].

Kyropoulos Method. The Kyropoulos method uses a seed crystal that is dipped into the melt, but growth is maintained by continuously lowering the crucible temperature (Fig. 24). Linear growth rates are low, but the area of the growth face is large so that volume growth rates are reasonable but significantly lower than those obtained by the Czochralski method. The Kyropoulos method is widely used to produce halide crystals for optical components. Crystal diameters and lengths are usually comparable. Crystals with dimensions greater than 50 cm have been grown. The major practical problem appears to

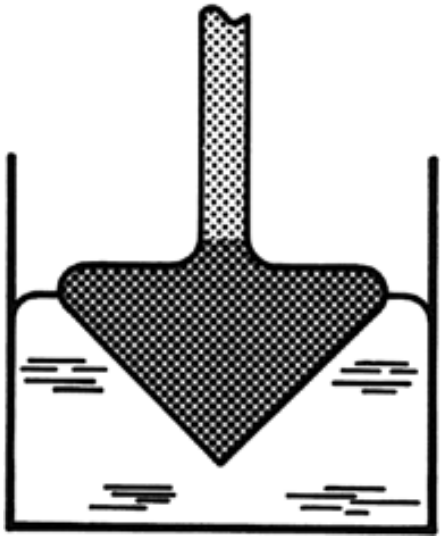

Figure 24. Kyropoulos method

be seed breakage. For this reason, seeds and crucible rotations are sometimes not used. Dislocation densities tend to be high ($> 10^4\,\mathrm{cm}^{-2}$).

Edge defined film-fed growth and the Stepanov method, which involve pulling crystals through shaped apertures, are shown schematically in Figures 25 and 26. The methods differ in their use of capillary action: in edge-fed growth, the die is wetted by the melt.

Edge defined film-fed growth (EFG) can be used to make single-crystal sapphire pipes but is employed on a large scale to make silicon ribbons for solar cells. Also thin-walled octagonal tubes are commercially produced by the EFG technique; they show reduced thermomechanical stress compared to edged ribbons. Octagons are then cut into wafers 10×10 cm, 300 mm thick with high-speed lasers. Crystalline quality is not usually important in such uses, and the plates, rods, and tubes made this way do contain some low-angle grain boundaries. Crystals grown by the Stepanov method are usually more crystallographically perfect but still tend to have large dislocation densities because of the large temperature gradients near the growth face.

Because the shaped crystals grown by these methods generally have at least one small dimension normal to the growth axis, high linear rates of growth (10 mm/min or more) can often be maintained. With the Stepanov method, the crystal need not be pulled vertically upward, and equipment in which crystals are pulled vertically downward or horizontally has been described.

A special branch of high-speed crystalline fiber pulling through wetting and nonwetting dies with micro-orifices has been developed [141]. Small-diameter (50–300 mm) long single-crystalline fibers of numerous oxide materials (e.g., sapphire, $LiNbO_3$, $KNbO_3$) are of considerable interest for miniaturization, especially of multifunctional nonlinear optical devices.

More details on shaped crystal growth are given in [142,143].

Dendritic Crystallization. Around 1960, the use of dendritic crystallization was expected to provide the thin sheets of semiconductors needed to make transistors. However, the crystal quality was inadequate: dislocation densities and impurity concentrations were too high. Some workers believed that the material might be useful for solar cells. Certainly, the linear growth rates are attractive (rates of up

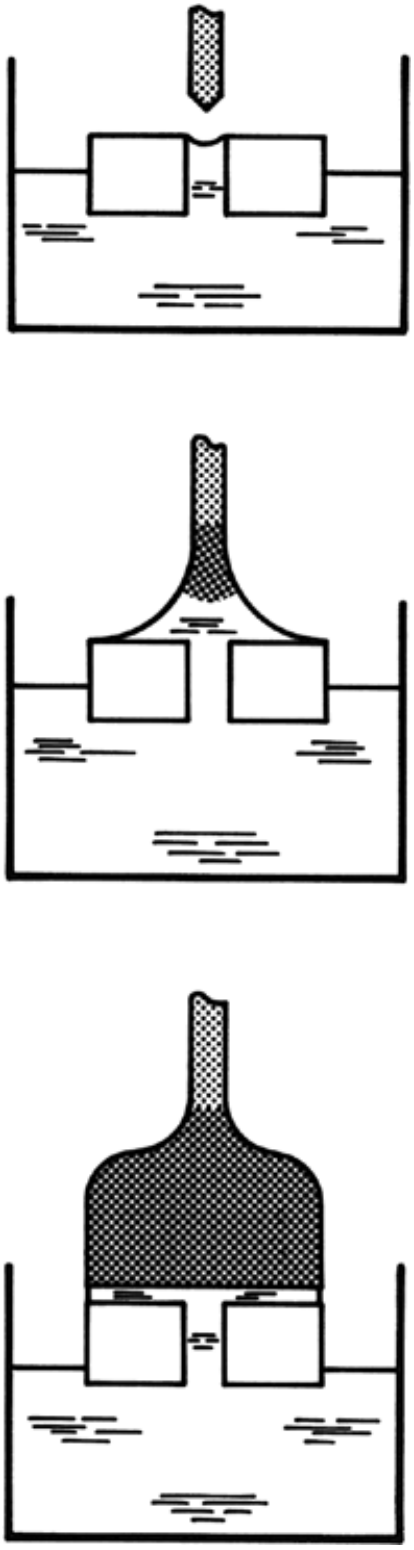

Figure 25. Edge defined film-fed growth

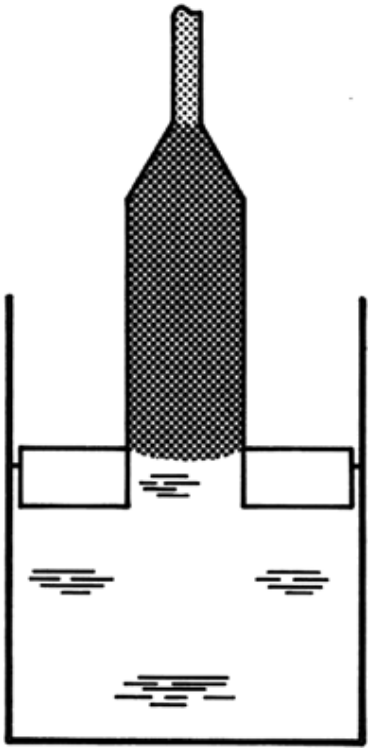

Figure 26. Stepanov method

to a few meters per minute have been reported). The method uses a multiply twinned seed crystal to grow tapelike crystals less than 1 mm thick. In diamond and zinc blende structure semiconductors, the preferred growth direction is <211>. In a typical process, a correctly oriented seed crystal is touched on the surface of a melt about 2 8C above its melting point. The melt temperature is then rapidly reduced by about 20 8C, and pulling commences. An ingenious modification of the method uses two seeds to pull a so-called web crystal (Fig. 27).

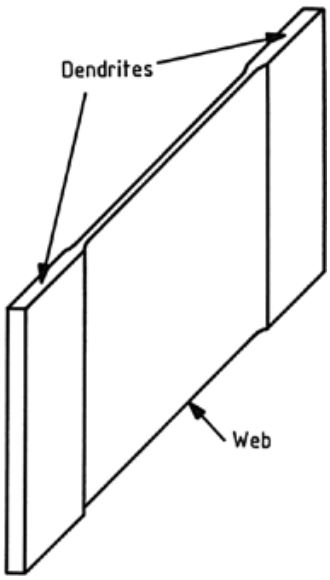

Figure 27. Web growth

6.2. Bridgman Method

A crucible (Fig. 28) is lowered through a temperature gradient which straddles the melting point T_M. If a seed crystal is used and the convex growth face shown can be maintained, a single crystal with the same shape as the crucible should result. The seed crystal can be omitted, and a long, narrow tube can be substituted at the lower end, for example. (If several crystals nucleate, only one will probably emerge from a long, narrow tube.)

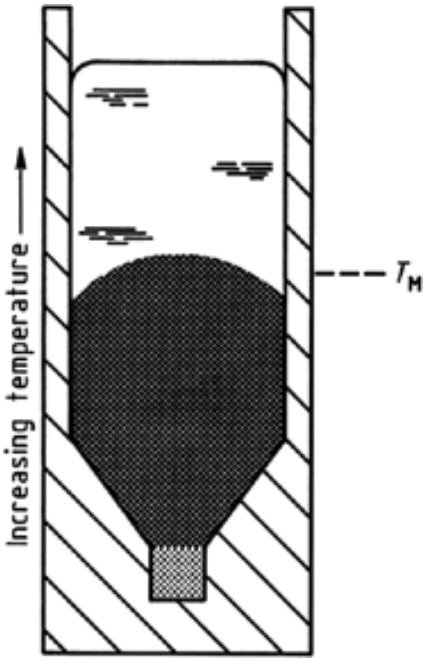

Figure 28. Bridgman crucible
Note the hatched seed crystal

In practice, two particularly important problems exist. The first is that it is difficult to find crucibles with the same thermal expansion coefficient as the crystal. If the crucible has a larger coefficient, it will damage the crystal during cooling. If the crucible has a smaller coefficient, damage will occur if the crystal sticks to the crucible.

The other major problem is to obtain and maintain the desired temperature distribution (i.e., the interface shape shown). This requires crucibles with thermal conductivities that are less than those of the materials grown.

Adding to these needs, the general requirement of no contamination makes crucible selection difficult. Common choices are graphite and silica which is often given a soft carbon coating. However, a variety of materials have been used, e.g., molybdenum for the growth of sapphire, iridium for $FeAl_2O_4$, boron nitride for gold, polyethylene for sodium nitrite, and polyester (e.g., Mylar) for ammonia.

Due to the rapid development of high-temperature construction materials in the 1990s and their application as growth containers (pBN, glassy carbon, etc.; see Section Containers and Atmospheres), the above-mentioned problems were solved for semiconductor compounds (GaAs, InP, GaP). Moreover, the sticking problem was suppressed by using a covering liquid layer (boron oxide) between the crucible wall and growing crystal. These technological improvements, together with the high diameter constancy and low defect density, led to a considerable renaissance of the Bridgman technique, which

has become a serious competitor to the Czochralski method in the modern electronics industry [121,134,144,145]. To prevent constitutional supercooling (Eq. 66), the growth rates (1–10 mm/h) are about one order of magnitude lower than in Czochralski growth because of the much lower axial temperature gradients used. Contemporary reviews on Bridgman growth of semiconductor compounds compared with Czochralski method are given in [121,146-148].

Horizontal Boat Method. This method was established in the 1950s for GaAs growth and is still the most widely used production method for Si-doped material for optoelectronics. Pretreated (sand-blasted or etched) quartz and pBN boats are used. Usually, the charge is produced by in-situ synthesis in a separate ampoule, in which the volatile component (As) is evaporated and reacts with gallium held at a suitable temperature. Either the charge or furnace is moved (Fig. 29).

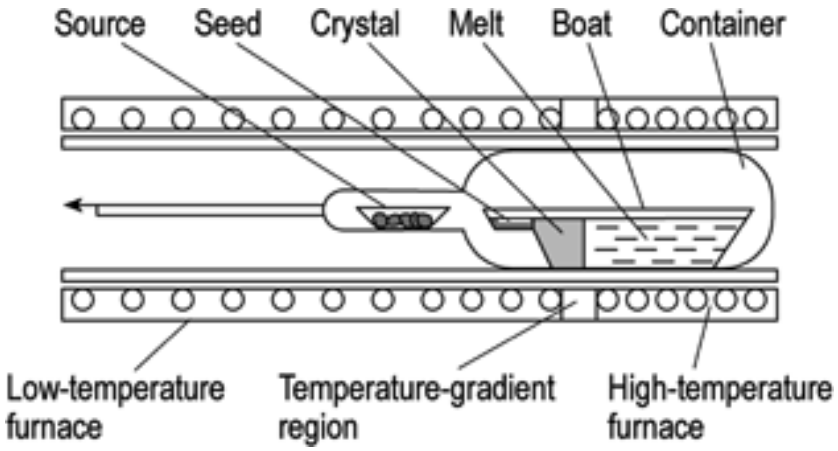

Figure 29. Horizontal boat configuration for the growth of semiconductor compounds

The major advantages are the possibility of stoichiometry control by means of the pressure of the volatile element from an additional source and the free growth of the shoulder region, which results in a low dislocation density of about 10^2 cm^{-2}. Main disadvantages are the noncircular cross section and the limited width of the shoulder. A review on semiconductor compound growth by this method is given in [149]. The succesful horizontal growth of single-crystalline sapphire and YAG plates by applying a restistance tungsten heater is described in [48].

Vertical Bridgman Method. The vertical bridgman method is characterized by the translation of the crucible containing the melt relative to the axial temperature gradient in a vertical furnace [150-152]. Whilst it is generally simpler in a mechanical sense to lower the crucible through the gradient, in some cases where vibration of the ampoule is a concern, the crucible is held stationary and the furnace is moved [134]. In the Bridgmann–Stockbarger mode [19], a high-temperature upper zone is followed by an adiabatic middle zone (for locating the position of the growing interface) and a low-temperature lower zone for afterheating and nearly gradient-free cooling. A wide range of materials (metals, semiconductors, oxides) are grown by vertical directional solidification. By connecting a third furnace in series, the stoichiometry of the growing crystal can be controlled by means of the partial vapor

pressure of the volatile component, which has been succesfully applied to II-VI growth, for example [153].

Gradient Freeze. In this configuration both the ampoule and the furnace are held stationary, and the freezing isotherm is moved by computer-controlled modification of the furnace temperature (Figure 30). A multifurnace system consisting of 5 to 10 (a maximum of 50 has been described [134]) independently controlled heating zones is used to tailor the temperature field during growth (dynamic gradient freezing). Presently, high-quality semi-insulating GaAs crystals up to 10–15 cm in diameter with low dislocation densities in the range from 500 to 5000 cm^{-2} are grown commercially for high-frequency microelectronics [144,145]. The reasons for such low dislocation density are the extremely low thermomechanical stress conditions (no sticking, no mechanical vibration, nearly uniaxial heat flow).

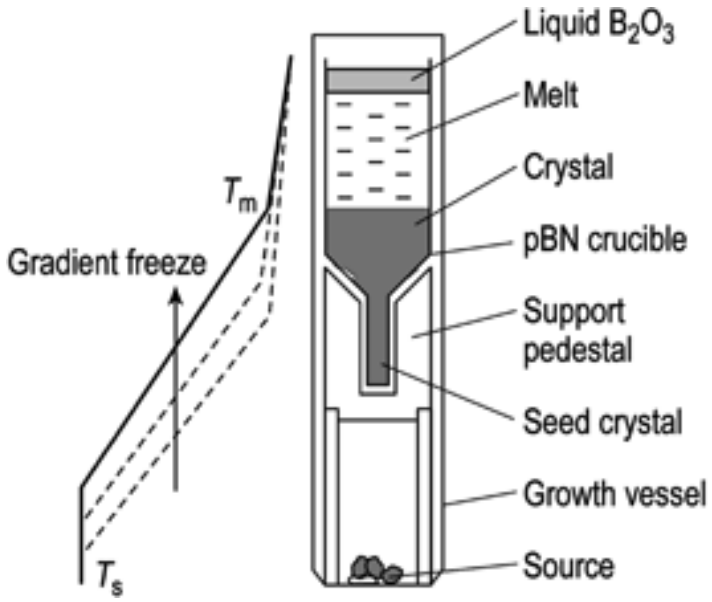

Figure 30. Vertical gradient freeze of semiconductor compounds (GaAs, InP) with stoichiometry control by means of a source of the volatile element (As, P) at T_s

Heat Exchanger Method. This container method, called HEM, is a modified directional solidification technique developed in the 1970s mainly for growth of large sapphire crystals from the melt [154]. But photovoltaic silicon, CdTe and BGO crystals have also been grown by this method. Large crystals can be grown by HEM since it has a unique feature for independently controlling the heat input and heat extraction, as shown in Figure 31. A crucible with a single-crystal seed centered at the bottom is loaded with sapphire meltstock and placed on a high-temperature, helium-cooled heat exchanger. During melting the seed is cooled by helium gas flowing through the heat exchanger. Then, after melting and homogenization, the growth is initiated and progressed by increasing the helium flow and decreasing the furnace temperature. After complete solidification the furnace temperature and helium flow are reduced to achive in-situ annealing of the boule before the crystal is cooled in a controlled manner.

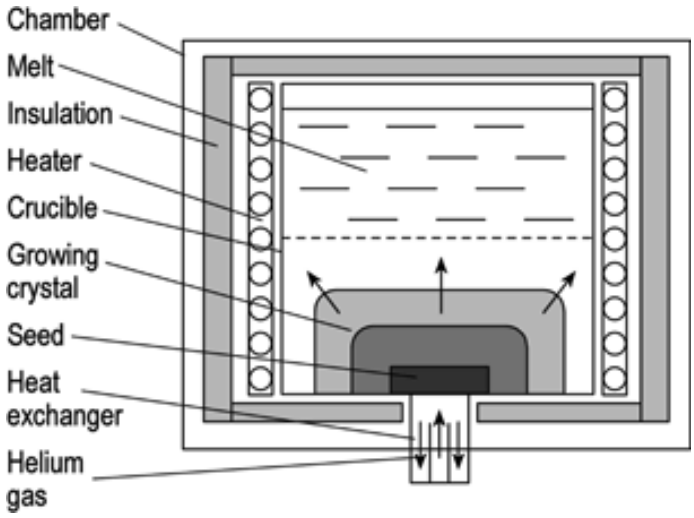

Figure 31. The principle of the heat-exchanger method

To remove trapped ambient gas from the liquid, the melt is overheated above the melting point without affecting the well-cooled seed. Morover, very low temperature gradients can be achieved. These features have allowed production of light-scatter-free sapphire crystals of 34 cm diameter and 65 kg weight. Growth of 50-cm diameter crystals is under investigation. Numerous cylindrical crystals can be prepared from such boules by core drilling.

6.3. Skull Melting Methods

Skull melting processes involve melting a powder charge (usually weighing over 50 kg) in a water-cooled container so that the melt is in contact only with an outer skull of sintered powder. When the system is cooled slowly, crystals nucleate at random and then progressively grow [155]. Figure 32 shows a version of the process using radio-frequency heating. Because the charge usually has an extremely high resistivity at room temperature, this version uses some lumps of the metal whose oxide is being grown to couple the radio-frequency energy to the charge. An alternative process [156] uses an arc to provide the power needed. The process is not very controllable and usually produces crystallographically imperfect crystals. However, for high-melting materials (MgO, CaO, SrO, BaO, and ZrO_2) the method has significant advantages and is used, for example, to grow about 1000 t of cubic zirconia per annum. For instance, Ceres Corporation (USA) produces approximately 20 t per month in 45 inch (117 cm) diameter skull furnaces holding 2.5–3.5 t of charge. The weight of the individual single crystals reaches 3–5 kg. At room temperature, pure ZrO_2 is monoclinic. The cubic form, which is stable at high temperature, can be made stable at lower temperature by doping (e.g., with CaO or La_2O_3). In addition, doping produces almost any color and this, combined with its hardness, large refractive index, and high dispersion, makes zirconia very attractive as a jewel. For further information on the growth, properties, and applications of this and other jewels, see [157].

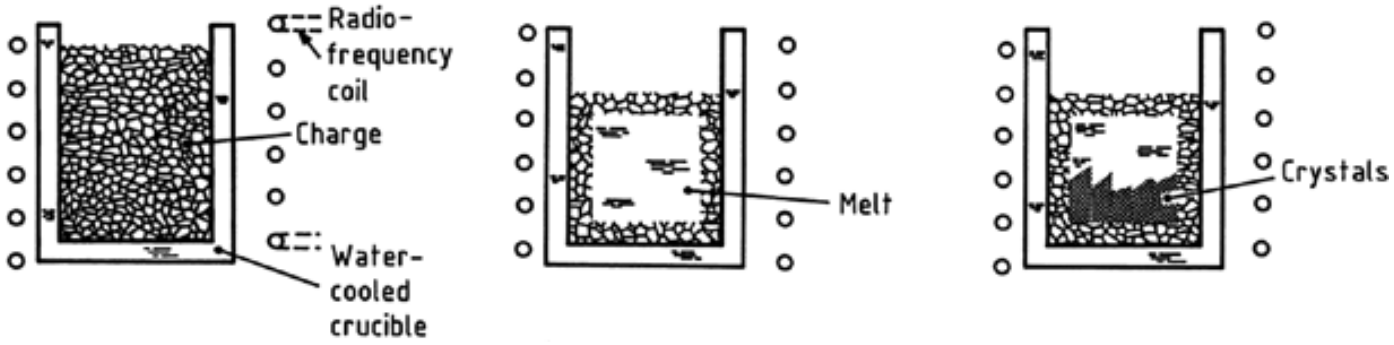

Figure 32. Skull melting. The sequence of operations starts at the left

6.4. Zone Melting

The methods described in Section Bridgman Method involve melting the entire charge and then progressively freezing it. However, the whole charge need not be molten. A crystal can also be grown by moving a molten zone through the charge [158]. This has the advantage that only part of the system must be at a high temperature at any time.

When the growth process is started with a charge having a uniform concentration c_0 of a solute with an effective distribution coefficient k, then the concentration in the crystal c_S at a distance x from the initial growth face is

$$c_S = k\,c_0(1 - x/L_0)^{k-1} \tag{68}$$

where L_0 is the length of the charge and the process considered is one in which the whole charge is initially molten and then frozen. However, if a zone process is used with a zone length L, then for $x < L_0 - L$,

$$c_S = c_0[1 - (1 - k)\exp(-k\,x/L)] \tag{69}$$

For $x > L_0 - L$, Equation (68 applies. Figure 33 gives an example of c_S as a function of x. The broken curve is the distribution obtained from Equation (65), i.e., the usual Bridgman case, which is referred to as normal freezing. The full curve labeled $n = 1$ is given by Equation (66) and is usually called a single-pass distribution. If the zone melting process is repeated (i.e., movement of another zone through the same bar), the distribution given by the curve for $n = 2$ is found. Further repetition gives curves for $n = 3$, 4, 5, etc., and an ultimate distribution is obtained which is shown by the line labeled $n = 1$. These multipass distributions are the basis of zone refining [158], which is a useful method for purification provided the impurities have k 9 0.2. Designing a zone refining process for purification is not easy. A set of impurities with different k values must usually be considered. However, a process for which $n\,L/L_0$ is between 0.5 and 1.5 is a reasonable starting point.

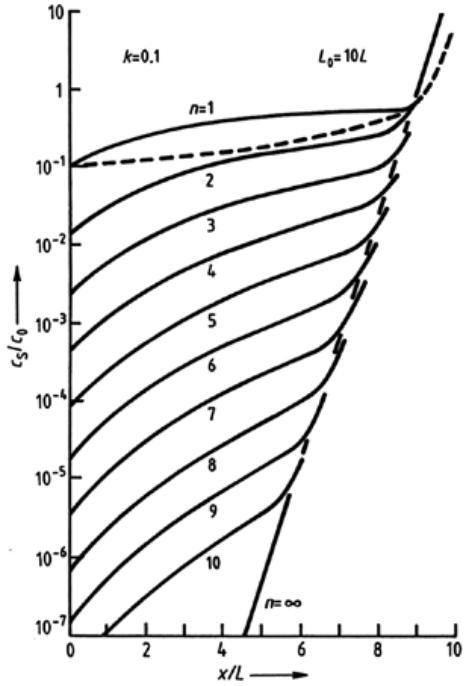

Figure 33. Concentrations (c_S) in the solid as a function of the initial charge concentration (c_0) and position x

In some processes, the charge is essentially pure, but doped crystals are to be produced by adding a dopant to the zone at the start of the process. If the concentration of dopant is c_0 in the zone, then the concentration in the solid is

$$c_S = k\,c_0 \exp(-kx/L) \tag{70}$$

If uniformly doped material is needed, the process is designed so that kx/L is small; in this way, crystals with very small gradients of dopant concentration can be obtained. When k is small, these gradients can be much less than those given by normal freezing, as shown when Equations (70) and (68) are compared.

The apparatus for zone melting a charge in a boat is fairly simple to design. All that is needed is a source of power which can heat a short length. Either the source or the boat can be moved.

In some cases, zone melting can be carried out without a boat [153]. A molten zone can exist between two solid rods, as shown in Figure 34. The power to maintain the molten zone can be supplied by electron bombardment, arc image systems, mirror-focused optical or thermal radiation, or laser beams. However, the use of radio-frequency heating as shown is the most popular method.

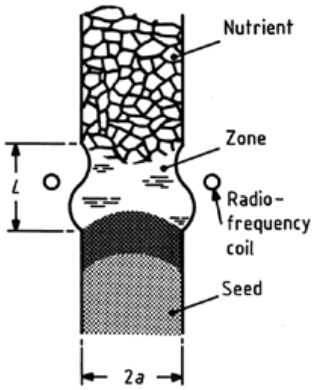

Figure 34. Floating zone
For explanation of symbols, see text

If the zone starts in contact with a seed crystal and is then moved away from the seed, it can melt a polycrystalline nutrient and deposit a single crystal. The advantage of this method is that the molten material is only in contact with its own solid and a vapor phase (which, at least in principle, does not contain harmful impurities). The method has obviously desirable features for the growth of crystals of many reactive materials, but the only large-scale use is for silicon [159]. Oxygen-free silicon in bulk form can be grown only by the floating zone method.

If gravity and surface tension are the only forces affecting the zone size, then the parameter which determines stability is the zone length L (not the rod radius a), based on the assumption that the melt perfectly wets the solid and that the interfaces are flat. If γ is the surface tension (about 0.72 J/m^2 for silicon) and ρ is the density, the maximum zone length is

$$L_{\max} \approx K(\gamma/\rho g)^{1/2} \tag{71}$$

where K is a constant for which values of 2.5–3.5 have been given [159]. In practice, zone lengths lie between about $0.5a$ and $2a$ so that, as a first approximation, the maximum zone radius is

$$a_{\max} \approx 3(\gamma/\rho g)^{1/2} \tag{72}$$

For silicon $(\gamma/\rho g)^{1/2}$, the capillary constant, is 5.37 mm.

However, these two relations are based on rather doubtful assumptions, and a more realistic model should take account of the extra stabilizing forces resulting from electromagnetic effects when radio-frequency heating is used and the destabilizing force resulting from rotation. In a typical case, the electromagnetic forces exceed the surface tension forces. The pressure resulting from rotation is about

$$p \approx \rho \int_0^a v^2 r\,dr$$

If this force should not exceed 10 % of the surface tension force (roughly γ/a), the rotation rate should not exceed

$$v_{\max} \approx (\gamma\rho/5\rho)^{1/2} a^{-3/2} \tag{73}$$

which for 10-cm diameter silicon gives a rotation rate of about 6 rpm. In general, Equation (70) appears to give values in the range used experimentally.

Global numerical models show that process optimization is sensitive to the shape of the field coil and the mass flow in the molten zone [160-162]. In addition to the flow caused by the relative rotations of the seed and nutrient rods, the large temperature gradients lead to density-gradient and surface tension-gradient (Marangoni) convection. There will also be electromagnetic forces causing flow when radio-frequency heating is used. If the aim is to produce uniformly doped silicon crystals, the best results appear to be obtained with short zones ($L \leq a$), rather low rotation rates (about half the value of v_{max}), and growth rates in the range 2–4 mm/min. As with crystal pulling, dislocation-free growth can be obtained by growing a narrow neck from the seed. Under these conditions, about 800 t of silicon up to 15 cm in diameter is produced each year. Float zone material is usually purer (lower oxygen concentration) and tends to be used for high-voltage (power) devices, whereas Czochralski material is used for low-voltage devices, which have a much larger market.

The floating zone method has been used in research for a large number of materials, but apart from silicon, its commercial use appears to be limited to a few metals grown at rates of a few kilograms per year. The optical zone heating technique in mirror furnaces is of special importance in space experiments due to its low power consumption. It is also widely used in fundamental research for growth of dielectric substances [160]. Laser heating arrangements are used for production of oxide fiber crystals by miniature-zone floating [163]. For further data, see [47,53,159,141,153].

6.5. Verneuil Process

The traditional Verneuil apparatus (shown schematically in Fig. 35) uses an oxygen–hydrogen flame to melt a powder that is sprinkled into one or more of the gas streams. Other flammable gases (acetylene, synthesis gas, natural gas) can be used, and arcs, arc images, and plasmas have been used as the power source. The melt exists as a thin (9 1 mm) film on the upper surface of the growing crystal. The powder must melt before or immediately after hitting the surface of this film. The process is controlled by the supply rates of heat and powder.

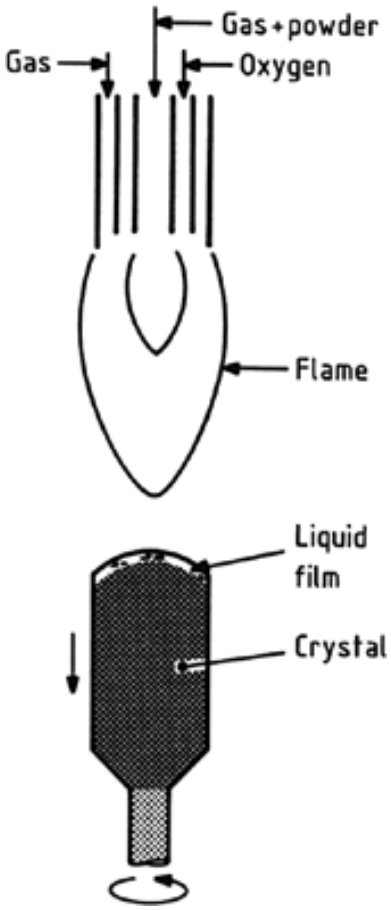

Figure 35. Verneuil process

The axial dopant and impurity distribution in Verneuil crystals follows the zone growth relation of Equation (66). This is due to the constancy of the liquid film volume continuously fed by molten source material.

An obvious refinement of the process is to surround the crystal by a furnace and so limit the temperature gradient in the crystal. This allows growth, for example, of ruby with dislocation densities below 500 cm^{-2}, but usually dislocation densities exceed 10^4 cm^{-2}. Typical growth rates range up to about 20 mm/h, but decrease roughly linearly as the crystal radius increases. Usual seed rotation rates are 5–50 rpm, with larger crystals requiring the slower rates. Diameters are, by modern standards, quite small: 20–50 mm is typical.

Up to the era of electronic clocks and watches, the largest use of the Verneuil process was to produce sapphire (undoped corundum) or preferably the harder ruby (chromium-doped corundum) for bearings in clocks and watches, at rates of up to 700 t/a. Because the hardness of the crystals increases, high dislocation densities could be an advantage for this type of application, although in practice, crystals with high dislocation densities tend to shatter when cut. Some ruby is still used for bearings, but the largest current use is for jewelry (a few hundred tons per year). Many refractory oxides and some other materials (e.g., niobium and silicon) have been grown for research purposes. Commercially available Verneuil-grown crystals include titania, strontium titanate, emerald, and a variety of spinels. The growth of 500 mm long laser crystals with a diameter of 40 mm has been reported [48].

7. Solution Growth Techniques

7.1. General Aspects

The properties of an ideal solvent are as follows:

1. Moderate reversible solubility of the material to be grown
2. Reasonable positive temperature coefficient of solubility
3. Production of crystals with useful habit
4. No formation of solid solutions with the solute
5. Low viscosity
6. Low volatility (except when evaporative methods are used)
7. Easy removal after growth
8. Compatibility with available containers
9. No reactivity with the gas phase
10. Ready availability
11. Inexpensiveness
12. Absence of toxicity

It is rare to find a solvent with all these properties. Many solvents are used for low-temperature solution growth (Table 4 lists some examples), but the only commercially significant solvent is water. High-temperature solution growth is employed on a much smaller scale than low-temperature processes. Table 5 contains some examples. In commercial processes, lead salts are used widely for the growth of oxidic materials. The other popular solvent is gallium, which is used for the growth of GaAs and similar materials.

Table 4. Non-aqueous solvents for low-temperature solution growth

Solvent	Solutes
Acetone	acridine, trilaurin
Ethanol	hexamethylenetetramine
Carbon tetrachloride	benzophenone
Carbon disulfide	sulfur
Mercury	tin, iron

The supersaturation needed to produce crystal growth is usually achieved in one of three ways: cooling, solvent evaporation, or temperature gradient transfer. In this last method, solid nutrient material is placed in contact with the solution at one temperature, while the crystal grows in a region where the solution temperature is lower. The solute concentration c is assumed to be a function of temperature approximated by

$$c = c_0 \exp(-\Delta H_S / RT) \tag{74}$$

where c_0 is a constant and ΔH_S is the enthalpy of solution for simple materials.

The solvent is actively involved in the growth process. Changing the solvent can have marked effects on the crystals; e.g., the shape may change. In many cases, small amounts of other materials are added to solvents to produce the desired effects; for discussion, see [3] and [26].

Table 5. Solvents for high-temperature solution growth

Solvent	Solutes
Lead difluoride, PbF_2	$ZnAl_2O_4$, ZnO
Lead oxide + lead difluoride, $PbO + PbF_2$	$Y_3Fe_5O_{12}$ and analogs, Al_2O_3, In_2O_3, $LiGaO_2$
Lead oxide, PbO	Al_2BeO_4, ferrites
Lead oxide + boric oxide, $PbO + B_2O_3$	$Y_3Al_5O_{12}$ and analogs
Bismuth oxide + boric oxide, $Bi_2O_3 + B_2O_3$	$GaFeO_3$, $Pb_3MgNb_2O_9$, garnets
Bismuth oxide, Bi_2O_3	$Bi_4Ti_3O_{12}$
Lead tungstate, $PbWO_4$	$Be_3Al_2Si_6O_{18}$
Potassium carbonate, K_2CO_3	$KTa_x Nb_{1-x} O_3$
Sodium tetraborate + boric oxide, $Na_2B_4O_7 + B_2O_3$	TeO_2
Potassium fluoride, KF	$KNbO_3$, $BaTiO_3$
Silicon, Si	SiC
Platinum, Pt	B
Gallium, Ga	GaAs, GaP, GaN, ZnTe
Tin, Sn	GaAs, ZnTe
Iron or iron + nickel, Fe or Fe + Ni	diamond
Tellurium, Te	CdTe

7.2. Low-Temperature Methods

Figure 36 shows an apparatus suitable for low-temperature solution growth by solvent evaporation.

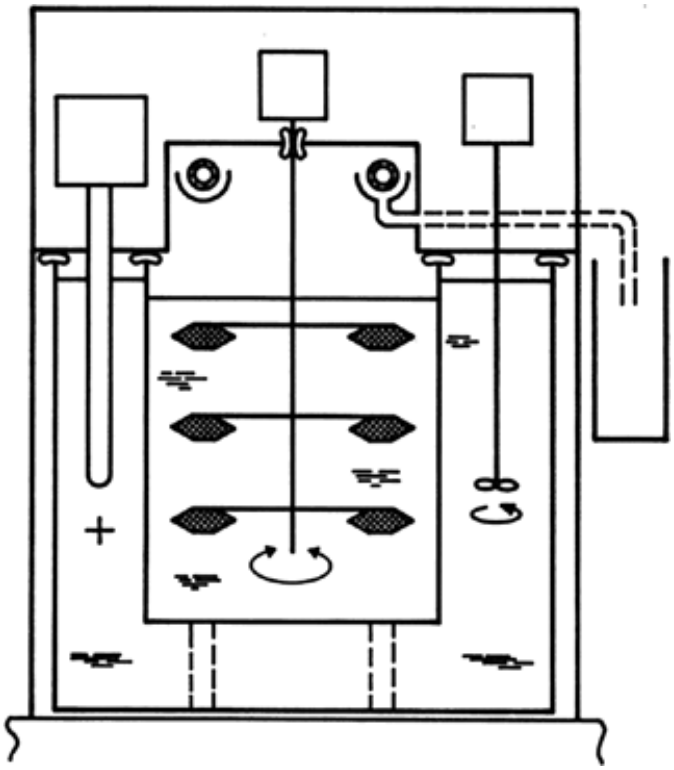

Figure 36. System for low-temperature solution growth by solvent evaporation

The basic components are an outer draught screen, an outer water bath with a propeller stirrer, and an immersion heater. A thermistor (+) below the immersion heater actuates the control system. In the inner solution bath, the crystals grow on seeds cemented to a ''spider'' which is rotated about the central axis alternately in clockwise and counterclockwise directions (one to four revolutions in each direction). The system has gaskets to seal all the joints; this is particularly necessary with deuterated solvents which are contaminated rapidly by atmospheric moisture.

By omitting the cooling pipe (shown hatched) and the gutter, the same apparatus could be used for growth by slow cooling. The solution surface is often covered with an immiscible liquid to suppress evaporation; e.g., a layer of a silicone oil on the surface of an aqueous solution allows the use of high growth temperatures which are not practical when evaporation at the free surface is high. In slow cooling methods, the rates of cooling are usually less than 2 K/d. For a given system, the rate depends on the ratio of the area of the growth face to the volume of the solution and on dc/dT.

Figure 37 shows an apparatus for temperature gradient growth.

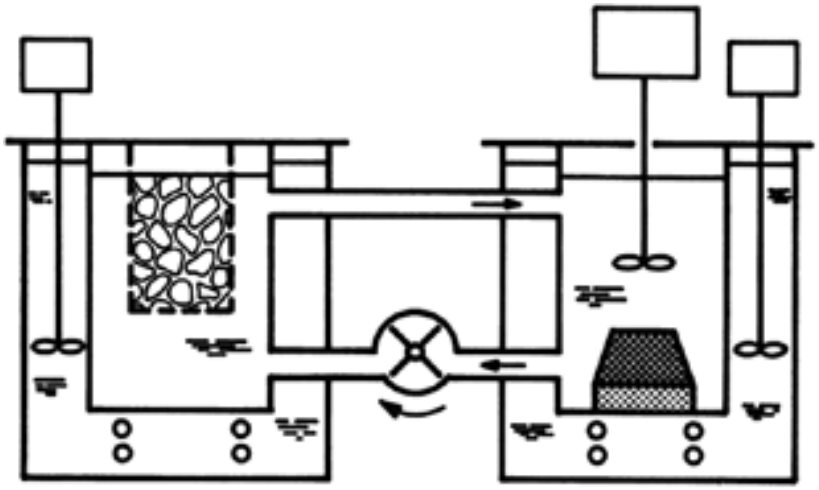

Figure 37. Growth by temperature gradient transfer

The system consists of two vessels in water baths, with appropriate stirring and temperature control. The crystal grows on a seed in the right-hand vessel at a temperature T_g, while in the left-hand vessel solution is saturated at a temperature $T_g + DT$ by solid nutrient in a porous container. Because the centrally located pump can sweep undissolved solute from left to right along the upper pipe, some workers insert an extra tank at a temperature greater than $T_g + DT$ at some point along the upper pipe. Cooling on the upper pipe and heating on the lower one may have to be provided if the temperatures in the two vessels are to be uniform.

In such systems the pump is the critical component: it can easily cause nucleation. Thus any pump should be placed in the flow from the crystallization tank. Pumps should be chosen to produce minimum pressure changes because nuclei tend to form in low-pressure regions.

Typical growth rates are small — usually less than 1 mm/d and occasionally below 0.01 mm/d. Hence, apparatus reliability is vital, and motors and bearings, for example, are usually much more robust than appears necessary for the loads borne. The possibility of power failures must be considered, and backup facilities capable of coping with the longest likely failure must be provided.

Numerous important oxide crystals, especially for applications in conventional and nonlinear optics, piezo- and pyroelectric devices, have long been grown commercially from aqueous solution. By controlling the pH of the solution very large perfect ammonium dihydrogenphosphate (ADP), potassium dihydrogenphosphate (KDP), potassium sodium tartrate (KNT), triglycine sulfate (TGS), and other crystals of dimensions $15 \times 15 \times 56$ cm weighing up to 20 kg (ADP, KDP) can be produced by modified temperature transfer techniques (Fig. 37) in growth periods of up to 6 weeks [4].

Growth from aqueous solutions is becoming increasingly important for the production of crystalline biological macromolecules such as proteins. Commonly, microdialysis cells or liquid–liquid diffusion of a solvent or solute into a macromolecular solution are used. Crystallization results from gradual change in a property of the protein solution, such as pH. Crystals of small dimensions in the range of some hundred micrometers are obtained, suitable for structural X-ray and neutron diffraction analysis. However, the crystallization of biological macromolecules is a complicated multiparameter

process, and extensive efforts are still required to understand the interactions of protein molecules in solution that govern nucleation and crystallization. More detailed information about this new important multidisciplinary branch of crystal growth are given in [164,165].

7.3. High-Temperature Methods

High-temperature solution growth is sometimes called *flux growth* or *growth from a fluxed melt* because the solvents (Table 5) are often the fluxes used to dissolve oxide and other scum from metal surfaces. The principles involved are similar to those in low-temperature solution growth, but the technology differs because of the high temperatures and reactive liquids used. Solvent evaporation has been used in research, but only slow cooling and — to a minor extent — gradient transfer are used commercially.

For seeded growth, equipment is often arranged so that a seed attached to the crucible walls is not in contact with the solution until immediately prior to growth. This allows some superheating of the solution, which is necessary to ensure that no solid particles remain. When the solution is cooled to near its saturation temperature, the crucible is tilted or even rotated by as much as 1808 about a horizontal axis to bring the seed into contact with the solution. At the end of growth, the tilting is reversed. To provide stirring, use is made of the accelerated crucible rotation technique (Section Boundary Layers), in which the crucible is rotated alternately clockwise and counterclockwise about a vertical axis (Fig. 38). The construction involves welded joints at the top and bottom of the crucible. With care, the welds can be cut, the crystal removed, fresh nutrient added, a new seed fastened on, and the crucible resealed. Furnaces are made from ceramic tubes and bricks, with outer metal cases and refractory-wool thermal insulation. The heating elements are often silicon carbide rods which should not be operated at temperatures much higher than about 1300 8C.

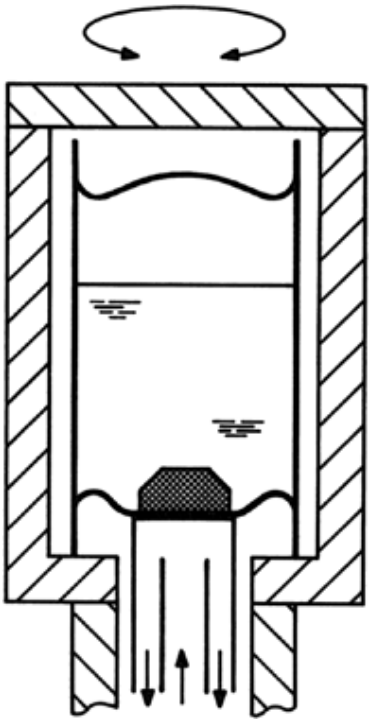

Figure 38. Crucible system for seeded high-temperature solution growth
Gas cooling is used to ensure that the seed is at the coldest point

A spherical platinum crucible, optimal for forced convection arround the vertical axisand separation of the as-grown crystal from the flux by rotating around the horizontal axis, has been used to grow high-perfection yttrium iron garnet (YIG) crystals of about 100 g [89].

Figure 39 shows a gradient transfer system that can be conveniently placed in a heated ceramic tube. In such systems, the bottom of the crucible can easily be well insulated; radiative and convective heat loss from the top of the system then maintains the indicated temperature difference D*T*.

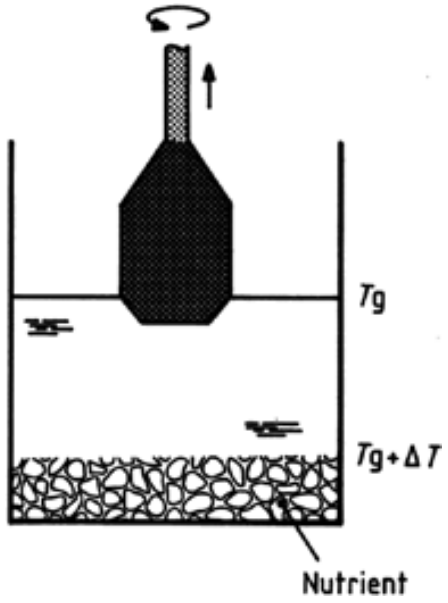

Figure 39. Crucible arrangement for seeded high-temperature solution growth by the gradient transfer method

For fluxes of low volatility, which allow the use of open crucibles, crystals can be grown at the surface of the melt when its temperature is lower than at the bottom. A seed crystal is introduced, as in Czochralski growth, but with a very small temperature gradient. The crucible temperature is continuously lowered at a cooling rate of 0.1–5 K/h. Such top-seeded solution growth (TSSG) is successfully applied to numerous perovskites and garnets.

High-temperature solution growth is widely used to produce thin crystalline plates of high-temperature superconductors like yttrium barium cuprous oxide $YBa_2Cu_3O_{7-x}$[166]. Flux growth under high pressure is becoming important for the growth of GaN plates from Ga-rich solutions [167]. Specimens of good quality have been grown at 1400–1500 8C in 20 h under high N_2 pressure. They are attractive as homoepitaxial substrates for GaN thin-film deposition. However, an increase of the area from presently a few mm^2 to 100 mm^2 is required before any commercial fabrication of blue lasers on GaN substrates could be started.

Small diamond crystals are produced from graphite by dissolving in metallic fluxes (Ni, Co, Mn) at 5–6 GPa and about 1500 8C [4].

Another form of temperature gradient growth is practiced by passing a solution zone along a rodlike bar. This can be done by making an assembly composed of a seed crystal, a disk of material with the initial solution composition, and a nutrient rod (probably of pressed powder) with the composition of the crystal to be grown. If this assembly is placed in a temperature gradient such

that the seed is at the coldest point, the solution will migrate up the temperature gradient by dissolving nutrient at the hot face and depositing solid at the cold face. This process has the disadvantage that the growth temperature (i.e., the cold face temperature) rises as growth proceeds. The system shown in Figure 40, known as the travelling heater method (THM), overcomes this problem by having a stable zone length due to the use of a zone heater with a temperature maximum between the dissolving and solidifying interfaces. This method has been applied successfully to growing semiconductor mixed crystals such as (Ga,In)P and (Hg,Cd)Te with reduced dislocation density and homogeneous axial composition distribution [4,168].

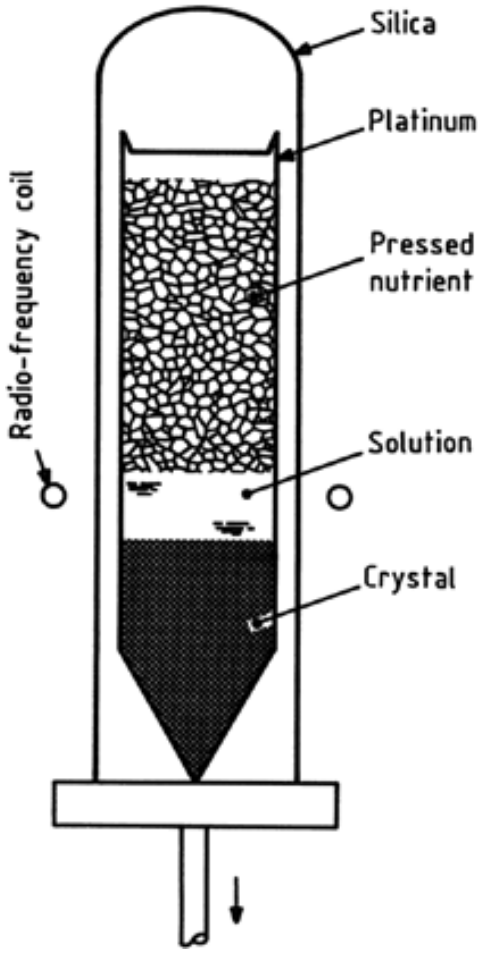

Figure 40. Traveling heater solution growth

7.4. Liquid-Phase Epitaxy

Liquid-phase epitaxy (LPE) consists of a set of methods used for growing thin layers onto substrates. Epitaxy implies that the film and substrate have identical structure. However, in current usage the word means that the film is a single crystal with some crystallographic relation to the substrate. Often, but not always, the film and substrate have a common symmetry axis. Films on substrates can be strained elastically (Section Phase Relations for Minor Components). This strain can be so large that brittle materials crack and other materials suffer plastic deformation, giving rise to edge dislocations.

These usually have a U shape, with the open end at the substrate surface and the closed end at a distance of about 2 h_c from that surface. It is possible to show that dislocations will not occur until the layer has a thickness h_c such that

$$h_c \approx \frac{3\,ba}{32\,\mathrm{D}a}\ln(h_c/b + 1) \tag{75}$$

for an abrupt change of the lattice constant by an amount Da. Complete relief of the elastic strain then suggests a dislocation density

$$N_D \approx 4(\mathrm{D}a/ab)^2 \tag{76}$$

but this neglects the energy needed to create the dislocations, and in general N_D is much lower than predicted by Equation (73). The discrepancy is usually a factor of 10 to 100. A reasonable empirical estimate is

$$N_D \approx 0.1(\mathrm{D}a/ab)^2 \tag{77}$$

In practice, abrupt junctions are rare: some interdiffusion will occur and when the strain is $s \approx \mathrm{D}a/a$, then the same geometrical arguments used to derive Equation (73) show that a dislocation density of $N_D \approx (1/b)(s/h)$ is obtained, where h is the distance from the substrate surface. Again this value is an overestimate. However, for $s \approx 0.1$ %, dislocation densities of 10^9–10^{10} cm^{-2} have been observed in regions within a few micrometers of the substrate surface. For further general discussion of epitaxy, see [169-171].

A wide variety of LPE methods have been used in research [56]. However, only two are employed on a large scale: the *dipping method* (see Fig. 41 for a representative example) and the *sliding boat process* (see example in Fig. 42). Dipping processes are used mostly for oxidic materials, and sliding boat processes for semiconductors.

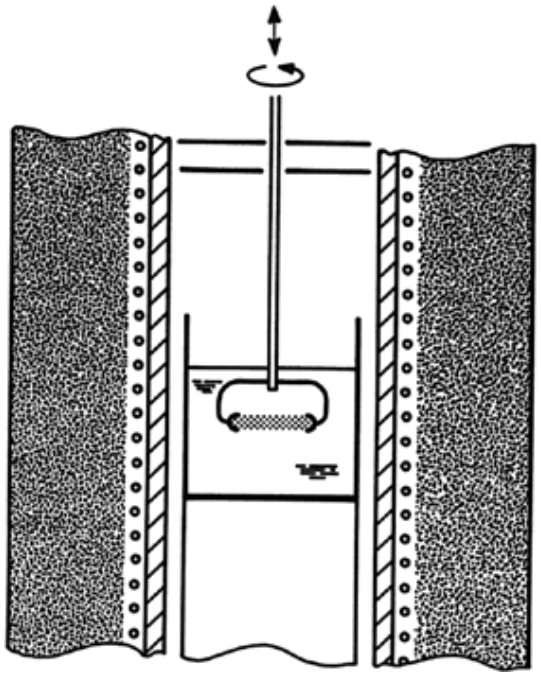

Figure 41. Liquid-phase epitaxy (LPE) by dipping
To produce growth, either the solution is supersaturated before the substrate is dipped, or it is marginally undersaturated before dipping and cooled while the substrate is immersed

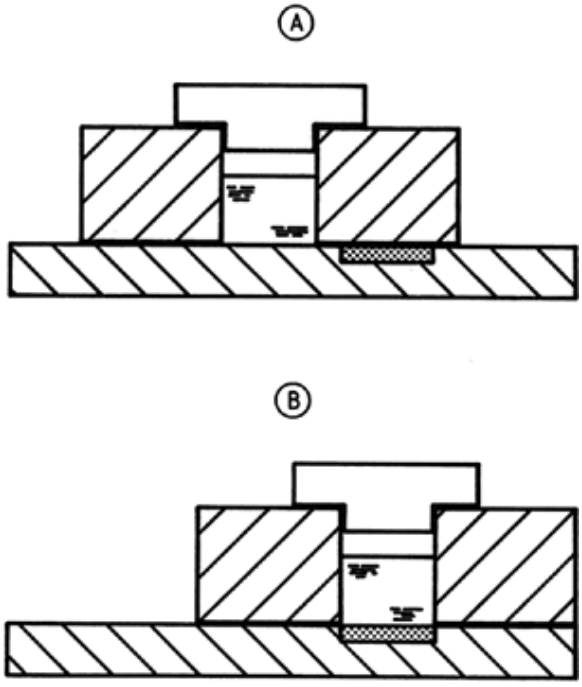

Figure 42. Liquid-phase epitaxy (LPE) in a sliding boat
Growth is produced by either supersaturating the solution before it is moved onto the substrate or cooling while it is over the substrate

Now as before, LPE is the most widley used thin-film deposition technique for large-scale production of light emitting diodes based on III-V semiconductors. The annual world production of LEDs amounts to 500×10^9.

Further information about LPE is given in references [53,56], and [169-171]. Detailed reviews on fundamentals and technology of LPE are given in [172,173].

7.5. Electrolytic Methods

Electroplating is a familiar process, and by using electrically conducting single-crystal substrates, single-crystal layers can be grown [174]. Bulk crystals can also be grown, but in general the process is rather slow. Thin layers of semiconductors have been grown from metallic solutions by this method; there is some dispute as to whether the principal effect is electroplating or whether growth results from the Peltier cooling which occurs at the semiconductor–metallic liquid interface. Both processes probably occur, and by suitable arrangement of the system, either can be made dominant. Layers can also be grown from nonmetallic solvents [175]. The limitation to conducting materials on conducting seeds, together with the fact that the process offers no particular advantages and some technological problems (e.g., the need to have both conducting and insulating materials in contact with the solution), has restricted the use of growth by electroplating, and there is no sign of its commercial use.

However, electroplating is only one of many electrolytic processes, and the use of electrolysis to change the valences of dissolved ions may be more important than direct electrolytic transport. The processes used include

1. Decomposition of the solvent to yield a supersaturated solution of the product, which is composed of atoms that were originally part of the solvent, e.g., MoO_2 crystals grown by electrochemical decomposition of $K_2Mo_2O_7$ at 600 8C
2. Decomposition of the solvent to reduce the solubility of a solute, e.g., the growth of $Co_x V_{3-x} O_4$ from solution in $Na_2WO_4 + WO_3$

For further information about these processes which can yield a wide variety of oxides, borides, carbides, phosphides, sulfides, and arsenides, see [176]. None of the processes seems to have been exploited commercially.

7.6. Hydrothermal Growth

Temperature gradient transfer under hydrothermal conditions is used on a large scale for the growth of quartz. Hydrothermal conditions are taken to be temperatures and pressures near the critical values (i.e., 374.2 8C and 221.23 bar) (Fig. 6). Thus, hydrothermal growth could be regarded as intermediate between solution growth and vapor growth. In practice, the solvent is almost invariably a solution of a mineralizer in water; the mineralizer and the solute decrease the saturation vapor pressure and increase the critical temperature. In general, temperatures are less than 400 8C and pressures exceed 250 bar so that the solution is usually a liquid. The mineralizers are usually alkaline (NaOHor, less often, Na_2CO_3 for quartz), but neutral (e.g., alkali metal halides) or acidic (e.g., HI, HBr) mineralizers are also used.

Figure 43 is a schematic sectional view of an autoclave system which exaggerates the horizontal dimensions. Typical autoclaves for pressures over 1000 bar have ratios of height to internal diameter in the range of 16–20, and heights can be 8 m or more. For lower pressures, larger diameters (up to 1 m) and smaller heights (2.5 m) are used. The optimum ratio of external to internal diameter is 1.8–2.5. Thicker walls do not give appreciably higher working pressures.

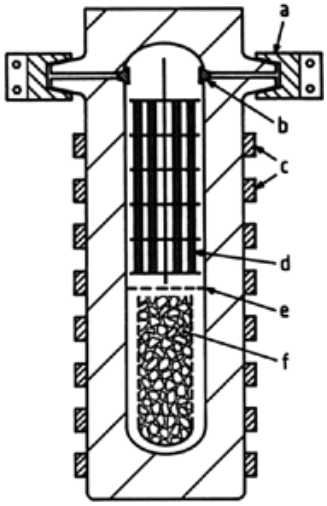

Figure 43. Hydrothermal growth
a) Split clamp; b) Seal ring; c) Heating elements; d) Crystals; e) Baffle; f) Granular nutrient in porous basket

The autoclave is loaded by putting the seed crystals in suitable racks, loading granular nutrient into the basket, and filling about 75 % of the free volume with the mineralizer solution. The concentration of this solution is usually about 1 mol/L. The autoclave is then sealed and heated to its working temperatures, e.g., 380 8C below the baffle and 350 8C above the baffle. The growth rate rises with the upper temperature, the temperature difference, the degree of fill (which governs the working temperature), the mineralizer concentration, and the amount of opening in the baffle (typically 2–10 %). For most applications of quartz, the growth temperature should be high, the mineralizer concentration should be less than 1 mol/L, and the other conditions are adjusted to limit the growth rate to less than 1 mm/d. Departing from these conditions gives crystals with too large a hydrogen content or too much other impurity to be useful in critical applications. According to the specifications to be met [177], the hydrogen content should not exceed about 200 atomic ppm (based on silicon); at higher hydrogen content, quartz is rather brittle. In current systems, up to 500 kg of quartz is grown in one run. Typical individual crystals weigh from a few hundred grams to several kilograms. For further data, see [47, Chap. 8], [54, Chap. 7.3] and [55, Chaps. 6 and 7]. A review is given in [178].

8. Vapor Growth Techniques

8.1. Sublimation and Evaporation Methods

Growth by evaporation and subsequent condensation is used widely to make thin epitaxial layers [133] and bulk crystals of a few materials (mostly compounds of cadmium or zinc with sulfur, selenium, or tellurium.)

For an element (e.g., zinc), two methods are available. The material can be evaporated in a vacuum and condensed on some region which is on the line of sight from the source, or it can be evaporated into a gas stream which can be conveyed around corners provided it is not cooled until the deposition region is reached. With compounds, the choice of methods is larger. Some compounds evaporate congruently; these can be treated like the elements. However, most compounds do not evaporate congruently. For these, multiple sources (one for each component) can be used. Thus, vacuum evaporation or evaporation with one gas stream per component into gas streams that are combined in the deposition region can be employed. However, only one source can be used for vacuum evaporation if a small volume of the material is vaporized at one time. This process, called *flash evaporation,* can be achieved in several ways. For example, grains of the compound are dropped onto a plate heated to a very high temperature, or a bulk solid is exposed either to a laser beam [179], which is scanned over the solid surface and run in a pulsed mode (*laser-assisted evaporation*), or to an energetic gas plasma (*sputtering*) [180]. Other possibilities also exist: for example, one component can be evaporated into an inert gas stream which in the deposition region reacts with a gas:

$$\mathrm{Cd(g)} + \mathrm{H_2S(g)} \rightarrow \mathrm{CdS} + \mathrm{H_2} \qquad (78)$$

where the CdS is first formed as a supersaturated vapor which then deposits, usually as plates of the solid. For further information, see [57].

Bulk growth from the vapor has become important for two optoelectronic materials: ZnSe and SiC. Both compounds are of special interest for blue and blue-green light emitting diodes and lasers.

Moreover, SiC is a suitable substrate for GaN epitaxy as well as for high-temperature high-power microelectronics. ZnSe monocrystals with diameters up to 6 cm and lengths of 3 cm are grown by seeded physical vapor transport [181]. SiC crystals are produced by the sublimation–condensation method in modified Lely reactors made of graphite, as shown in Figure 44[182].

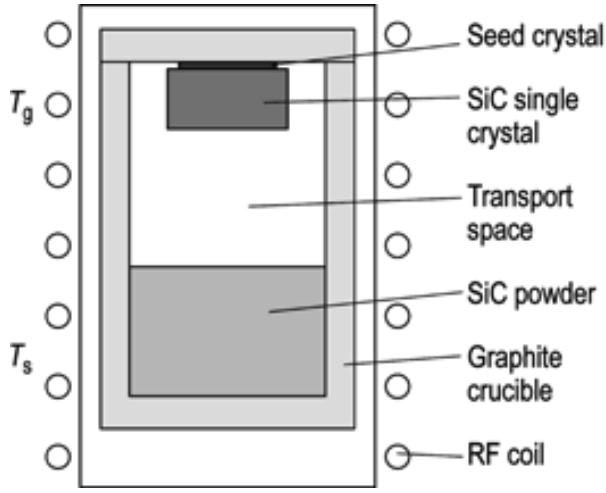

Figure 44. Schematic of a Lely reactor for the vapor growth of SiC single crystals (T_s = sublimation temperature, T_g = growth temperature)

Temperatures of ≥ 2200 8C are required for evaporation. The seed wafer is mounted to directly face the source of SiC powder. Usually, induction heating with frequency of 10 kHz or about 1 MHz and an argon atmosphere with a pressure of 130–5300 Pa are employed during growth at rates of 0.2–2 mm/h. Boules with diameters of 3–5 cm and a length of 2 cm are already produced commercially. Diameters 7.5 cm and 10 cm are under investigation. The main efforts are still directed towards the control of characteristic polytypes, lowering of dislocation density, and preventation of micropipes for growth in the <0001>direction. Such holes, with diameter of several micrometers, are caused by the strain field arround screw dislocations combined with the large value of the Burgers vector in this material. More information is given in [182].

8.2. Molecular Beam Epitaxy

Molecular beam epitaxy (MBE) is a refined evaporation process. Conventional evaporation sources have a rate of evaporation governed by the area of the evaporant and its temperature (or the partial pressure of the evaporant in the source region). Most MBE sources have large evaporant areas but are almost sealed. The rate of efflux from the source is governed by the area of the opening in the source and the partial pressure of the evaporant inside the source. Outside the source, the atmosphere is almost invariably an ultrahigh vacuum (usually less than 10^{-12} bar). Figure 45 shows the working region of a system and a typical source. To minimize the time to reach the desired vacuum, the substrates and sources are often loaded and unloaded through a vacuum lock so that the main vacuum system is not routinely exposed to the atmosphere. The extreme vacuum used enables MBE films to be grown with very low substrate temperatures (< 100 8C), but in general, somewhat higher temperatures are needed (e.g., 200 8C) to obtain the desired properties. In the MBE growth of binary compounds, the flux of one component usually governs the growth rate, provided the other is available in excess; the excess of noncritical component is not consumed [183].

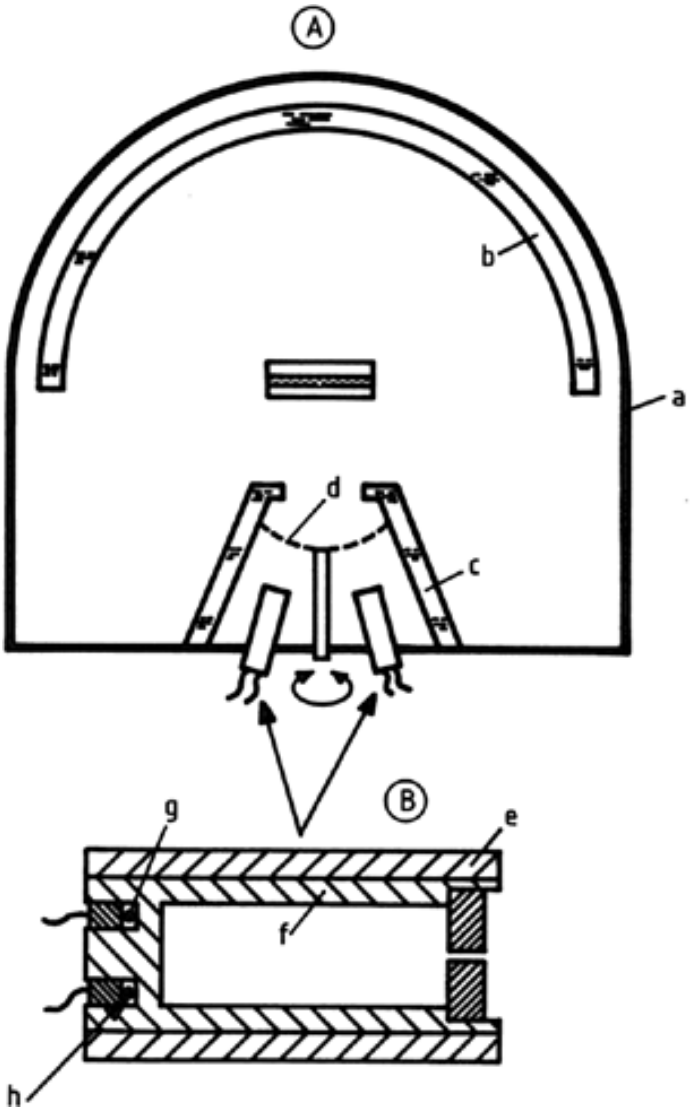

Figure 45. Simple system for molecular beam epitaxy (A) and typical source (B)
a) Outer vacuum jacket; b) Cryogenic screens; c) Source holders; d) Shutters; d) Cylindrical heater; f) Crucible; g) Thermocouples; h) Heater

Molecular beam epitaxy is a powerful method for making multiple-layer structures, such as multiple sandwich structures containing alternate layers of GaAs and AlAs, only two or three atomic layers thick. Such superlattices or quantum well materials have properties that differ radically from either bulk crystal [184]. Very sharp composition changes with dopants can also be obtained. However, MBE is usually a very slow process. Growth rates rarely exceed 1 mm/h so that the method is only viable for very thin layers. Molecular beam epitaxy is used in the production of semiconductor devices to a rapidly increasing extent. For further information, see [171] and [184-135].

8.3. Chemical Vapor Transport

The bulk polycrystalline silicon, the nutrient material used in the Czochralski and floating zone processes, is prepared by decomposing volatile silicon compounds on hot silicon filaments by reactions

of the type

$$2\,SiHCl_3 + 2\,H_2 \rightarrow 2\,Si + 6\,HCl$$

Such reactions can be used to deposit single crystal films onto single crystal substrates. This type of process is usually described as vapor-phase epitaxy (VPE). Because the reactants are produced outside the growth system, VPE is not strictly identical to chemical vapor deposition (CVD) in the sense described [186,187], which involves in situ reactions such as

$$CdS(s) + I_2(g) \rightleftharpoons CdI_2(g) + \tfrac{1}{2}S_2(g) \tag{79}$$

However, all depositions involving chemical reactions are now described as CVD which is taken to include also mixed forms, for example,

$$AsCl_3 + Ga \rightarrow GaCl_3 + \tfrac{1}{2}As_2 \tag{80}$$

$$GaCl_3 + \tfrac{1}{2}As_2 + \tfrac{3}{2}H_2 \rightarrow GaAs + 3\,HCl \tag{81}$$

(the reactions are schematic only). The $AsCl_3$ is provided from an external source.

Figures 46-48 give examples of these three types of growth. The first and last of these processes are widely used, and in some cases, there is an advantage in using a reduced pressure which increases the diffusion coefficients to give faster growth. For the growth of semiconducting compounds, use of the appropriate organometallic compounds can be a significant advantage [188].

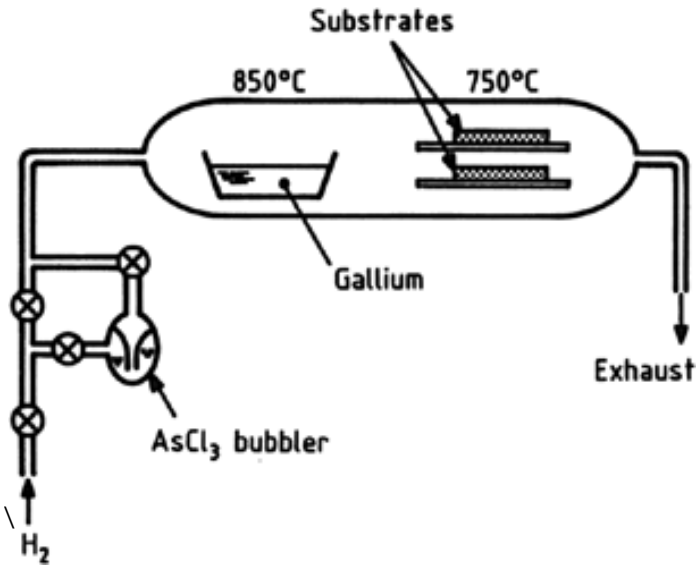

Figure 46. Vapor-phase epitaxy of gallium arsenide

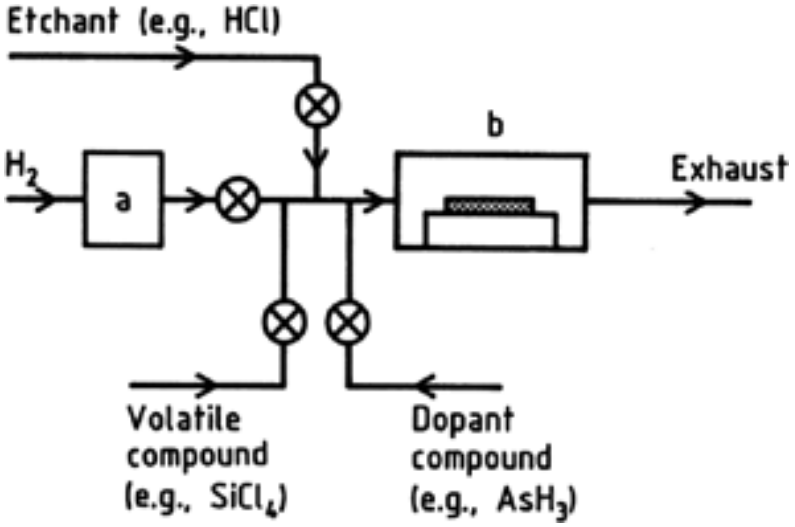

Figure 47. Vapor-phase epitaxy of silicon
a) Purifier; b) Reactor (1100–1200 8C)
Commercial reactors may contain up to 100 substrates; in these large reactors, the susceptor (often heated by radiofrequency) is tilted so that a greater gas flow rate (thinner boundary layer) compensates for the decrease of reactant concentration in the gas after it has passed over many substrates

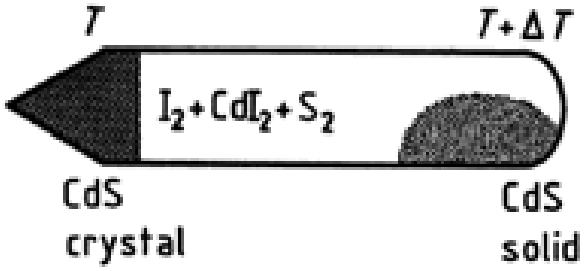

Figure 48. Transport of cadmium sulfide by means of iodine

The use of these materials allows good control over growth so that complex structures composed of very thin layers can be grown. These structures have electronic properties not exhibited by bulk samples [189,190]. Table 6 gives some examples of the layers that can be grown and the reactants used. For further information on VPE and CVD, see [54,55,57,170,171,191-197]. Organometallic vapor-phase epitaxy is summarized in [198]

Table 6. Organometallic chemical vapor deposition

Layer	Substrates	Reactants	Growth temperature, 8C
AlAs	GaAs, Al_2O_3	$Al(CH_3)_3 + AsH_3$	700
AlN	Si, Al_2O_3, a-SiC	$Al(CH_3)_3 + NH_3$	1250
CdS	Al_2O_3	$Cd(CH_3)_2 + H_2S$	475
CdSe	Al_2O_3	$Cd(CH_3)_2 + H_2Se$	600
CdTe	Al_2O_3, BeO, GaAs	$Cd(CH_3)_2 + Te(CH_3)_2$	500
GaAs	GaAs, Ge, Al_2O_3	$Ga(CH_3)_3$ or $Ga(C_2H_5)_3$ + AsH_3	650–700
$GaAs_xP_{1-x}$	GaAs, $MgAl_2O_4$	$Ga(CH_3)_3 + PH_3 + AsH_3$	700–725
$Ga_xIn_{1-x}As_yP_{1-y}$	InP	$Ga(CH_3)_3 + In(CH_3)_3 + AsH_3 + PH_3$	670
GaN	Al_2O_3, a-SiC	$Ga(CH_3)_3 + NH_3$	950
GaP	GaAs, Si	$Ga(CH_3)_3 + PH_3$ or $P(C_2H_5)_3$	700 or 500
ZnS	Al_2O_3, BeO	$Zn(C_2H_5)_2 + H_2S$	750
ZnSe	Al_2O_3, $MgAl_2O_4$	$Zn(C_2H_5)_2 + H_2Te$	725
ZnTe	Al_2O_3	$Zn(C_2H_5)_2 + Te(CH_3)_2$	500

8.4. Vapor-Liquid-Solid Growth

In 1964 [37] the vapour-liquid-solid (VLS) mechanism was proposed for the first time to use such phase transition sequence for the growth of whisker crystals. A review is given by SIVARGIZOV, *Rost nitevidnykh i plastinchatykh kristallov iz para.*, Nauka, Moscow 1977. Today, such mechanism is of increasing importance for controllable production of nanowires and nanometer-sized structures–a rapidly expanding area with numerous applications, e.g., in electronics, photonics, biology, and medicine [199]. In the VLS growth mechanism, the reactants are supplied in the vapor phase by MBE, MOCVD, for example, and the diameters of the crystal whiskers are dictated by the size of metallic seed particles acting in molten form as localized solvent on a substrate. The material to be grown translates first from the vapor into the droplet due to the much higher absorption rate at the vapor–liquid surface compared with that at the surrounding solid substrate surface. The crystallization starts at the melt–solid interface between the droplet and substrate. The driving force for crystallization is the supersaturation within the droplet, which is continuously maintained by the material supply diffusing from the vapor–liquid interface to the liquid–solid one. As a result, a crystalline wire is growing under the continuously raising microdroplet (Fig. 49).

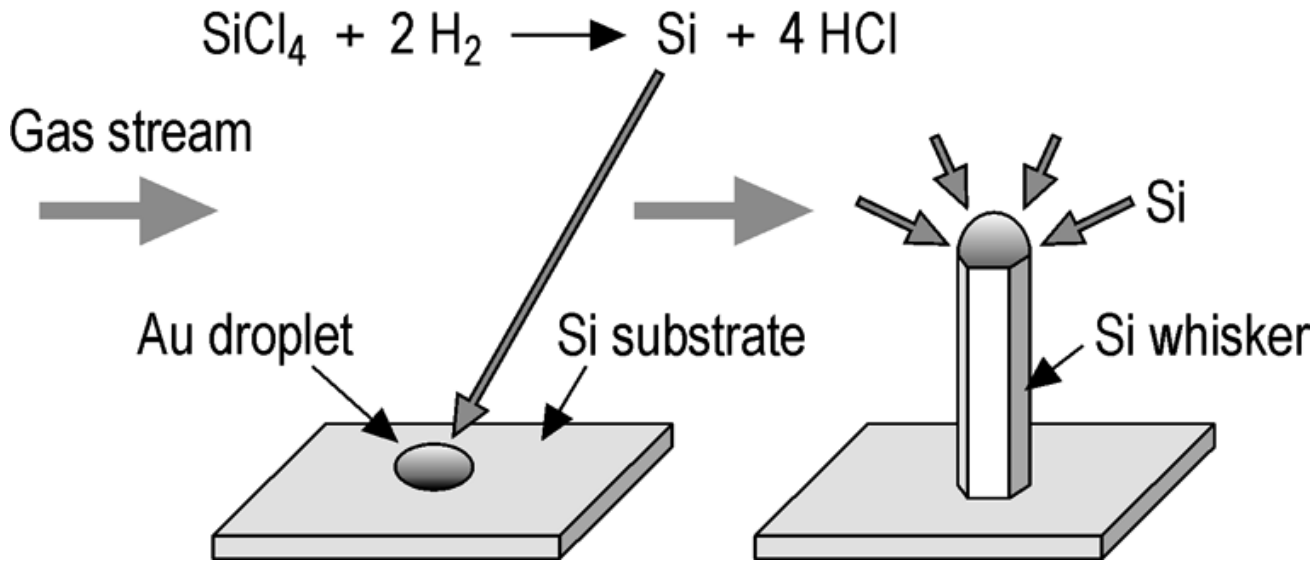

Figure 49. The VLS mechanisms demonstrating the growth of a silicon whisker crystal by using a gold microdroplet as solvent during a CVD or MOCVD process

9. Solid-Phase Growth Techniques

9.1. Strain–Anneal Method

Before methods for handling materials without contamination were developed, growth from the solid state had very significant advantages. Contamination from surfaces in contact with other solids or with reactive atmospheres penetrated only a small distance because diffusion in the solid state is usually several orders of magnitude slower than in a liquid phase. Also, the apparatus was simple: almost any furnace would serve. At that time, the great interest was in metals or other ductile materials that could safely be strained. Later interest centered on rather brittle materials and, usually, on crystals with great crystallographic perfection. Thus, solid-phase growth techniques which tend to produce heavily dislocated crystals are of interest only when rather imperfect crystals of ductile materials are needed, such as materials with low loss and high permeability for very efficient transformers and motors.

In the strain-anneal method, the sample is first heated to a temperature high enough to ensure that it is not brittle (about half the absolute melting temperature for metals) and then subjected to a strain, usually between 1 and 10 %. The strain employed is critical. If s_{opt} is the optimum strain, then strains less than 0.9 s_{opt} or larger than 1.5 s_{opt} will be less effective by a factor of two or more. The second stage of the process is annealing, which may be carried out to advantage with a temperature gradient across the sample. The annealing temperature is usually at an absolute temperature *T* which

is an appreciable fraction (50–95 %) of the melting temperature on the same scale. If growth is going to occur, it is usually fast: 5–50 mm/h can be expected, but much higher rates (about 1 m/s) have been recorded [200]. The free energy to drive the process is the excess energy attributable to dislocations or small clusters of dislocations and grain boundaries. Ordered arrays of dislocations (small-angle grain boundaries) have lower energies per dislocation than isolated dislocations so that many samples grown by the strain-anneal method contain low-angle boundaries. For further data, see [4,54,201].

9.2. Methods Not Involving Applied Strain

In theory, the excess free energy of grain boundaries should be a driving force for crystallization. Although the energy per dislocation in a grain boundary is less than that for isolated dislocations, reducing the area of the boundaries (i.e., increasing the grain size) should decrease the sample free energy. This process occurs in many materials: metal workers exploit it on a large scale to control the properties of their materials. The extend to which it occurs is often related to purity. In particular, precipitated impurities stop grain boundary movements, and a common method for obtaining hard or creep-free metals is to add impurities that migrate to the grain boundaries. Thus, if impurities can be removed, grain growth can be expected. Solid-state electrolysis removes impurities and also heats the samples. To be effective, solid-state electrolysis should involve large current densities (several amperes or even hundreds of amperes per square centimeter). Subsidiary heating can be applied to raise the sample temperature to a suitable value (55–90 % of the absolute melting temperature is usual). Growth rates can be 3–50 mm/h. For further information, see [202] and [203].

9.3. Solid-Phase Epitaxy

A solid in an amorphous (glassy) state has a higher free energy than the same solid in the form of a single crystal. The recrystallization of silicate glass over the centuries is a familiar process. This process is slow but can be accelerated by heating. It is now possible to create amorphous samples of many materials such as metallic alloy glasses by rapid quenching, and amorphous semiconductors by sputtering, for example, in hydrogen. For semiconductors, selective recrystallization of amorphous layers is now practiced on an increasing scale by the use of layer heating or other energy beam techniques [204-212]. Spatial control gives this process an obvious advantage. A less obvious but still significant advantage is that layers with much higher doping densities can be made by this method than by any other. Indeed, dopant concentrations can exceed the maximum equilibrium value.

9.4. Gel Growth

Gels can be regarded as soft pseudosolids. They are actually three-dimensional solid skeletons with liquid-filled interstices. The solid phase is often a network of silicon atoms surrounded by oxygen atoms in a tetrahedral geometry, which is made by hydrolysis of sodium silicate at about pH 8. Other gel-

forming materials include gelatin, pectin, or potassium salts of fatty acids. Crystallization in a gel has the advantage of occurring in a strain-free environment, which is useful for some fragile solids that can deform under their own weight. Growth is usually produced by diffusing two solutions (one from each side of the gel) so that a supersaturated solution is created within the gel. With care or by providing a seed, one crystal can be grown. The diffusion rate in the gel is only slightly lower than in the pure fluid phase so the gel process is relatively rapid. The size L of a crystal generally increases with the square root of the time. This gives rapid growth when L is small but rather slow growth as L increases. Typically, L^2 increases at rates measurable in units of square millimeters per day or per week.

Examples of pairs of diffusants are:

1. Aqueous $(NH_4)_2CO_3$ and aqueous $CaCl_2$ to yield $CaCO_3$ crystals
2. CuCl in hydrochloric acid and pure water to yield CuCl crystals
3. Aqueous $AgNO_3$ and sulfuric acid to yield Ag_2SO_4 crystals
4. $Pb(CH_3COO)_2$ in acetic acid and aqueous KI to yield PbI_2 crystals

The technique does not appear to be used commercially. For further information, see [59].

10. Trends

Many methods are obviously available for crystal growth. The extent to which various methods are now used is discussed in Section Commercial Aspects, which shows that only few methods are employed to any significant degree. As the range of materials and uses increases, other methods will be employed more often; for example, the use of thin-film techniques is increasing. Table 7 gives production rates and their trends for the more extensively produced materials. Two other trends are also obvious. The first is that for economic reasons, larger crystals will be demanded. Costs of growth and subsequent processing decrease as crystal sizes increase. The second trend is the increasing demand for higher quality because greater purity and perfection, as well as tighter control over dopant distribution, are needed to raise yields and device performance. Decreases in device dimensions and increases in yields may change the quantities of particular materials needed, and some substitution of noncrystalline materials can be expected, e.g., amorphous semiconductors. However, an increasing demand for crystals and for crystals grown to tighter specifications can confidently be expected. To meet these demands at reasonable cost will require better apparatus with more extensive use of automation and better understanding of the mechanisms of crystal growth. Thus, although fewer people may be involved with crystal production, more effort is likely to be required in process development and research.

Table 7. Annual production rates and trends

Crystal [a]	Production [b]>, t/a	Trends [c]
Silicon	10 000	up
Metals	4000	up [d]
Quartz	2500	constant
III-V compounds [e]	800	constant
Ruby	500	down
Alkali halides	400	down
Germanium	400	constant
Garnets	100	up
Lithium niobate	100	up
Phosphates [f]	20	down
Lithium tantalate	15	constant
Cubic zirconia	2000	up
TGS [g]	10	constant
Diamond	10	up
II-VI compounds [h]	5	up

[a] Crystals of more than 100 other materials can be bought.
[b] Averages; data for Russia, China, etc., are rare so that errors could range from —20 % to + 30 %.
[c] Trends are averaged; some materials show rapid fluctuations, e.g., quartz.
[d] The upward trend for metal crystals is very rapid.
[e] GaAs, GaP, InP, InSb, etc.
[f] Ammonium and potassium dihydrogen phosphates and their analogs.
[g] Triglycine sulfate and similar materials used mainly for pyroelectric devices.
[h] CdS, CdTe, etc.

REFERENCES

1. A. van Hook: *Crystallization*, Reinhold Publ. Co., New York 1961.
2. J. G. Burke: *Origin of the Science of Crystals*, University of California Press, Berkeley 1966.
3. H. Scheel in D. T. J. Hurle (ed.): *Handbook of Crystal Growth*, vol. 1a, North Holland Publ., Amsterdam 1993, p. 1.
4. K.-Th. Wilke, J. Bohm: *Kristallzu¨chtung*, VEB Deutscher Verlag der Wissenschaften, Berlin 1988 und Verlag H. Deutsch, Thun, Frankfurt/M. 1988.
5. A. Verneuil, *Compt. Rend.* 135 (1902) 791.
6. A. Verneuil, *Ann. Chim. Phys.* 3 (1904) 20.
7. G. Spezia, *Accad. Sci. Torino Atti a. Sci. Fis. Mat. Nat.* 40 (1905) 254.
8. G. Spezia, *Accad. Sci. Torino Atti a. Sci. Fis. Mat. Nat.* 41 (1905) 51.
9. G. Spezia, *Accad. Sci. Torino Atti a. Sci. Fis. Mat. Nat.* 44 (1908) 95.
10. A. Sauveur, *Proc. Int. Assoc. Test. Mater. 6th Congress* 11 (1912) Section 1.

11. J. Pintsch, *Grosses Jahrb. Radiotechn. und Elektrotechnik* 15 (1918) 270.
12. J. Czochralski, *Z. Phys. Chem. (Leipzig)* 92 (1918) 184.
13. R. Nacken, *Zs. Instrumentenkunde* 36 (1916) 12.
14. S. Kyropoulos, *Zs. anorg. allg. Chemie* 154 (1926) 308.
15. F. Koref, *Z. Elektrochem.* 28 (1922) 511.
16. G. Tammann: *Lehrbuch der Metallographie*, Leopold Voss, Leipzig 1914.
17. P. W. Bridgman, *Proc. Am. Acad. Arts Sci.* 60 (1925) 303.
18. F. Stober, *Z. Kristallogr.* 61 (1925) 299.
19. D. C. Stockbarger, *Rev. Sci. Instrum.* 7 (1936) 133.
20. P. Kapitza, *Proc. R. Soc. London Ser. A* 119 A (1928) 358.
21. W. Nernst, *Z. Phys. Chem. (Leipzig)* 47 (1904) 52.
22. M. Volmer, *Z. Phys. Chem. (Leipzig)* 102 (1922) 267.
23. W. Kossel, *Nachr. Ges. Wiss. Goettingen Jahresker. Math. Phys. Klasse* 1927, 135.
24. I. N. Stranski, *Z. Phys. Chem. (Leipzig)* 136 (1928) 259.
25. *Discuss. Faraday Soc.* 5 (1949) .
26. H. E. Buckley: *Crystal Growth*, J. Wiley, New York 1951.
27. G. K. Teal, J. B. Little, *Phys. Rev.* 25 (1950) 16.
28. G. K. Teal, E. Buehler, *Phys. Rev.* 87 (1952) 190.
29. W. G. Pfann, *Trans. AIME* 194 (1952) 747.
30. H. C. Theurer, US 3 060 123, 1952.
31. P. H. Keck, M. J. E. Golay, *Phys. Rev.* 89 (1953) 1297.
32. W. G. Pfann: *Zone Melting*, J. Wiley, New York 1958.
33. J. A. Burton, R. C. Prim, W. P. Slichter, *J. Chem. Phys.* 21 (1953) 1987.
34. J. A. Burton, E. D. Kolb, W. P. Slichter, J. D. Struthers, *J. Chem. Phys.* 21 (1953) 1991.
35. Advanced Semiconductors Buyers' Guide 2003/2004, Special issue of III-Vs Review, Elsevier, ûtown û 2005.
36. M.-P. Pileni (ed.): *Nanocrystals Forming Mesoscopic Structures*, Wiley-VCH, Weinheim 2005.
37. R. S. Wagner, W. C. Ellis, *Appl. Phys. Letters* , 4 (1964) 89.
38. H. Nelson, *RCA Review* 24 (1963) 603.
39. B. A. Joyce, *J. Cryst. Growth* 3/4 (1968) 43.
40. H. M. Manasevit, W. I. Simpson, *J. Electrochem. Soc.* 116 (1969) 1725.
41. A. Y. Cho, J. R. Arthur, *Progr. Solid State Chem.* 10 (1975) no. 3,157.
42. H. Hirayama, H. Asahiin D. T. J. Hurle (ed.): *Handbookof Crystal Growth,* vol. 3a, North Holland Publ., Amsterdam1994, p. 184.
43. B. V. Spitsyn in D. T. J. Hurle (ed.): *Handbook of Crystal Growth*, vol. 3a, North Holland Publ., Amsterdam 1994, p. 401.
44. A. Holden, P. Singer: *Crystals and Crystal Growing*, Heinemann, London 1961. I. Tarjan, M. Matrei: *Laboratory Manual on Crystal Growth*, Akademiai Kiado, Budapest 1972.
45. P. Kratochvil: *Crystals*, Iliffe, London 1967.
46. B. R. Pamplin: *Crystal Growth*, Pergamon Press, Oxford 1980.
47. J. C. Brice: *Crystal Growth Processes*, Blackie, Glasgow 1986.
48. A. A. Chernov: *Modern Crystallography III*, Springer Verlag, Berlin 1984.

49. W. A. Tiller: *The Science of Crystallization*, Cambridge University Press, Cambridge, 1991 and 1995.
50. I. V. Markov: *Crystal Growth for Beginners*, World Scientific, Singapore 1995.
51. A. van Hook: *Crystallization*, Reinhold Publ. Co., New York 1961.
52. R. F. Strickland-Constable: *Kinetics and Mechanisms of Crystallization*, Academic Press, New York 1968.
53. J. C. Brice: *The Growth of Crystals from Liquids*, North Holland, Amsterdam 1973.
54. R. A. Laudise: *The Growth of Single Crystals*, Prentice-Hall, Englewood Cliffs 1970.
55. P. Hartman: *Crystal Growth*, An Introduction, North Holland, Amsterdam 1973.
56. D. Elwell, H. J. Scheel: *Crystal Growth from High-Temperature Solutions*, Academic Press, New York 1975.
57. M. M. Faktor, I. Garrett: *Growth of Crystals from the Vapour*, Chapman and Hall, London 1974.
58. F. Rosenberger: *Fundamentals of Crystal Growth I*, Springer Verlag, Berlin 1979.
59. H. K. Henisch: *Crystal Growth in Gels*, Pennsylvania State University Press, University Park 1970.
60. B. Wunderlich: *Macromolecular Physics,* vol. 2, Academic Press, New York 1976.
61. H. L. Anderson: *Physics Vademecum*, American Institute of Physics, New York 1981, pp. 54 and 315.
62. K. Fujiwara et al., *J. Crystal Growth* 243 (2002) 275.
63. A. A. Chernov in E. Kaldis (ed.): *Crystal Growth of Electronic Materials*, Elsevier, Amsterdam 1985, p. 87.
64. J. C. Brice, *J. Cryst. Growth* 28 (1975) 249. J. C. Brice, J. M. Robertson, W. T. Stacy, J. C. Verplanke, *J. Cryst. Growth* 30 (1975) 66.
65. V. M. Glazov, S. N. Chizevskaya, N. N. Glagoleva: *Liquid Semiconductors*, Plenum Press, New York 1969.
66. C. H. P. Lupis: *Chemical Thermodynamics of Materials*, North Holland Publ., New York 1983.
67. A. D. Pelton in P. Haasen (ed.), *Mat. Sci. and Technol.*, vol. 5, VCH Verlagsgesellschaft, Weinheim, Germany 1991.
68. W. Hume-Rothery, J. W. Christian, W. B. Pearson: *Metallurgical Equilibrium Diagrams*, Chapman and Hall, London 1952.
69. P. Gordon: *Principles of Phase Diagrams in Materials Systems*, McGraw-Hill, New York 1968.
70. F. A. Kroger: *Chemistry of Imperfect Crystals*, North Holland, Amsterdam 1973.
71. A. M. Alper: *Phase Diagrams: Materials Science and Technology*, Academic Press, London 1970.
72. A. Prince: *The Constitutional Diagrams of Alloys*, Institute of Metals, London 1956.
73. M. Hansen: *Constitution of Binary Alloys*, McGraw-Hill, New York 1958.
74. R. P. Elliott: *Constitution of Binary Alloys*, First Supplement, McGraw-Hill, New York 1965.
75. F. A. Shunk: *Constitution of Binary Alloys*, Second Supplement, McGraw-Hill, New York 1969.
76. E. A. Brandes: *Smithells Metals Reference Book*, Butterworth, London 1983.
77. G. V. Samsonov: *The Oxide Handbook*, Plenum Publishing, New York 1973.
78. E. H. Levin, C. R. Robbins, H. F. McMurdie: *Phase Diagrams for Ceramists*, American Ceramic Society, Columbus 1964 and 1969 Supplement.
79. E. H. Levin, H. F. McMurdie: *Phase Diagrams for Ceramists*, 1975 Supplement, American Ceramic Society, Columbus 1975.

80. R. H. Doremus: *Glass Science*, J. Wiley, New York 1973.
81. H. Stephen, T. Stephen: *Solubilities of Inorganic and Organic Compounds*, Pergamon Press, Oxford 1963.
82. F. D. Rossini: *Selected Values of Chemical Thermodynamic Properties*, NBS, Washington 1952.
83. JANAF: *Thermochemical Tables*, NSRDS-NBS, Washington 1971.
84. D. E. Gray: *American Institute of Physics Handbook*, McGraw-Hill, New York 1972.
85. W. G. Moffatt: *Handbook of Binary Phase Diagrams*, General Electric Company, Schenectady, continuing.
86. D. P. Woodruff, *The Solid-Liquid Interface*, Cambridge University Press, 1973.
87. J. H. Greenberg, *J. Cryst. Growth* 161 (1996) 1.
88. P. Rudolph, *Prog. Cryst. Growth Charact.* 29 (1994) 275.
89. W. Tolksdorf in D. T. J. Hurle (ed.): *Handbook of Crystal Growth*, vol. 2a , North Holland, Amsterdam 1994, p. 563.
90. H. H. Farrell, J. P. Harbison, L. D. Peterson, *J. Vac. Sci. Technol.* B5 (1987) 1482.
91. P. Rudolph in R. Fornari, C. Paorici (eds.): *Theoretical and Technological Aspects of Crystal Growth*, Trans Tech Publ., Zürich 1998, p. 1.
92. A. Zunger, *MRS Bulletin* 22 (1997) 20;G. B. Stringfellow, *MRS Bulletin* 22 (1997) 27.
93. K. A. Jackson: *Liquid Metals and Solidification*, Amer. Soc. Metals, Novelty, Ohio, 1958, p. 174.
94. D. E. Temkin in N. N. Sirota (ed.): *Mechanism and Kinetics of Crystallization*, Nauka i Technika, Minsk 1964, p. 68.
95. P. Bennema in D. T. J. Hurle (ed.): *Handbook of Crystal Growth*, North Holland, Amsterdam 1993, p. 477.
96. S. Glasstone, K. J. Laidler, H. Eyring: *The Theory of Rate Processes*, McGraw-Hill, New York 1941.
97. W. B. Hillig in W. Kingery (ed.): *Kinetics of High Temperature Processes*, J. Wiley, New York 1959, p. 627.
98. J. C. Brice, *J. Cryst. Growth* 1 (1967) 218.
99. D. Walton, *J. Chem. Phys.* 37 (1962) 2182.
100. D. Walton, *Philos. Mag.* 7 (1962) 1691.
101. W. K. Burton, N. Cabrera, F. C. Frank, *Philos. Trans. R. Soc. London Ser. A* 243, (1951) 299.
102. A. A. Chernov, *Sov. Phys. Usp. (Engl. Transl.)* 4 (1961) 776.
103. P. Bennema, G. H. Gilmer in *Crystal Growth*, An Introduction, North Holland, Amsterdam 1973", Chap. 10".
104. H. J. Scheel, *J. Crystal Growth* 287 (2006) 214.
105. K. T. Zawilski, M. ClaudiaC. Custodio, R. C. DeMattei, R. S. Feigelson, *J. Crystal Growth* , 282 (2005) 236.
106. G. N. Kozhemyakin, *J. Crystal Growth* 257 (2003) 237.
107. E. W. Sparrow, J. L. Gregg, *J. Heat Transfer* 81 (1959) 249.
108. G. Müller, A. Ostrogorsky in D. T. J. Hurle (ed.): *Handbook of Crystal Growth*, vol. 2b, North Holland, Amsterdam 1994, p. 709.
109. F. Dupret, N. van den Bogaert in D. T. J. Hurle (ed.): *Handbook of Crystal Growth*, vol. 2b, North Holland, Amsterdam 1994, p. 875.

110. J. J. Derby et al. in R. Fornari, C. Paorici (eds.): *Theoretical and Technological Aspects of Crystal Growth*, Trans Tech Publ., Zürich 1998, p. 119.
111. J. J. Derby, A. Yeckel in G. Müller, M J.-J. Metois and P. Rudolph (eds.): *Crystal Growth — from Fundamentals to Technology*, Elsevier, Amsterdam 2004, p. 143.
112. K. Kakimoto in G. Müller, M J.-J. Metois and P. Rudolph (eds.): *Crystal Growth — from Fundamentals to Technology*, Elsevier, Amsterdam 2004, p. 169.
113. H. J. Scheel, *J. Cryst. Growth* 13/14 (1972) 560.
114. W. C. Johnston, W. A. Tiller, *Trans. AIME* 221 (1961), 331,224 (1962) 214.
115. O. Pätzold, I. Grants, U. Wunderwald, K. Jenker, A.- Cröll, G. Gerbeth, *J. Crystal Growth* 245 (2002) 237.
116. A. Krauze et al., *J. Crystal Growth* 265 (2004) 14.
117. T. P. Lyubimova, A. Croell, P. Dold, O. A. Khlybov, I. S. Fayzrakhmanova, *J. Crystal Growth* 266 (2004) 404.
118. P. Schwesig, M. Hainke, J. Friedrich, G. Mueller, *J. Crystal Growth* 266 (2004) 224.
119. S. Yesilyurt, S. Motakef, R. Grugel, K. Mazuruk, *J. Crystal Growth* 263 (2004) 80.
120. A. Mitric et al., *J. Crystal Growth* 287 (2006) 224.
121. G. Müller in R. Fornaci, C. Paorici (eds.): *Theoretical and Technological Aspects of Crystal Growth*, Trans Tech Publ., Zürich 1998, p. 87.
122. M. Abricka, J. Krümins, Yu. Gelfgat, *J. Cryst. Growth* 180 (1997) 388.
123. A. Cröll, P. Dold, Th. Kaiser, F. R. Szofran, K. W. Benz in H. R. Huff, H. Tsuyga, U. Gösele (eds.): *Silicon Materials Science and Technology*, Proc. vol. 98–1, The Electrochem. Soc. Inc., Pennington NJ 1998, p. 429.
124. D. T. J. Hurle, R. W. Series in D. T. J. Hurle (ed.): *Handbook of Crystal Growth*, vol. 2a, North Holland, Amsterdam 1994, p. 259.
125. J. Fainberg, H.-J. Leister, G. Müller, *J. Cryst. Growth* 180 (1997) 517.
126. V. L. Indenbom, *Kristall und Technik* 14 (1979) 493.
127. J. Völkl in D. T. J. Hurle (ed.): *Handbook of Crystal Growth*, vol. 2b, North Holland, Amsterdam 1994, p. 821.
128. S. Pendurti, V. Prasad, H. Zhang, *Modelling Simul. Mater. Sci. Eng.* 13 (2005) 249 and 267.
129. W. A. Tiller, K. A. Jackson, J. W. Rutter, B. Chalmers, *Acta Metallurg.* 1 (1953) 428.
130. J. R. Carruthers in N. Hannay (ed.): *Treatise on Solid State Chemistry*, vol. 5, Plenum Press, New York 1975, p. 325.
131. A. A. Chernov, *J. Cryst. Growth* 24/25 (1974) 11.
132. M. Althaus, K. Sonnenberg, E. Küssel, R. Naeven, *J. Cryst. Growth* 166 (1996) 566.
133. R. V. Stuart: *Vacuum Technology*, Thin Films and Sputtering, Academic Press, London 1983.
134. E. Monberg in D. T. J. Hurle (ed.): *Handbook of Crystal Growth*, vol. 2a, North Holland, Amsterdam 1994, p. 51.
135. C. T. Foxon in D. T. J. Hurle (ed.): *Handbook of Crystal Growth*, vol. 3a, North Holland, Amsterdam 1994, p. 93.
136. B. K. Tanner: *X-ray Diffraction Topography*, Pergamon Press, Oxford 1976.
137. D. Betteridge, H. E. Hallam: *Modern Analytical Methods*, The Chemical Society, London 1974.
138. E. J. Millett, *J. Cryst. Growth* 48 (1980) 666.
139. P. Rudolph, M. Neubert, S. Arulkumaran, M. Seifert, *Cryst. Res. Technol.* 32 (1997) 35.

140. D. T. J. Hurle, B. Cockayne in D. T. J. Hurle (ed.): *Handbook of Crystal Growth*, vol. 2a, North Holland, Amsterdam 1994, p. 99.
141. P. Rudolph, T. Fukuda, *Cryst. Res. Technol.* 34 (1999) 3.
142. P. Rudolph: *Profilzu¨chtung von Eiskristallen*, Akademie-Verlag, Berlin 1982.
143. V. A. Tatarchenko in D. T. J. Hurle (ed.): *Handbook of Crystal Growth*, vol. 2b, North Holland, Amsterdam 1994, p. 1011.
144. X. Liu, *III-Vs Review* 8 (1995) 14.
145. M. Tatsumi, K. Fujita in M. Isshiki (ed.): *Recent Development of Bulk Crystal Growth*, Research Signpost, Trivandrum 1998, p. 47.
146. J. B. Mullin in K. A. Jackson (ed.): *Compound Semiconductor Devices. Structures and Processing*, Wiley-VCH, Weinheim, Germany 1998, p. 1.
147. P. Rudolph, M. Jurisch, *J. Cryst. Growth* 198/199 (1999) 325.
148. M. Jurisch et al., *J. Crystal Growth* 275 (2005) 283.
149. P. Rudolph, F. Kiesling, *Crystal Res. Technol.* 23 (1988) 1207.
150. M. J. Reiner, K. E. Taylor, EP-A 092 496, 1983.
151. D. N. Duhl, M. L. Gell, GB 2 112 812, 1982.
152. GB 2 112 309, 1982 (G. J. S. Higginbotham, J. R. Marjoram, F. J. Horrocks).
153. P. Rudolph in M. Isshiki (ed.): *Recent Development of Bulk Crystal Growth*, Research Signpost, Trivandrum 1998, p. 127; *Prog. Crystal Growth and Charact.* 29 (1994) 275.
154. F. Schmid, C. P. Khattak, D. M. Felt, *Am. Ceramic Soc. Bull.* 73 (1994) 39.
155. A. Rabenau, *Chem. Ing. Tech.* 36 (1964) 542.
156. C. T. Butler, B. J. Sturm, R. B. Quincy, *J. Cryst. Growth* 8 (1971) 187.
157. M. O'Donoghue: *Identifying Man-Made Gems*, NAG Press, London 1983.
158. W. G. Pfann: *Zone Melting*, J. Wiley, New York 1958.
159. W. Keller, A. Muhlbauer: *Floating Zone Silicon*, Dekker, New York 1981.
160. J. Bohm, A. Lüdge, W. Schröder in D. T. J. Hurle (ed.): *Handbook of Crystal Growth*, vol. 2a, North Holland, Amsterdam 1994, p. 213.
161. H. Riemann et al., *J. Electrochem. Soc.* 142 (1995) 1007.
162. A. Mühlbauer, A. Muiznieks, J. Virbulis, A. Lüdge, H. Riemann, *J. Crystal Growth* 151 (1995) 66.
163. R. S. Feigelson, *J. Crystal Growth* 79 (1986) 669.
164. A. McPherson in D. T. J. Hurle (ed.): *Handbook of Crystal Growth*, vol. 2a, North Holland, Amsterdam 1994, p. 417.
165. F. Rosenberger in R. Fornari, C. Paorici (eds.): *Theoretical and Technological Aspects of Crystal Growth*, Trans Tech Publ., Zürich 1998, p. 241.
166. H. J. Scheel in R. Fornari, C. Paorici (eds.): *Theoretical and Technological Aspects of Crystal Growth*, Trans Tech Publ., Zürich 1998, p. 201.
167. S. Porowski, *J. Crystal Growth* 166 (1996) 583.
168. R. Triboulet, *Progress Cryst. Growth and Charact.* 28 (1994) 85.
169. G. B. Stingfellow, *Rep. Prog. Phys.* 45 (1982) 469.
170. B. A. Joyce, *Rep. Prog. Phys.* 37 (1974) 363.
171. J. W. Matthews: *Epitaxial Growth*, Parts A and B, Academic Press, New York 1975.

172. M. B. Small, E. A. Giess, R. Ghez in D. T. J. Hurle (ed.): *Handbook of Crystal Growth*, vol. 3a, North Holland, Amsterdam 1994, p. 223.
173. E. Bauser in D. T. J. Hurle (ed.): *Handbook of Crystal Growth*, vol. 3b, North Holland, Amsterdam 1994, p. 879.
174. J. G. Wright in J. W. Matthews: *Epitaxial Growth*, Academic Press, New York 1975", Chap. 2.3".
175. D. Elwell, in E. Kaldis, H. J. Scheel (eds.): *Current Topics in Materials Science*, vol. 2, North Holland, Amsterdam 1977, Chap. 11.6.
176. W. Kunnmann in R. A. Lefever (ed.): *Preparation and Properties of Solid State Materials*, vol. 1, Dekker, New York 1971, Chap. 1.
177. J. C. Brice, *Rep. Prog. Phys.* 40 (1977) 567.
178. K. Byrappa in D. T. J. Hurle (ed.): *Handbook of Crystal Growth*, vol. 2a, North Holland, Amsterdam 1994, p. 465.
179. J. T. Cheung, T. Magee, *J. Vac. Sci. Technol. A* 1 (1983) 1604.
180. S. A. Barnett, G. Bajor, J. E. Greene, *Appl. Phys. Lett.* 37 (1980) 734.
181. G. Cantwell et al., *J. Appl. Phys.* 71 (1992) 2931.
182. N. Ohtani et al. in M. Isshiki (ed.): *Recent Development of Bulk Crystal Growth*, Research Signpost, Trivandrum 1998, p. 231.
183. C. T. Foxon, B. A. Joyce in E. Kaldis (ed.): *Current Topics in Materials Science*, vol. 7, North Holland, Amsterdam 1981, Chap. 1.
184. A. C. Gossard: *Treatise on Materials Science and Technology*, vol. 24, Academic Press, New York 1982.
185. B. A. Joyce, *Phys. Educ.* 18 (1981) 328.
186. H. Schäfer in *Crystal Growth*, An Introduction, North Holland, Amsterdam 1973 , p. 143.
187. H. Schäfer: *Chemical Transport Reactions*, Academic Press, New York 1964.
188. G. B. Stringfellow, *J. Cryst. Growth* 62 (1983) 225.
189. J. C. Portal et al., *Semicond. Sci. Technol.* 1 (1986) 3.
190. M. S. Skolnick et al., *Semicond. Sci. Technol.* 1 (1986) 29.
191. J. Bloem, W. A. P. Claassen, *Philips Tech. Rev.* 41 (1983) 60.
192. J. Bloem, Y. S. Oei, H. H. de Moor, J. H. L. Hanssen, L. J. Giling, *J. Cryst. Growth* 65 (1983) 399.
193. L. J. Giling, *J. Electrochem. Soc.* 129 (1982) 634.
194. J. H. L. Hanssen, A. A. Saaman, H. H. de Moor, L. J. Giling, J. Bloem, *J. Cryst. Growth* 65 (1983) 406.
195. G. R. Srinivasan in D. G. Gupta (ed.): ''Silicon Processing,'' *ASTMSTP 804*, ASTM, New York 1983, p. 151.
196. G. B. Stringfellow, *J. Cryst. Growth* 62 (1983) 225.
197. G. B. Stringfellow, *Rep. Prog. Phys.* 45 (1982) 469.
198. D. W. Kisker, T. F. Kuech in D. T. J. Hurle (ed.): *Handbook of Crystal Growth*, vol. 3a, North Holland, Amsterdam 1994, p. 93.
199. A. I. Persson, M. W. Larsson, S. Stenström, B. J. Ohlsson, L. Samuelson, L. R. Wallenberg, *Nature Materials* 3 (2004) 677.
200. A. Mineo, A. Matsuda, T. Kurosu, M. Kikuchi, *Solid State Commun.* 13 (1973) 329.
201. K. T. Aust, *J. Cryst. Growth* 13/14 (1972) 57.
202. R. C. Jordan, D. W. Jones, V. H. Hems, *J. Less. Common Met.* 42 (1975) 101.

203. C. M. Muirhead, D. W. Jones, *J. Less Common Met.* 50 (1976) 73.
204. J. S. Williams et al., *Appl. Phys. Lett.* 33 (1978) 542.
205. D. H. Auston, J. A. Golovchenko, P. R. Smith, C. M. Surko, *Appl. Phys. Lett.* 33 (1978) 539.
206. E. F. Kennedy, L. Csepregi, J. W. Mayer, *J. Appl. Phys.* 48 (1977) 4241.
207. L. N. Aleksandrov: *Growth of Crystalline*, Semiconductor Materials on Crystal Surfaces, Elsevier, Amsterdam 1983.
208. L. N. Aleksandrov, *Prog. Cryst. Growth Charact.* 9 (1984) 227.
209. J. C. Fan, N. M. Johnson: *Energy Beam Solid Interactions and Transient Thermal Processing*, North Holland, Amsterdam 1984.
210. J. M. Poate, G. Foti, D. C. Jacobson: *Surface Modificationand Alloying*, Plenum, New York 1983.
211. F. A. Smidt: *Ion Implantation for Materials Processing*, Noyes Data Corp., Park Ridge, N.J., 1983.
212. C. W. White, S. P. Pearcy: *Laser Beam and Electron Beam Processing of Materials*, Academic Press, New York 1980.

Symbols:

a: lattice constant, crystal radius
A: radius of fluid, constant
b: Burger's vector
B: magnetic induction
c: concentration
C: specific heat
D: diffusion coefficient
f: growth rate
g: acceleration due to gravity
G: free energy, shear modulus
h: height of nucleus, heat transfer coefficient
H: enthalpy, depth
J: flux
k: segregation coefficient
K: thermal conductivity
L: face size
N_d: dislocation density
Q: addition rate of particles
S: entropy, radial spacing
t: time
T: temperature
u: number of nearest neighbors
V_m: molar volume
v: velocity of growth face, flow velocity
w: number of nearest neighbors on surface
x: atom fraction
a: expansion coefficient, crystal face parameter, ratio of spacing

b: volume expansion coefficient
g: surface tension
d: thickness of boundary layer
h: dynamic viscosity
~: thermal diffusivity
n: kinematic viscosity
l: layer spacing
r: mass density
σ: relative supersaturation, strain
t: time constant
w_2: rotation rate
r : Laplacian operator $\frac{@^2}{@x^2} + \frac{@^2}{@y^2} + \frac{@^2}{@z^2}$

Related Articles

Industrial Crystallization is treated in ! Crystallization and Precipitation